

**PREPARATION, CHARACTERIZATION AND
PHARMACOKINETIC INTERACTIONS STUDY OF GREEN
SYNTHESIZED SILVER NANOPARTICLES OF *Pterocarpus
marsupium* WITH ANTIDIABETIC DRUG**

A Dissertation submitted to
**THE TAMIL NADU Dr. M.G.R. MEDICAL UNIVERSITY
CHENNAI – 600 032**

In partial fulfillment of the requirements for the award of the Degree of
**MASTER OF PHARMACY
IN
BRANCH- I - PHARMACEUTICS**

Submitted by
BAVYA .C
REGISTRATION No: 261910154

Under the guidance of
DR. J. BAGYALAKSHMI M.Pharm., Ph.D.
Department of Pharmaceutics



**COLLEGE OF PHARMACY
SRI RAMAKRISHNA INSTITUTE OF PARAMEDICAL SCIENCES
COIMBATORE – 641044**

OCTOBER 2021

CERTIFICATE

This is to certify that the M. Pharm dissertation entitled “**PREPARATION, CHARACTERIZATION AND PHARMACOKINETIC INTERACTIONS STUDY OF GREEN SYNTHESIZED SILVER NANOPARTICLES OF *Pterocarpus marsupium* WITH ANTIDIABETIC DRUG**” being submitted to The Tamil Nadu Dr. M.G.R. Medical University, Chennai was carried out by **Ms. C. Bavya (Registration No: 261910154)** in the Department of Pharmaceutics, College of Pharmacy, Sri Ramakrishna Institute of Paramedical Sciences, Coimbatore, under my direct supervision, guidance and to my fullest satisfaction.

Dr. J. BAGYALAKSHMI, M.Pharm., Ph.D.,
Professor,
Department of Pharmaceutics,
College of Pharmacy,
SRIPMS,
Coimbatore – 641 044.

Place: Coimbatore

Date:

CERTIFICATE

This is to certify that the M. Pharm dissertation entitled “**PREPARATION, CHARACTERIZATION AND PHARMACOKINETIC INTERACTIONS STUDY OF GREEN SYNTHESIZED SILVER NANOPARTICLES OF *Pterocarpus marsupium* WITH ANTIDIABETIC DRUG**” being submitted to The Tamil Nadu Dr. M.G.R. Medical University, Chennai was carried out by **Ms. C. Bavya (Registration No: 261910154)** in the Department of Pharmaceutics, College of Pharmacy, Sri Ramakrishna Institute of Paramedical Sciences, Coimbatore under the direct supervision and guidance of **Dr. J. Bagyalakshmi, M.Pharm., Ph.D., Professor**, Department of Pharmaceutics, College of Pharmacy, Sri Ramakrishna Institute of Paramedical Sciences, Coimbatore.

**Dr. M. GOPAL RAO, M. Pharm, Ph.D.,
Vice Principal & HOD,
Department of Pharmaceutics,
College of Pharmacy,
SRIPMS,
Coimbatore - 641 044.**

Place: Coimbatore

Date:

CERTIFICATE

This is to certify that the M.Pharm dissertation entitled “**PREPARATION, CHARACTERIZATION AND PHARMACOKINETIC INTERACTIONS STUDY OF GREEN SYNTHESIZED SILVER NANOPARTICLES OF *Pterocarpus marsupium* WITH ANTIDIABETIC DRUG**” being submitted to The Tamil Nadu Dr. M.G.R. Medical University, Chennai was carried out by **Ms. C. Bavya (Registration No: 261910154)** in the Department of Pharmaceutics, College of Pharmacy, Sri Ramakrishna Institute of Paramedical Sciences, Coimbatore, under the direct supervision and guidance of **Dr. J. Bagyalakshmi, M. Pharm, Ph.D., Professor**, Department of Pharmaceutics, College of Pharmacy, Sri Ramakrishna Institute of Paramedical Sciences, Coimbatore.

Dr. T.K. RAVI, M. Pharm, Ph.D., FAGE.

**Principal,
College of Pharmacy,
SRIPMS
Coimbatore -641 044.**

Place: Coimbatore

Date:

ACKNOWLEDGEMENT

I thank **God Almighty** for the wisdom and perseverance that had been bestowed upon me during this research project. It's because of His grace I was able to successfully complete my project.

Words are insufficient to express my gratitude and respect towards my guide, **DR. J. BAGYALAKSHMI M. Pharm., Ph.D.**, Professor, Department of Pharmaceutics, who mentored me in this innovative pharmaceutical research work at every stage and took great care in making me proceed on the right path, through her valuable suggestions and inspirations.

My sincere gratitude to our beloved Principal **Dr. T.K. Ravi, M. Pharm., Ph.D., FAGE.**, for supporting and providing every need from time to time to complete this work successfully.

I express my deep sense of gratitude and indebtedness to **Dr. M. Gopal Rao, M. Pharm., Ph.D.**, Vice principal and Head of Department of Pharmaceutics, for his valuable suggestions and support during this project.

I submit my sincere thanks to our beloved Managing Trustee **Late. Thiru. R. Vijayakumar**, and **Thiru. P. Lakshmi Narayanaswamy** Managing Trustee, SNR Sons Charitable Trust, Coimbatore for providing all the facilities to carry out this work.

I owe my profound gratitude to **Dr. M. Gandhimathi, M. Pharm., Ph.D., and Dr. Susheel John Varghese M. Pharm, Ph.D.**, for helping me to carry out the analytical studies and also for being a beacon of wisdom in resolving any challenges I faced during the course of work.

I owe my profound gratitude to **Dr. Ashok Kumar M. Pharm, Ph.D.**, for helping me to carry out the in vitro study, and also for being a beacon of wisdom in resolving any challenges I faced during the course of work.

My sincere thanks to my dear teachers **Dr. S. Krishnan M.Pharm., Ph.D., Dr. K. Muthuswamy, M.Pharm., Ph.D., Dr. R.M. Akila, M. Pharm., Ph.D., Dr. A.S. Manjula Devi M. Pharm., Ph.D., and Dr. Amutha Gnana arasi., M.Pharm., Ph.D.** for their moral support and guidance during the course of work.

I would also like to thank Dr. **Venkata Swamy, M.Sc., Ph.D., Mr. Muruganandham., Mrs.Visalakshi** and for their kind co- operation during this work.

I remain greatly indebted to my parents Mr. **A. Chinnamuniappan** and **Mrs. V. Meenakshi**, my brother Mr. **C. Manibalan** for their precious love, affection and moral support which kept me on high spirits and are also the backbone for all successful endeavors in my life.

I wish to extend my sincere thanks to all my batchmates, **Agneeshwaran, Aravindh raj, Arul Packiadhas, Hari, Janani, Navaneethakrishnan, Nithin, Sapthasri, Sweety Kuriakose** who directly or indirectly helped me during my work.

I express my gratitude to all my dear teachers, friends and relatives for their support during my work.

My sincere thanks to all those who have directly or indirectly helped me to complete this project work.

C.Bavya

LIST OF ABBREVIATIONS

DDS	-	Drug delivery system
NDDS	-	Novel Drug Delivery System
NP	-	Nanoparticles
AgNPs	-	Silver nanoparticles
AEPM	-	Aqueous extract of <i>Pterocarpus marsupium</i>
PMAgNPs	-	<i>Pterocarpus marsupium</i> silver nanoparticles
FTIR	-	Fourier Transform Infrared spectroscopy
UV	-	Ultraviolet
SEM	-	Scanning Electron Microscope
rpm	-	Rotation per minute
cm	-	Centimeter
nm	-	Nanometer
mM	-	Milli Molar
<i>et al.</i>	-	and others
g	-	Gram(s)
hrs	-	Hour(s)
min(s)	-	Minutes
mg	-	Milligrams
ml	-	Milliliter
nm	-	Nanometer
µg	-	Micrograms
λ_{\max}	-	Absorption maxima
KBr	-	Potassium Bromide

BSA	-	Bovine serum albumin
WHO	-	World Health Organization
$t_{1/2}$	-	Biological half life
M	-	Molarity
CAM	-	Combination and Alternative Medicine

CONTENTS

Sl. No.	TITLES	PAGE No.
	LIST OF ABBREVIATIONS	
	LIST OF TABLES	
	LIST OF FIGURES	
1	INTRODUCTION	1
2	LITERATURE REVIEW	17
3	AIM AND OBJECTIVE	28
4	PLAN OF WORK	30
5	MATERIALS AND EQUIPMENTS	32
6	PLANT PROFILE	33
7	DRUG PROFILE	37
8	EXCIPIENT PROFILE	40
9	EXPERIMENTAL METHODS	41
10	RESULT AND DISCUSSION	56
11	SUMMARY AND CONCLUSION	91
12	BIBLIOGRAPHY	96
	ANNEXURE- AUTHENTICATION CERTIFICATE	

LIST OF TABLES

TABLE NO	TITLE	PAGE NO
1	Materials and equipment	32
2	Experimental properties	38
3	Pharmacokinetic data	39
4	Diffusion mechanism and diffusion exponent	50
5	Phytochemical analysis	57
6	Solubility studies	58
7	Calibration data of <i>Pterocarpus marsupium</i> bark	59
8	FTIR interpretation of <i>Pterocarpus marsupium</i> bark	61
9	FTIR interpretation of silver nitrate	62
10	FTIR interpretation of <i>Pterocarpus marsupium</i> silver nanoparticles	66
11	Drug entrapment efficiency	67
12	<i>In vitro</i> drug release study of <i>Pterocarpus marsupium</i> silver nanoparticles	73
13	Correlation coefficient values of various kinetic models	76
14	Alpha amylase inhibitory effect of positive control acarbose	77
15	Alpha amylase inhibitory effect of <i>Pterocarpus marsupium</i> silver nanoparticles	77
16	Calibration curve of metformin	79
17	Unbound concentration and percentage protein binding of metformin individual	80

18	Unbound concentration and percentage protein binding of metformin in presence of <i>Pterocarpus marsupium</i> silver nanoparticle	82
19	Calibration curve of glimepiride	85
20	Unbound concentration and percentage protein binding of glimepiride individual	86
21	Unbound concentration and percentage protein binding of glimepiride in presence of <i>Pterocarpus marsupium</i> silver nanoparticle	88

LIST OF FIGURES

FIG NO	TITLE	PAGE NO
1	<i>Pterocarpus marsupium</i> Roxb	36
2	UV visible spectra of <i>Pterocarpus marsupium</i> bark	59
3	Calibration curve of <i>Pterocarpus marsupium</i> bark	60
4	FTIR spectra of <i>Pterocarpus marsupium</i> Roxb. bark	62
5	FTIR spectra of silver nitrate	63
6	Formation of <i>Pterocarpus marsupium</i> silver nanoparticles by green synthesis method	64
7	UV- visible spectra of <i>Pterocarpus marsupium</i> silver nanoparticles	65
8	FTIR spectra of <i>Pterocarpus marsupium</i> silver nanoparticles	67
9	SEM analysis of <i>Pterocarpus marsupium</i> silver nanoparticles with 1500 magnification	68
10	SEM analysis of <i>Pterocarpus marsupium</i> silver nanoparticles with 3000 magnification	69
11	SEM analysis of <i>Pterocarpus marsupium</i> silver nanoparticles with 5000 magnification	69
12	SEM analysis of <i>Pterocarpus marsupium</i> silver nanoparticles with 15000 magnification	70
13	Particle size measurement of <i>Pterocarpus marsupium</i> silver nanoparticles	71
14	Determination of Zeta potential of <i>Pterocarpus marsupium</i> silver nanoparticles	72
15	Zero order plot of <i>Pterocarpus marsupium</i> silver nanoparticle	74
16	First order plot of <i>Pterocarpus marsupium</i> silver nanoparticle	74

17	Higuchi plot of <i>Pterocarpus marsupium</i> silver nanoparticle	75
18	Korsmeyer plot of <i>Pterocarpus marsupium</i> silver nanoparticle	75
19	Alpha amylase Inhibitory effect of <i>Pterocarpus marsupium</i> silver nanoparticles and acarbose	78
20	Calibration curve of metformin	79
21	Protein binding of metformin individual	81
22	Protein binding of metformin in presence of <i>Pterocarpus marsupium</i> silver nanoparticle	83
23	Scatchard plot for protein binding of metformin individual	84
24	Scatchard plot for protein binding of metformin in presence of <i>Pterocarpus marsupium</i> silver nanoparticle	84
25	Calibration curve of glimepiride	85
26	Protein binding of glimepiride individual	87
27	Protein binding of glimepiride in presence of <i>Pterocarpus marsupium</i> silver nanoparticle	89
28	Scatchard plot for protein binding of glimepiride individual	89
29	Scatchard plot for protein binding of glimepiride in presence of <i>Pterocarpus marsupium</i> silver nanoparticle	90

INTRODUCTION

NANOPARTICLES

Nanomedicine and nano delivery systems are a relatively new but rapidly developing science where materials in the nanoscale range are employed to serve as means of diagnostic tools or to deliver therapeutic agents to specific targeted sites in a controlled manner. Nanotechnology offers multiple benefits in treating chronic human diseases by site-specific, and target-oriented delivery of precise medicines. Nanotechnology plays a significant role in advanced medicine/drug formulations, targeting area and their controlled drug release and delivery with immense success. Nanomaterials can be well-defined as a material with sizes ranged between 1 and 1000 nm. As nanoparticles comprise materials designed at the atomic or molecular level, they are usually small sized nanospheres. Hence, they can move more freely in the human body as compared to bigger materials. Nanoscale sized particles exhibit unique structural, chemical, mechanical, magnetic, electrical, and biological properties. Being nanosized, these structures penetrate in the tissue system, facilitate easy uptake of the drug by cells, permit an efficient drug delivery, and ensure action at the targeted location. The uptake of nanostructures by cells is much higher than that of large particles with size ranging between 1 and 10 μm . Hence, they directly interact to treat the diseased cells with improved efficiency and reduced or negligible side effects. **(Patra et al., 2018)**

Targeting of drugs is another significant aspect that uses nanomaterials or nano formulations as the drug delivery systems and, is classified into active and passive. In active targeting, moieties, such as antibodies and peptides are coupled with drug delivery system to anchor them to the receptor structures expressed at the target site. In passive targeting, the prepared drug carrier complex circulates through the bloodstream and is driven to the target site by affinity or binding influenced by properties like pH, temperature, molecular site and shape. **(Patra et al., 2018)**

Classification of Nanoparticles

The nanoparticles are generally classified into the organic, inorganic and carbon based.

Organic nanoparticles

- Dendrimers, micelles, liposomes and ferritin, etc. are commonly known as the organic nanoparticles or polymers. These nanoparticles are biodegradable, non-toxic, and

some particles such as micelles and liposomes have a hollow core, also known as nano capsules and are sensitive to thermal and electromagnetic radiation such as heat and light.

- These unique characteristics makes them an ideal choice for drug delivery. The drug carrying capacity, its stability and delivery systems, either entrapped drug or adsorbed drug system determines their field of applications and their efficiency apart from their normal characteristics such as the size, composition, surface morphology, etc.
- The organic nanoparticles are most widely used in the biomedical field for example drug delivery system as they are efficient and also can be injected on specific parts of the body that is also known as targeted drug delivery. (**Anu Mary Ealias. et al., 2017**)

Inorganic nanoparticles

Inorganic nanoparticles are particles that are not made up of carbon. Metal and metal oxide-based nanoparticles are generally categorised as inorganic nanoparticles.

- **Metal based** - Nanoparticles that are synthesised from metals to nanometric sizes either by destructive or constructive methods are metal based nanoparticles. Almost all the metals can be synthesised into their nanoparticles. The commonly used metals for nanoparticle synthesis are aluminium (Al), cadmium (Cd), cobalt (Co), copper (Cu), gold (Au), iron (Fe), lead (Pb), silver (Ag) and zinc (Zn).
- **Metal oxides based** - The metal oxide-based nanoparticles are synthesised to modify the properties of their respective metal-based nanoparticles. Metal oxide nanoparticles are synthesised mainly due to their increased reactivity and efficiency. The commonly synthesised are Aluminium oxide (Al₂O₃), Cerium oxide (CeO₂), Iron oxide (Fe₂O₃), Magnetite (Fe₃O₄), Silicon dioxide (SiO₂), Titanium oxide (TiO₂), Zinc oxide (ZnO).

Carbon based

The nanoparticles made completely of carbon are known as carbon based. They can be classified into fullerenes, graphene, carbon nano tubes (CNT), carbon nanofibers and carbon black and sometimes activated carbon in nano size.

- **Fullerenes** (C₆₀) is a carbon molecule that is spherical in shape and made up of carbon atoms held together by sp² hybridization. About 28 to 1500 carbon atoms forms the spherical structure with diameters up to 8.2 nm for a single layer and 4 to 36 nm for multi-layered fullerenes.
- **Graphene** is an allotrope of carbon. Graphene is a hexagonal network of honeycomb lattice made up of carbon atoms in a two-dimensional planar surface. Generally, the thickness of the graphene sheet is around 1 nm.
- **Carbon Nano Tubes (CNT)**, a graphene nano foil with a honeycomb lattice of carbon atoms is wound into hollow cylinders to form nanotubes of diameters as low as 0.7 nm for a single layered and 100 nm for multi-layered CNT and length varying from a few micrometres to several millimetres. The ends can either be hollow or closed by a half fullerene molecule.
- **Carbon Nanofiber**, the same graphene nano foils are used to produce carbon nanofiber as CNT but wound into a cone or cup shape instead of a regular cylindrical tube.
- **Carbon black**, an amorphous material made up of carbon, generally spherical in shape with diameters from 20 to 70 nm. The interaction between the particles is so high that they bound in aggregates and around 500 nm agglomerates are formed.
(Anu Mary Ealias. et al., 2017)

SILVER NANOPARTICLES

- Silver nanoparticles (AgNPs) are one of the most vital and fascinating nanomaterials among several metallic nanoparticles that are involved in biomedical applications. AgNPs play an important role in nanoscience and nanotechnology, particularly in nanomedicine.
- Nanosized metallic particles are unique and can considerably change physical, chemical, and biological properties due to their surface-to-volume ratio; therefore, these nanoparticles have been exploited for various purposes. In order to fulfil the requirement of AgNPs, various methods have been adopted for synthesis.
- Generally, conventional physical and chemical methods seem to be very expensive and hazardous.

- Interestingly, biologically-prepared AgNPs show high yield, solubility, and high stability. Among several synthetic methods for AgNPs, biological methods seem to be simple, rapid, non-toxic, dependable, and green approaches that can produce well-defined size and morphology under optimized conditions for translational research. In the end, a green chemistry approach for the synthesis of AgNPs shows much promise. (Xi-Feng Zhang et al., 2016)

Synthesis of AgNPs

- In general, silver nanomaterials can be obtained by two methods, classified as “**top-down**” and “**bottom-up**”.

Top-down approach

- In top to bottom approach, suitable bulk material is broken down into smaller fine particles by size reduction using various techniques like grinding, milling, sputtering, thermal/laser ablation, etc.
- The “top-down” method is the mechanical grinding of bulk metals with subsequent stabilization using colloidal protecting agents.

Bottom-up approach

- In bottom to top approach, nanoparticles are synthesized using chemical and biological methods by self-assembly of atoms to new nuclei, which grow into nano size particles.
- The “bottom-up” methods include chemical reduction, electrochemical methods, and sono-decomposition.
- The biggest advantage of “bottom to top” approach method is the production of a large quantity of nanoparticles within a short span of time.

PHYSICAL METHODS

- In physical methods, nanoparticles are prepared by evaporation-condensation using a tube furnace at atmospheric pressure. Conventional physical methods including spark discharging and pyrolysis were used for the synthesis of AgNPs.

- The advantages of physical methods are speed, radiation used as reducing agents, and no hazardous chemicals involved, but the downsides are low yield and high energy consumption, solvent contamination, and lack of uniform distribution.

CHEMICAL METHODS

- Chemical methods use water or organic solvents to prepare the silver nanoparticles. This process usually employs three main components, such as metal precursors, reducing agents, and stabilizing/capping agents.
- The major advantage of chemical methods is high yield, contrary to physical methods, which have low yield. **(Xi-Feng Zhang et al., 2016)**

BIOLOGICAL METHODS

- Production of silver nanoparticles by physical and chemical processes is expensive, time consuming and eco-unfriendly. Hence, it is very important to develop an environmentally and economically friendly method, which does not involve toxic chemicals and avoids the other problems associated with chemical and physical means of production.
- Biological methods fill these gaps and have various applications in health management through regulation of various biological activities.
- Biological production of silver nanoparticles mainly involves the use of microorganisms and plant sources. It has been reported that nanoparticle production methods based on microorganisms and plants are safe, economic and are relatively less harmful to the environment than chemical synthesis. **(Ahmad Almatroudi, 2020)**

GREEN SYNTHESIS OF METAL NANOPARTICLE

- The green synthesis of nanoparticles is having added advantage when it combines with the metal precursors to give the metal nanoparticles.
- The metal nanoparticles are having its own application with respective to their metal precursors. The metals like platinum, gold, copper, zinc, silver, selenium, titanium, iron, etc.

- The stability of the green synthesis of metal nanoparticles is attained from the plant extract which acts as both reducing and stabilizing agent.
- The plant extracts in the normal decoction method are more suitable for the green metal nanoparticle as a capping and stabilization agent.
- The reduction of metal nanoparticles with the help of biomolecules present in the plant extracts is being the eco-friendly and low-cost approach without any side effects. (D. Ashwini, 2020)

Green Chemistry Approach for the Synthesis of AgNPs

- The development of eco-friendly and reliable techniques for synthesis of silver nanoparticles is a vital step in the area of nanotechnology.
- The concept of green chemistry was introduced to nanoparticle synthesis strategy to decline the use of toxic chemicals and eliminate the production of undesirable or toxic products. The well-known process for synthesis of metal nanoparticles is a chemical reduction of organic and inorganic solvents act as reducing agents
- Green synthesis approach are the choice of the solvent medium (preferably water), an environmentally friendly reducing agent, and a nontoxic material for the stabilization of the nanoparticles
- Biological systems have long been known to reduce metal ions into nano-sized particles and many researchers have recently reported the biogenic synthesis of silver and gold nano-particles using a wide range of biological resources like bacteria, fungi and plants.

Benefits of Green Synthesis Silver Nanoparticles:

- Simple
- Cost-effective
- High product yielding capacity
- Environmentally friendly (Ravindra B. Chintamani, et al., 2018)

Diabetes mellitus

Diabetes mellitus (DM) also known as simply diabetes, is a group of metabolic diseases in which there are high blood sugar levels over a prolonged period. This high blood sugar produces the symptoms of frequent urination, increased thirst, and increased hunger.

Untreated, diabetes can cause many complications. Acute complications include diabetic ketoacidosis and nonketotic hyperosmolar coma. Serious long-term complications include heart disease, stroke, kidney failure, foot ulcers and damage to the eyes.

Diabetes is due to either the pancreas not producing enough insulin, or the cells of the body not responding properly to the insulin produced. There are three main types of diabetes mellitus:

- Type 1 DM results from the body's failure to produce enough insulin. The cause is unknown. This type is an autoimmune disease, meaning your body attacks itself. In this case, the insulin-producing cells in your pancreas are destroyed. Up to 10% of people who have diabetes have Type 1. It's usually diagnosed in children and young adults (but can develop at any age). This form was previously referred to as "insulin-dependent diabetes mellitus" (IDDM) or "juvenile diabetes". People with Type 1 diabetes need to take insulin every day.
- Type 2 DM begins with insulin resistance, a condition in which cells fail to respond to insulin properly. As the disease progresses a lack of insulin may also develop. This form was previously referred to as "non-insulin-dependent diabetes mellitus" (NIDDM) or "adult-onset diabetes". The primary cause is excessive body weight and not enough exercise. Up to 95% of people with diabetes have Type 2. It usually occurs in middle-aged and older people. Other common names for Type 2 include adult-onset diabetes and insulin-resistant diabetes.
- Gestational diabetes, is the third main form and occurs when pregnant women without a previous history of diabetes develop a high blood glucose level. (**Hossam A. Shouip,2015**)

Signs and symptoms:

Symptoms of diabetes include:

- Increased thirst.
- Weak, tired feeling.
- Blurred vision.
- Numbness or tingling in the hands or feet.

- Slow-healing sores or cuts.
- Unplanned weight loss.
- Frequent urination.
- Frequent unexplained infections.
- Dry mouth

Other symptoms

- In women: Dry and itchy skin, and frequent yeast infections or urinary tract infections.
- In men: Decreased sex drive, erectile dysfunction, decreased muscle strength.

Determination of diabetes mellitus

Diabetes can be determined in one of three different ways (tests):

- **The A1C test**
 - at least 6.5% means diabetes
 - between 5.7% and 5.99% means prediabetes
 - less than 5.7% means normal
- **The FPG (fasting plasma glucose) test**
 - at least 126 mg/dl means diabetes
 - between 100 mg/dl and 125.99 mg/dl means prediabetes
 - less than 100 mg/dl means normal

(An abnormal reading following the FPG means the patient has impaired fasting glucose (IFG))
- **The OGTT (oral glucose tolerance test)**
 - at least 200 mg/dl means diabetes
 - between 140 and 199.9 mg/dl means prediabetes
 - less than 140 mg/dl means normal

(An abnormal reading following the OGTT means the patient has impaired glucose tolerance (IGT) (**B. Suresh Lal, 2016**))

Data Analysis of Diabetes in India

- The pervasiveness of diabetes is rising everywhere throughout the world because of populace development, maturing, urbanization and expansion of obesity and physical latency. Diabetes is a major global public health problem currently affecting 463 million individuals and projected to affect 700 million by 2045.
- Estimates of prevalence suggest that the diabetes burden is increasing at a faster pace in low- to middle income countries (LMICs) than in high-income countries (HICs). In India, 77 million adults currently have diabetes and this number is expected to almost double to 134 million by 2045.
- One in six people with diabetes in the world is from India. The numbers place the country among the top 10 countries for people with diabetes, coming in at number two with an estimates 77 million diabetes. China leads the list with over 116 million diabetes.
- India is on the top of the table of clutch of countries in from southeast Asia – Bangladesh, Sri Lanka, Nepal, and Mauritius. Bangladesh, which is second on the list of top five countries with diabetes (20-79 years), however, has only 8.4 million diabetes. **(Shammi Luhar, et al., 2020)**
- A study revealed a varying range of complementary and alternative medicine (CAM) use rates among diabetic patients in India (**67.7%**). Many patients with chronic diseases such as diabetes mellitus are reliant on CAM use because of its perceived efficacy, low cost, and safety. **(Zemene demelash kifle, 2021)**
- CAM can affect the management of diabetes by either herb-drug interaction with the use of herbal remedies or indirectly by affecting medication adherence when using herbal or any other CAM types. **(Abdulaziz S. Alzahrani, et al.,2021)**

PROTEIN BINDING OF DRUGS

The formation of a protein drug complex is termed as protein binding of drugs. Drug protein binding may be a reversible or an irreversible process. Irreversible drug protein binding is usually as a result of chemical activation of drug, when then attaches strongly to protein or macromolecule by covalent chemical bonding. Reversible drug protein binding implies that the drug binds the protein with weaker chemical bonds such as hydrogen bonds or Vander

Waals forces. The amino acids that compose the protein chain have hydroxyl, carboxyl or other sites available for reversible drug interaction.

Drug may bind to various macromolecular components in the blood including albumin, α 1 acid glycoprotein, lipoproteins, immunoglobulins (IgG) and erythrocytes (RBC). Albumin is a protein synthesized by the liver with a molecular weight of 66KD. Albumin is the major component of plasma proteins responsible for reversible drug binding. In the body, albumin is distributed in the plasma and in the extra cellular fluids of sin, muscle and various other tissues.

Albumin is responsible for maintaining osmotic pressure of the blood and for the transport of endogenous and exogenous substances. Lipoproteins are responsible for the transport of plasma lipids and may be responsible for the transport of plasma lipids may be responsible for binding of the drug if the albumin sites become saturated.

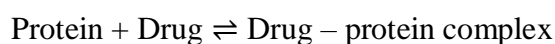
Reversible drug-protein binding is a major interest in pharmacokinetics. The protein bound drug is a large complex that cannot easily cross cell membranes and therefore has a restricted distribution. The protein bound drug is usually pharmacologically inactive. In contrast, the free or unbound drug crosses cell membranes and is therapeutically active.

Drug protein binding is influenced by a number of factors like,

- Drug
- Protein
- Affinity between drug and protein
- Drug interactions
- Pathological condition of patient (**Brahmankar and Jaiswal, 1995**)

KINETICS OF PROTEIN BINDING

The kinetics of reversible drug-protein binding site can be described by law of mass action as follows.



From this equation and law of mass action, an association constant, K_a can be expressed as the ratio of molar concentrations of the reactants. It assumes only one binding site per protein molecule

$$K_a = \frac{[PD]}{[P][D]} \text{ -----(2)}$$

To study the binding behaviour of drugs, a determinable ratio, R is defined as follows.

$$r = \frac{\text{Moles of drug bound}}{\text{Total moles of protein}}$$

$$r = \frac{[PD]}{[PD]+[P]} \text{ -----(3)}$$

According to eqn 2 $[PD] = K_a [P] [D]$ by substitution into eqn 3.

$$r = \frac{K_a [P][D]}{K_a [P]+[P]}$$

$$r = \frac{K_a [D]}{1+K_a [D]} \text{ -----(4)}$$

The eqn describes 1 mole of drug binds to 1 mole of protein in a 1:1 complex. Therefore, this assumes only one independent binding site for each molecule of drug.

If there are “n” independent identical binding sites eqn 4 becomes

$$r = \frac{n K_a [D]}{1+K_a [D]} \text{ -----(5)}$$

In terms of $K_d = 1 / K_a$ eqn 5 reduces to

$$r = \frac{n [D]}{K_d+[D]} \text{ -----(6)}$$

since protein molecules are large in size, more than one type of binding site is present and drugs bind independently on each binding site with its own association constant and hence eqn 6 becomes,

$$r = \frac{n_1 k_1 [P]}{1+k_1 [D]} + \frac{n_2 k_2 [P]}{1+k_2 [D]}$$

where, 1,2 – different binding sites

K - binding constants

n - number of binding sites

As per the equations we assume that each drug binds to the protein at an independent binding site and the affinity of a drug for one binding site does not influence binding to other sites.

In reality a drug protein binding sometimes exhibits a phenomenon called cooperativity. For these drugs the binding of first drug molecule at one site on the protein molecule influences successive binding of other drug molecules. **(Brahmankar and Jaiswal 1995)**

DETERMINATION OF BINDING CONSTANTS AND BINDING SITES BY GRAPHIC METHODS

IN VITRO METHODS

$$r = \frac{n [D]}{Kd + [D]} \text{-----(1)}$$

As per the equation quoted above, as free drug concentration increases number of moles of drug bound per mole of protein becomes saturated and plateaus. Thus, drug protein binding resembles a Langmuir adsorption isotherm which is also similar to adsorption of a drug to an adsorbent becoming saturated as drug concentration increases.

$$r = \frac{1 + Ka [D]}{n Ka [D]} \text{-----(2)}$$

$$r = \frac{1}{n Ka [D]} + \frac{1}{n} \text{-----(3)}$$

The values for n and Ka give a general estimate of the affinity and binding capacity of the as plasma contains a complex mixture of proteins. The drug protein binding in plasma may be influenced by competing substances such as ions, free fatty acids, drug metabolites and other drugs. Measurements of drug protein binding should be obtained over a wide range of concentration range, because at low drug concentration range, because at low drug concentrations a high affinity low-capacity binding site might be missed or at a higher drug concentration saturation of the protein binding sites may occur.

CLINICAL SIGNIFICANCE OF DRUG PROTEIN BINDING

Most drugs bind to plasma proteins to some extent. When the clinical significance of the fraction of drug bound is considered it is important to know whether the study was performed using pharmacological or therapeutic plasma drug concentrations. The fraction of drug bound can change with plasma drug concentration and dose of drug administered.

When a highly protein bound drug is displaced from binding by a second drug or agent, a sharp increase in the free drug concentration in the plasma may occur leading to toxicity. Displacement occurs when a second drug is taken that competes for the same binding site in the protein as initial drug. this will lead to increased apparent volume of distribution and an increased half-life, but clearance will remain unaffected. If administered by multiple doses, the mean steady state remains unaffected; however, the mean steady state free drug level will be increased due to displacement. The therapeutic effect will therefore increase. **(Leon Shargel, Susanna wu-pong, 2012).**

DRUG – DRUG INTERACTIONS

A drug interaction results when the effects of a drug are altered in some way by the presence of another drug, by food, or by environmental exposure. A cause of a drug interaction involves one drug which alters the pharmacokinetics of another medical drug. Alternatively, drug interactions result from competition for a single receptor or signalling pathway. Both synergy and antagonism occur during different phases of the interaction between a drug and an organism. Drug–drug interactions can occur when two or more drugs administered simultaneously mutually interact in a manner which results in alteration of the pharmacokinetic profile, pharmacological or toxicological response to one or both of the compounds. Drugs may interact via inhibition of absorption or elimination processes or induction of enzymes responsible for the metabolism of drugs. drugs may affect endogenous metabolic processes (e.g., 6 β -hydroxylation of cortisol increases with cytochrome P4503A4 induction); drugs may interact with ‘foodstuffs’ (e.g., furafylline inhibits caffeine clearance) or ‘foodstuffs’ which contain potent pharmacological principles may interact with drugs (e.g., components of grapefruit juice can block terfenadine metabolism). Drug interaction results into increased or decreased efficacy or toxicity of drug which is very dangerous in some time to the patient. There are large numbers of drug interactions associated with use of anticoagulants, oral hypoglycaemic agents, use of cytotoxic drugs, use of digoxin, etc... **(Evans, G., 2004)**

TYPES OF DRUG INTERACTION

Drug Interaction mechanisms can be broadly divided into two groups

- Pharmacodynamic interactions
- Pharmacokinetic interactions

PHARMACODYNAMIC INTERACTIONS

A pharmacodynamic interaction is caused by the concurrent administration of two drugs that have the opposite effect or similar effects. In this type of interaction, there is a change in the patient's response to the drug without altering the drug's pharmacokinetics (absorption, distribution, metabolism, and excretion). That is, there is a change in drug action without altering the plasma concentration. The interaction of drugs having similar effects such as alcohol, opioids, and sedatives is considered synergistic. Pharmacodynamic interactions may result from one drug changing the environment necessary for the safe and effective use of a second drug. An example of this interaction is a loop diuretic that produces potassium wasting and can increase the cardiotoxic effects of digoxin.

PHARMACOKINETIC INTERACTIONS

A pharmacokinetic (or dispositional) drug interaction is where one drug alters the rate or extent of any of the four basic pharmacokinetic processes: absorption, distribution, metabolism, or excretion (ADME) of a second drug. This type of interaction is measured by a change in one or more of the kinetic parameters, such as maximum serum concentration, half-life amount of drug excreted in the urine, area under the concentration time curve, etc.

MECHANISMS OF DRUG INTERACTIONS

Interactions Affecting Drug Absorption

Interactions affecting drug absorption may result in changes in the rate of absorption, the extent of absorption, or a combination of both. The extent to which a drug is absorbed can be affected by changes in drug transport time or gastrointestinal motility, gastrointestinal pH, intestinal cytochrome P450 (CYP) enzyme and transport protein activity, and drug chelation in the gut. In general, a change in the extent of drug absorption that exceeds 20% is generally considered to be clinically significant.

Interactions Affecting Drug Distribution

Theoretically, drugs that are highly protein bound (>90%) may displace other highly protein-bound drugs from binding sites, thereby increasing drug distribution. For restrictively metabolized drugs, as the fraction of unbound drug increases due to displacement of drug from protein binding sites, elimination of unbound drug increases, to return unbound concentrations to their previous levels. The transient increase in unbound concentration may

be clinically important for drugs with a limited distribution, a narrow therapeutic index, or a long elimination half-life. As no restrictively metabolized drugs rely on hepatic blood flow for their elimination, increases in the fraction of unbound drug in plasma do not result in immediate compensatory elimination of unbound drug. (**Beverly J. McCabe, Eric H. Frankel,2004**)

Interactions Affecting Drug Metabolism

Drug metabolism is composed of two distinct pathways of biochemical processing, Phase I and Phase II. Phase I is a chemical modification (typically oxidation, hydrolysis, or reduction reactions) performed primarily by members of the CYP enzyme family. Phase II metabolism consists of the biotransformation of endogenous compounds by reactions such as glucuronidation, sulfation, methylation, acetylation, and glycine conjugation. Modulation of CYP-mediated metabolism is the primary mechanism by which one drug interacts with another. The most common CYP subfamilies include CYP1A2, CYP2C9, CYP2C19, CYP2D6, CYP2E1, CYP3A4. These enzymes may be induced or inhibited by other agents, thereby leading to an increase or decrease in the metabolism of the primary drug.

Enzyme Inhibition

Inhibition of enzyme activity is a common mechanism of clinically significant metabolic drug interactions. Enzyme inhibition decreases the rate of drug metabolism, thereby increasing the amount of drug in the body, leading to accumulation and potential toxicity.

Enzyme Induction

Enzyme induction may increase the intestinal and hepatic clearance of drugs, subsequently altering serum concentrations. Enzyme inhibition may result from non-competitive or competitive inhibition of CYP enzymes by a second drug, an effect may occur rapidly. The result of non-competitive enzyme inhibition by addition of a second agent is slower metabolism of the first drug, higher plasma drug concentrations, and a risk for toxicity. In the case of competitive inhibition, the metabolism of both drugs can be reduced, resulting in higher than expected concentrations of each drug.

Interactions Involving Drug Transport Proteins

A variety of transport proteins may be involved to different extents in drug interactions that alter the absorption, distribution, metabolism, and elimination of medications. Transporters

such as the MDR proteins, P-glycoprotein, multidrug resistance related proteins (MRPs), organic anion transport polypeptides (OATPs), organic cation transporters (OCTs), and organic anion transporters (OATs) may be altered by xenobiotics, thereby affecting the disposition of coadministered drugs that are transported by these proteins.

Interactions Affecting Renal Excretion

The pharmacokinetic properties of drugs that are primarily renally excreted may be altered by changes to active transport systems, urinary pH, and renal blood flow. Passive diffusion of molecules into and out of the tubule lumen is dependent upon their extent of ionization, with only the nonionized form able to diffuse through the lipid membrane. Changes in pH alter the ionization of weakly acidic and basic drugs, thereby affecting their degree of passive diffusion. Since most weakly acidic and basic drugs are metabolized to inactive compounds prior to renal excretion, changes in urinary pH do not affect the elimination of most drugs.

(Arthur J. Atkinson Jr., et al., 2012)

Food-Drug Interactions

The term “food” can be defined as materials that consist of different chemical components such as proteins, carbohydrates and fat that can be used in an organism as nutrients to sustain growth, repair and maintain vital processes as well as furnish energy. Food can affect drug absorption via different mechanisms such as changing gastric emptying time, the pH and residence time of the drug in the gastrointestinal tract, the hepatic blood flow and by modulating efflux transporters as well as pre-systemic metabolism. One of the classical pharmacokinetic interactions of food components with drugs is that of grapefruit juice with nifedipine. Certain recently discovered pharmacokinetic interactions of selected food components that may enhance drug bioavailability. **(Werner Gerber., et al., 2018)**

Herb-Drug Interactions

The term “herb” refers to a plant or plant part that is valued specifically for its medicinal, savoury or aromatic qualities. Herbal medicines are often used by patients in conjunction with their conventional medicines. Herb-drug interactions being capable of modulating pharmacodynamic and pharmacokinetic profiles of drugs. **(Werner Gerber., et al., 2018)**

REVIEW OF LITERATURE

Kanmani R. and Irudaya Irin Scleeva P., (2021) This research work is mainly focused to study the anti-oxidant and anti-diabetic activities of biologically synthesis of silver nanoparticles (AgNPs) from the flaxseed extract of *Linum usitatissimum*. The In vitro antioxidant and antidiabetic activities of *L. usitatissimum* mediated AgNPs were analyzed by using the DPPH, alpha-amylase, and alpha glycosides assays respectively. The DPPH result shows that the AgNPs possess 59.01% of radical scavenging property and the standard ascorbic acid reveals 48.63% at 100 µg/mL concentration. Similarly in anti-diabetic activity, AgNPs shows the maximum inhibition of 79.84% in the alpha-amylase assay, and for alpha-glucosidase, AgNPs showed 58.86% at 100 µg/ ml concentration. The aqueous extract of *L. usitatissimum* showed the great capability to synthesize the silver nanoparticles. The synthesized nanoparticle has 59% of elemental silver with noticeable activities of anti-oxidant and anti-diabetic. This study suggests that *L. usitatissimum* mediated silver nanoparticles can be alternate antioxidants and antidiabetic agents for the treatments which is less toxic and more effective than the existing one.

Ngan Tran. et al., (2020) Diabetes mellitus has been considered to be a major cause affecting the economy of patients, their families and society. In order to decrease this problem, researches on new antidiabetic agents are concerned. Because of the adverse effects of modern therapies, many traditional medicines have been noticed. Moreover, herbal extracts nowadays can be used with standard drugs for combinatorial therapies. Each herb has its own active ingredients that can lower blood sugar levels as well as control the complications of diabetes. Similar to most herbs, *P. marsupium* is a rich source of phenolic and flavonoid compounds. It has been reported that this plant contains alkaloids, steroids, terpenoids, tannins, amino acids, proteins, etc. The potential antidiabetic constituents in this plant have been identified successfully, including epicatechin. It is also reported to be rich in polyphenolic compounds which have been considered major bioactive compounds, such as marsupsin, pterosupin and pterostilbene and flavonoids pteroside, pteroisouroside, carsupin and marsupol. These compounds have many biological effects, e.g., anti-inflammatory, anti-bacterial, anti-oxidant activity, especially antidiabetic activity. It was found to be effective in lowering the glucose level. Epicatechin, isolated from *P. marsupium* showed the ability of regeneration of the β -cells of the pancreas islets.

Sivanageswararao Mekala. et.al, (2020) Pterocarpus marsupium is a medicinal plant used in Ayurvedic system of medicine to control blood sugar and strong antidiabetic. The study evaluated the hypoglycemic effect of the ethanolic extract of Pterocarpus marsupium seeds in diabetic rats. The work was designed to evaluate the anti-hyperglycemic activity of Pterocarpus marsupium seed extract (100 mg/kg and 200 mg/kg) on gabapentin induced hyperglycemia in wistar albino rats. Blood glucose level, serum triglycerides, total cholesterol, HDL cholesterol and LDL cholesterol were evaluated in gabapentin induced diabetic rats. The results of the test drug were compared with the standard drug. Ethanolic seed extract of Pterocarpus marsupium at 100 mg/kg and 200 mg/kg had significantly reduced the blood glucose level compared to disease control rats on day 1, 7, 14 and 21. Pterocarpus marsupium shows significant decrease in triglycerides levels, serum cholesterol levels, LDL levels and increased HDL levels, total protein levels compared to the disease control group. They have concluded that the ethanolic seed extract of Pterocarpus marsupium has potential antidiabetic action in gabapentin induced diabetic rats and the effect was found to be more similar to the standard drug metformin.

Dr. Aruna. et al., (2020) The present study involves an efficient and sustainable route of AgNPs preparation using P. marsupium bark extract which is well adorned for their medicinal properties. The green synthesis of silver nanoparticles from P. marsupium bark extract was accomplished. In vitro cytotoxicity effect of biosynthesized AgNPs in SKOV-3 ovarian cancer cell line by MTT assay was also carried out. Results of the UV-VIS spectrum of silver nanoparticles revealed a characteristic Surface Plasmon Resonance (SPR) peak at 435nm. SEM study showed a spherical shaped AgNPs and size of AgNPs were about 240nm. XRD photograph indicated AgNPs were in crystalline face-centered cubic structure and the size range of 15-30 nm, further confirming the result of SEM. FTIR result also showed that the synthesized nanoparticles were capped with bimolecular compounds which are responsible for the reduction of silver ions. The AgNPs nanoparticles have shown a potential antibacterial, antioxidant and cytotoxicity activities when compared with their respective standards. The present study concluded that the biosynthesized AgNPs from P. marsupium bark extract were found to be ecofriendly, easy, cost effective and have promising pharmacological activities.

D. Jini. et al., (2019) The present study was concentrated on the green synthesis of silver nanoparticles by using *Allium cepa* and evaluation of its antidiabetic activity by inhibiting the carbohydrate hydrolyzing enzymes. The results of UV–vis Spectrophotometer, FT-IR and SEM analysis revealed that the synthesized particles were nano in size and spherical in shape and was adhered by the functional groups of metabolites from the *Allium cepa* extract. The synthesized silver nanoparticles showed higher level of antidiabetic activity by inhibiting the carbohydrate metabolizing enzymes such as α -amylase and α -glucosidase. In addition, it also exhibited good antioxidant activity which will scavenge the free radicals produced due to hyperglycemia. From the study, it was proved that the green synthesized silver nanoparticles from *Allium cepa* have antioxidant and antidiabetic activities with less cytotoxicity. So, the synthesized nanoparticles will be a good therapeutic agent for the management of diabetes through the inhibition of carbohydrate hydrolyzing enzymes.

Govindappa M. et al., (2018) The current study developed an easy and eco-friendly method for the synthesis of AgNPs using aqueous leaf extract of *Calophyllum tomentosum* (CtAgNPs) and evaluated the extract to know the effects of anti-bacterial, antioxidant, anti-diabetic, anti-inflammatory and anti-tyrosinase activity. The leaf extract of *C. tomentosum* yielded flavonoids, saponins, tannins, alkaloids, glycosides, phenols, terpenoids and coumarins. AgNPs formation was confirmed by UV-vis spectra at 438 nm. Crystalline structure with a face centered cubic (fcc) of AgNPs was observed in XRD. FTIR had shown that the phytochemicals were responsible for the reduction and capping material of silver nanoparticles. The size and shape of the AgNPs were determined using SEM. From EDX study analyzed the strong absorption property of AgNPs. The CtAgNPs have showed significant antibacterial activity on multi drug resistance bacteria. The CtAgNPs had shown strong antioxidant (DPPH, H₂O₂ scavenging, nitric oxide scavenging power, reducing power) activities. The CtAgNPs had strongly inhibited the α -glucosidase and DPPIV compared to α -amylase. The CtAgNPs exhibited strong anti-inflammatory activity (albumin denaturation, membrane stabilization, heat hemolytic, protein inhibitory, lipoxigenase, xanthine oxidase) and tyrosinase inhibitory activity.

Agarwal. et al., (2018) In the present study they optimized synthesis of silver nanoparticles (Ag NPs) using lemongrass and visualizing its in-vitro antidiabetic potential. This study involves the

comparative analysis of Conventionally heated (CH) and Microwave irradiated (MI) technique for the synthesis of Ag NPs from lemongrass for the first time. The crystalline nature of the nanoparticles was confirmed using X-ray diffraction assay (XRD) with average size range of 75 nm, the size, and shape of the nanoparticles were confirmed as spherical shaped using scanning electron microscope (SEM), atomic force microscopy (AFM) demonstrated aggregate formation of size range 138 nm with mean average size of individual nanoparticle as 80 nm, elements present in the nanoparticles confirmed using elemental dispersive analysis of X-ray (EDAX) and the functional groups of plant extract responsible for nanoparticles synthesis have been confirmed using Fourier transform infrared spectroscopy (FT-IR). Surface morphology and the dispersity were observed by Transmission electron microscopy (TEM) analysis. The anti-diabetic potential of nanoparticle synthesized was studied using amylase activity inhibition Assay and glucose diffusion-inhibitory Assay. EDAX analysis confirmed the presence of elemental silver Synthesized nanoparticle proved to have anti-diabetic activity clearly demonstrated by the results.

J Bagyalakshmi and Haritha, (2017) In present study, green synthesis of silver nanoparticles from aqueous extract of Pterocarpus marsupium bark and wood. Synthesis of Pterocarpus marsupium silver nanoparticles was done by drop wise addition of 1 mM silver nitrate to Pterocarpus marsupium bark and wood extract. Aqueous extract of Pterocarpus marsupium bark and wood extract were mixed with the aqueous solution of silver nitrate. The surface Plasmon band in the silver nanoparticles was found to be 431 nm. The FTIR study concluded that hydroxyl and carboxyl groups act as reducing and stabilizing agent and phenolic group function as capping agent. Average particle size was found to be 148.5 nm. Its polydispersity index was 0.336 and zeta potential was measured and found to be -28 mV with the peak area of 100% intensity. This indicates that formed nanoparticles were stable. The in vitro anti-diabetic study confirms that Pterocarpus marsupium is having anti-diabetic activity. The study concluded that: Pterocarpus marsupium silver nanoparticles are found to be effective for anti-diabetic activity. The study found without using any chemical reagent as stabilizing agent the silver nanoparticles are stable.

Rijuta G. Saratale.et al., (2017) In this study reports the novel synthesis of silver nanoparticles (AgNPs) using a Punica granatum leaf extract (PGE). The synthesized AgNPs were characterized by various analytical techniques including UV–Vis, FTIR, XRD, XPS, field emission scanning electron microscopy and energy-dispersive spectra and high-resolution transmission electron microscopy (HRTEM). FTIR analysis revealed that the involvement of biological macromolecules of P. granatum leaf extract were distributed and involved in the synthesis and stabilization of AgNPs. A surface-sensitive technique of XPS was used to analyze the composition and oxidation state of synthesized AgNPs. The analytical results confirmed that the AgNPs were crystalline in nature with spherical shape. The zeta potential study revealed that the surface charge of synthesized AgNPs was highly negative (-26.6 mV) and particle size distribution was ranging from 35 to 60 nm and the average particle size was about 48 nm determined by dynamic light scattering (DLS). The PGE-AgNPs antidiabetic potential exhibited effective inhibition against α -amylase and α -glucosidase (IC₅₀; 65.2 and 53.8 μ g/mL, respectively). The PGE-AgNPs showed a dose-dependent response against human liver cancer cells (HepG2) (IC₅₀; 70 μ g/mL) indicating its greater efficacy in killing cancer cells. They also possessed in vitro free radical-scavenging activity in terms of ABTS (IC₅₀; 52.2 μ g/mL) and DPPH (IC₅₀; 67.1 μ g/mL) antioxidant activity. PGE-AgNPs displayed strong antibacterial activity and potent synergy with standard antibiotics against pathogenic bacteria. Thus, synthesized PGE-AgNPs show potential biomedical and industrial applications.

Gupta. et al., (2017) Diabetes is a complex condition with a variety of causes and pathophysiology. The current single target approach has not provided ideal clinical outcomes for the treatment of the disease and its complications. Herbal medicine has been used for the management of various diseases such as diabetes over centuries. Many diabetic patients are known to use herbal medicines with antidiabetic properties in addition to their mainstream treatments, which may present both a benefit as well as potential risk to effective management of their disease. In this review they evaluated the clinical and experimental literature on herb–drug interactions in the treatment of diabetes. Pharmacokinetic and pharmacodynamic interactions between drugs and herbs are discussed, and some commonly used herbs which can interact with antidiabetic drugs summarized. Herb–drug interactions can be a double-edged sword presenting both risks (adverse drug events) and benefits (through enhancement). Based on the results

presented above, it is clear that numerous herbal medicines, when taken in conjunction with antidiabetic pharmaceutical agents, could potentially alter their pharmacokinetic and/or pharmacodynamic properties. These interactions are complex given the large number of pathophysiological/pharmacological targets associated with the disease and the multicomponent properties of herbal medicine.

Kannan Balan. et al., (2016) In the present study the green synthesis of silver nanoparticles (AgNPs) using the aqueous leaf extract of *Lonicera japonica*. A color change from pale yellow to brown was observed during the synthesis process. Ultraviolet-visible (UV-vis) studies show an absorption band at 435 nm due to surface plasmon resonance of the AgNPs, further characterized using the average size and stability of the AgNPs, which were 53 nm and -35.6 mV as determined by a zeta sizer. The spherical, hexagonal shape and the face centered cubic crystalline structure of metallic silver were confirmed by high resolution transmission electron microscopy (HR-TEM) and X-ray diffraction (XRD). The functional group of biomolecules present in the AgNPs was characterized by Fourier transform infrared spectra (FTIR). The synthesized AgNPs exhibited strong antioxidant activity. The antidiabetic ability of AgNPs was shown by the effective inhibition against carbohydrate digestive enzymes such as α -amylase and α -glucosidase with IC₅₀ values of 54.56 and 37.86 mg ml⁻¹, respectively. The inhibition of the kinetic mechanism was analyzed with LB and Dixon plots. AgNPs were identified to be reversible noncompetitive inhibitors and K_i values of 25.9 and 24.6 mg were found for key enzymes of diabetes (α -amylase and α -glucosidase). They concluded that the results suggest that the AgNPs were found to show remarkable potential antidiabetic activity against the key enzymes of diabetes and were found to be an appropriate nanomedicine for nano biomedical applications.

Karthik VP. et al., (2016) Diabetes mellitus is a metabolic disorder which has emerged as a global public health threat in the present century. The present oral hypoglycemic agents produce undesirable side effects and oxidative stress. Thus, there is a need for a safe, cost effective and complementary therapy for Diabetes mellitus. To evaluate the Nitric oxide scavenging activity and Alpha amylase inhibitory activity of *Pterocarpus marsupium*. The antioxidant activity was determined by nitric oxide radical scavenging activity according to the method of Garrat (1964).

Alpha-amylase inhibitory activity was evaluated according to the method of Bernfield (1955). % Inhibition of Nitric Oxide by *Pterocarpus marsupium* extract at 20, 40, 60, 80, 100µg/ml was 14.24±0.10, 24.43±0.18, 40.22±0.27, 60.87±0.22, 82.25±0.78 respectively. % Inhibition of Alpha amylase by extract of *Pterocarpus marsupium* at 20, 40, 60, 80, 100µg/ml are 22.54±0.18, 30.64±0.52, 40.92±0.56, 56.08±0.07 and 72.25±0.76 respectively. Based on the results they conclude that *Pterocarpus marsupium* as strong in vitro nitric oxide scavenging activity and alpha amylase inhibitory activity. Thus, *Pterocarpus marsupium* is a potential antidiabetic agent.

Behara Chandra Rekha. et al., (2016) In present study, Albino rats of Wister strain weighing 180 – 225 gm were procured from our animal house. They employed Alloxan monohydrate 5% fresh solution (125mg/kg body weight) administered intraperitoneally to induce diabetes. Animals were divided into four groups with six animals in each group, kept separately in different cages. Group N: - Non-diabetic rats served as control group and received plain water, Group C: -Diabetic control group (Alloxan +2% Gum Acacia), Group G: -Standard group (Alloxan +0.5mg/kg BW Glibenclamide) and Group PM: -Test group (Alloxan +700mg/kg BW *Pterocarpus marsupium* leaves). Acute toxicity study was conducted using doses 100-1000 mg/kg body weight of *Pterocarpus marsupium* on healthy rats, additionally; 24-hour antidiabetic profile was also conducted on animals of four groups. 700mg/kg body weight *Pterocarpus marsupium* leaves showed its peak action in 24-hour antidiabetic activity and also was found to be safe in acute toxicity study. In 24 Hour, antidiabetic study with methanol extract of leaves of *Pterocarpus marsupium* on alloxan induced diabetic rats: After administration of 700mg/kg methanolic extract of *Pterocarpus marsupium* leaves, we observed the fall in blood glucose concentrations were 56.12% at a 1st hour & 14.61% at a 2nd hour with ($p < 0.0001$). The results indicate that methanol extract of leaves of *Pterocarpus marsupium* plant has significant & sustained oral hypoglycemic activity, comparable with the oral hypoglycemic effect of insulin secretagogue like glibenclamide, a sulphonyl urea. Hence, it was concluded, that this antidiabetic effect may be due to increased secretion of insulin.

Neelam Seedher. et al., (2015) For the highly protein-bound anti-diabetic drugs with a small volume of distribution, competitive binding to human serum albumin can significantly influence the pharmacological activity of drugs resulting in serious fluctuations in the blood glucose levels

of diabetic patients. In this paper, competitive binding studies using fluorescence spectroscopic technique have been reported for a wide range of drug combinations involving oral hypoglycemic (anti-diabetic) agents. The results indicated that the combination of gliclazide and repaglinide with the studied competing drugs can increase the risk of hypoglycemia in diabetic patients and should be avoided. On the other hand, the corresponding combinations involving glimepiride and glipizide were found safe. The therapeutic efficacy of studied competing drugs, on the other hand decreased in the presence of antidiabetic drugs in most cases. Competitive binding mechanism based on the site-specificity and conformational changes in the human serum albumin molecule has been proposed.

Ajithadas Aruna. et al., (2014) Cost effective and eco-friendly technique for green synthesis of silver nanoparticles from the methanolic extract of *Costus pictus* leaf and characterization of synthesized silver nanoparticles was carried out in this study. The biological synthesis of silver nanoparticles using *Costus pictus* extract was shown to be rapid and produced particles of fairly uniform size and shape. As the methanolic leaf extracts of *Costus pictus* D. Don were mixed with the aqueous solution of silver nitrate, it changed into brown color due to the excitation of surface Plasmon vibrations, which indicated the formation of methanolic extract of *Costus pictus* silver nanoparticles (MECPAgNPs). UV-Visible spectroscopy analysis of nanoparticles showed the broadening of the peak indicated the particles are poly dispersed. The surface Plasmon band in the silver nanoparticles in the solution remains close to 420nm. Throughout the reaction period indicating the particles are dispersed in the aqueous solution of silver nitrate, with no evidence for aggregation. The average particle size (average) was found to be 132.6nm, its polydispersity index was 0.248 and zeta values were measured and it was found to be -25.1mV with the peak area of 100% intensity. This indicates that the formed silver nanoparticle is stable. A SEM images showed that the silver nanoparticles formed were spherical in shape, with an average size of around 100nm. SEM showed uniformly distributed silver nanoparticles on the surface of the cells was observed. Conclusion: The Biomedical application of silver nanoparticles can be rendered more effective by using biologically synthesized nanoparticles that are found to be exceptionally stable, and also minimize toxicity and cost.

Ali Alkaladi. et al., (2014) In the present study, zinc oxide and silver nanoparticles were evaluated for their antidiabetic activity. Fifty male albino rats with weight 120 ± 20 and age 6 months were used. Animals were grouped as follows: control; did not receive any type of treatment, diabetic; received a single intraperitoneal dose of streptozotocin (100 mg/kg), diabetic + zinc oxide nanoparticles (ZnONPs), received single daily oral dose of 10 mg/kg ZnONPs in suspension, diabetic + silver nanoparticles (SNPs); received a single daily oral dose of SNP of 10 mg/kg in suspension and diabetic + insulin; received a single subcutaneous dose of 0.6 units/50 g body weight. Zinc oxide and silver nanoparticles induce a significant reduced blood glucose, higher serum insulin, higher glucokinase activity higher expression level of insulin, insulin receptor, GLUT-2 and glucokinase genes in diabetic rats treated with zinc oxide, silver nanoparticles and insulin. In conclusion, zinc oxide and silver nanoparticles act as potent antidiabetic agents.

Rastogi Archit. et al., (2013): in present study, In vitro analysis of the anti-diabetic effect of aqueous extracts from the medicinal plants *Hemidesmus indicus*, *Ficus bengalensis*, *Pterocarpus marsupium* Roxb. An aqueous extract of each of the plants were prepared by soxhlation at 60°C. 1mL of the extract was then placed in a bio-membrane along with a glucose solution (0.22 mM in 0.15 M NaCl) and the bio-membrane was immersed in a beaker containing 40mL of 0.15 M NaCl + 10mL of distilled water. The control contained 1mL of 0.15 M NaCl containing 22 mM glucose and 1mL of distilled water. Half-hourly observations of the concentration of glucose in mg/dL in the beaker were done. A significant hindrance to the flow of glucose across the bio-membrane results was seen. The medicinal plants were found to show potent inhibition of glucose diffusion across the membrane. They concluded that, these results indicate that these plants could quite possibly show hypoglycemic activity due to this inhibitory action. However, further studies at a molecular level are essential to confirm this mechanism.

A. Maruthupandian and V.R. Mohan, (2011) In present study, the ethanol extracts of *Pterocarpus marsupium* wood, bark and combined extract of wood and bark were investigated for its antidiabetic effect in Wistar albino rats. Diabetes was induced in Albino rats by administration of alloxan monohydrate (150mg/kg, i.p). The ethanol extracts of *Pterocarpus marsupium* wood and bark at a dose of 150mg/kg of body weight respectively and combined

extracts of wood and bark at a dose of 150 +150mg/kg of body weight were administered at single dose per day to diabetes induced rats for a period of 14 days. The ethanol extracts of *Pterocarpus marsupium* resulted significant reductions of blood glucose($p<0.001$). lipid parameters except HDL-C, serum enzymes and significantly increased HDL-C and antioxidant enzymes. The extracts also caused significant increase in plasma insulin($p<0.01$) in the diabetic rats. From the above results it was concluded that ethanol extracts of *Pterocarpus marsupium* possesses significant antidiabetic, antihyperlipidemic and antioxidant effects in alloxan induced diabetic rats.

Aninda Kumar Nath. et al., (2011) The in vitro study of protein binding of metformin hydrochloride and its 1:1 mixture with levofloxacin has been conducted by equilibrium dialysis method at physiological pH and temperature. In this study, the number of binding sites and affinity constants of metformin hydrochloride and its 1:1 mixture with levofloxacin were calculated by Scatchard method. The Scatchard plots revealed that the interaction of metformin hydrochloride with levofloxacin lowered the affinity and decreased the percentage of binding of metformin hydrochloride in the mixture to bovine serum albumin (BSA). Thus, the interaction of metformin hydrochloride with levofloxacin can increase the free drug concentration of metformin hydrochloride in the blood plasma. This may change the pharmacokinetic and pharmacodynamic properties of metformin hydrochloride.

Mohammad Mohiuddin. et al., (2009) The in vitro study of protein binding of caffeine and its 1:1 mixture with gliclazide and metformin HCl has been conducted by equilibrium dialysis method performing measurement by direct spectrophotometric method at temperature $37\pm 0.5^{\circ}\text{C}$ and at pH 7.4. In this study, number of binding sites and affinity constants of caffeine and its 1:1 mixture with gliclazide and metformin HCl were calculated by scatchard method. Scatchard plots were prepared to reveal the number of binding sites and the affinity for protein binding. It has been found that both gliclazide and metformin HCl cause lowering the affinity and percentage of binding of the drugs in the mixture to bovine serum albumin. Thus, the interaction of caffeine with gliclazide and metformin HCl can increase the free drug concentration of caffeine in blood plasma. This may change the pharmacokinetic and pharmacodynamic properties of the drug.

SM-Mahbubul-Alam.et al., (2004) The study of drug-drug interaction between Ciprofloxacin and Captopril at binding sites of Bovine Serum Albumin (BSA) was studied by equilibrium dialysis (ED) method. During concurrent administration of these drugs, Captopril (an ACE inhibitor) and Ciprofloxacin HCl (a broad-spectrum antibacterial drug) have been found to increase the free concentration of Captopril due to Ciprofloxacin causing reduced binding to BSA. The increment in free concentration of Captopril was more prominent in presence of site-II specific probe (diazepam) than in absence of same probe. When no probe and no Ciprofloxacin was added the free concentration of Captopril was only 5% whereas this release was 23% when Ciprofloxacin was added with an increasing concentration from 1×10^{-5} to 12×10^{-5} M. The increment of free concentration of Captopril was from 9.5% to 43% in presence of site-II specific probe upon the addition of Ciprofloxacin with an increasing concentration from 0×10^{-5} to 12×10^{-5} M. During concurrent administration site-to-site displacement has taken place.

Mats A.L. Eriksson. et al., (2004) The plasma protein binding of three model compounds was investigated using a variant of equilibrium dialysis, denoted comparative equilibrium dialysis (CED), and the results were compared with those obtained with ultrafiltration (UF). For the first model compound, having an unbound fraction (f_u) of about 0.05% in human plasma, the time to reach equilibrium was too long (≥ 40 h) to make the CED technique feasible in practice. For the second model compound, the weaker bound drug NAD-299 (with an unbound fraction of about 2% in human plasma), the CED equilibration times were considerably shortened (≤ 16 h), and the technique was applied to plasma from three different species. Large discrepancies between the CED and UF results were seen, CED always giving rise to much lower C_{tot} differences than expected from the UF results. It is suspected that this discrepancy was due to equilibration between the dialysis chambers of all plasma components with a molecular weight less than the cut-off of the membrane. This equilibration causes altered binding properties compared to the initial plasma. When performing ultrafiltration on plasma where drug was added to untreated plasma or added to blank plasma that was equilibrated against plasma from the same or from another species, the change of binding properties was confirmed. To ensure that the results were not specific for NAD-299, a third model compound, tolterodine, was also included. The same trends as for NAD-299 were seen.

AIM AND OBJECTIVE

AIM

The aim of the present research work was to formulate and evaluate the antidiabetic effect of green synthesized silver nanoparticles from aqueous extract of *Pterocarpus marsupium* and to study its pharmacokinetic interactions with antidiabetic drug.

OBJECTIVE

Diabetes mellitus is a major health problem worldwide. Diabetes mellitus is a metabolic disorder in which the body does not produce enough respond normally to insulin, causing blood sugar levels to be abnormal which leads to the serious damage to blood vessels, heart, kidney, eyes and nerves. Increased blood sugar level gives rise to many complications like diabetes retinopathy, depression, hypertension, hyperlipidemia, Alzheimer's disease, hearing impairment etc... Adults with diabetes have increased risk of heart attack and strokes. In pregnancy, increases the risk of fetal death and other severe complications.

Numerous medicinal plants are mentioned in India and other ancient systems of the world for the treatment of diabetes and some of them have been experimentally evaluated. Since the chemically synthesized drugs have unsatisfactory adverse effects, the World Health Organization (WHO) has advised the usage of traditional plant for the management of diabetes. The medicinal plant metabolites have a lesser side effect and have the good hypoglycemic potential.

The bark and heartwood of *Pterocarpus marsupium* is very effective in hypoglycemic activity and it was very popular in traditional medicine.

The metal NPs are being researched extensively for use in high technology applications such as sensory probes, electric conductors, therapeutic agents, drug delivery in biomedical applications. Among the wide range of metal nanoparticles, silver nanoparticles were the most popular, due to their unique physical, chemical, and biological properties. Nowadays, the nanoparticles synthesized by the green method is getting popular.

An attempt has been made to formulate silver nanoparticles with the herbal drug and to evaluate its anti-diabetic activity. Also, this research work focuses on green chemistry which is an eco-

friendly & environmentally accepted procedure. Herbal substances act as chelating agent for biosynthesized nanoparticles and because of such property the drug gets easily absorbed in the body and they target drug delivery and easily eliminated out of body.

Hence the objective of present study is to investigate antidiabetic effect of green synthesized silver nanoparticles from aqueous extract of *Pterocarpus marsupium* and to study its pharmacokinetic interactions with antidiabetic drug.

PLAN OF WORK

PART – A

PREPARATION AND CHARACTERIZATION OF *Pterocarpus marsupium* SILVER NANOPARTICLE

STEP 1

Review of literature.

STEP 2

Collection & authentication of the bark of *Pterocarpus marsupium*.

STEP 4

Aqueous extraction of the bark of *Pterocarpus marsupium*.

STEP 5

Processing of the material into silver nanoparticles.

STEP 7

Characterization of *Pterocarpus marsupium* silver nanoparticles.

STEP 8

Invitro antidiabetic activity.

PART – B

**PHARMACOKINETIC INTERACTION STUDY OF GREEN SYNTHESIZED
NANOPARTICLE AND ANTIDIABETIC DRUGS**

STEP 1

Analytical method – development of calibration curve using UV spectroscopy

STEP 2

Protein binding studies by using equilibrium dialysis method

STEP 3

Green synthesized nanoparticle and drug interaction

- ✚ Interaction study of *Pterocarpus marsupium* silver nanoparticle with Metformin
- ✚ Interaction study of *Pterocarpus marsupium* silver nanoparticle with Glimepiride

STEP 4

Evaluation of protein binding studies and silver nanoparticle - drug interaction

- ✚ To find out no of binding sites and intrinsic association constant

STEP 5

Tabulation and compilation of results obtained.

MATERIALS AND EQUIPMENT

S. No	MATERIALS USED	SOURCE
1	Silver Nitrate	Qualigens fine chemicals, Mumbai
2	<i>Pterocarpus marsupium</i> Roxb Bark	Natural Source., Thalassery
3	α - amylase enzyme	Himedia, Mumbai
4	Drugs	Microlabs
5	Bovine Serum Albumin	S D fine chemicals
6	Di sodium hydrogen phosphate	S D fine chemicals
7	Sodium chloride	S D fine chemicals
8	Potassium dihydrogen phosphate	S D fine chemicals
9	Methanol	Qualigens Fine chemicals

S. No	EQUIPMENT	SOURCE
1	Magnetic Stirrer	REMI – 2MLH
2	Probe sonicator	LAB SONICATOR
3	Bath sonicator	LEELA SONIC
4	Centrifuge	REMI
5	UV Spectrophotometer	JASCO V-530
6	FT-IR Spectrometer	FTIR JASCO – 4100
7	pH meter	pH TESTER 1,2 (EUTECH)
8	Zeta Sizer	MALVERN
9	SEM	Hitachi X650, Tokyo, Japan
10	Dialysis membrane 50	Himedia, Mumbai
11	pH Tester	Eutech instrument

PLANT PROFILE

SCIENTIFIC CLASSIFICATION

Family	: Fabaceae
Domain	: Eukaryota
Kingdom	: Plantae
Subkingdom	: Viridaeplantae
Phylum	: Magnoliophyta
Subphylum	: Euphyllophytina
Class	: Magnoliopsida
Subclass	: Rosidae
Super order	: Fabanae
Order	: Fabales
Genus	: Pterocarpus
Species	: Marsupium

VERNACULAR NAMES

Urdu	: Bijasar
Sanskrit	: Bijaka, Pitasara, Asana, Bijasara
English	: Indian Kino
Gujrati	: Biyo
Hindi	: Vijayasara, Bija
Kannada	: Bijasara, Asana
Malayalam	: Venga

Tamil : Vengai

Telugu : Yegi, Vegisa

ORIGIN, DISTRIBUTION AND HABITAT

P. marsupium is growing in defoliate and evergreen jungles of Southern, Western and Central regions of India. It is present generally in Gujarat, Bihar, West Bengal, Orissa, Uttar Pradesh, Western Ghats, Kerala, Karnataka, and Madhya Pradesh, of prominent India, Srilanka and Nepal. It develops generally on hills or undulating lands or rocky grounds up to a height of 150 to 1100 meter. The usual rainfall of its habitat ranges starting from 750 to 2000 mm and even more in Southern India. The maximum temperature was ranged from 35°C to 48°C and minimum temperature was ranged from 0°C to 18°C. It can increase in huge variety of soils and geographical situations like quartzite, shale, conglomerates, lateritic, gneiss and sandstone. It favors well-drained sandy and sedimentary soil to loamy soil. The species is adequate light loving and the young seedlings are frost-tender. (Mohd Saidur Rahman et al., 2018)

PLANT DESCRIPTION

Description: It is a deciduous tree about 90 feet or more high.

Bark: stem bark is grey brown. The heartwood is golden yellowish-brown with darker streaks and occurs as uneven pieces of erratic sizes and thickness.

Leaves: 3-5 inches long have 5-7 leaflets long, margin wavy and obtuse. The petioles are round, smooth and waved from leaflet, 5 or 6 inches long and no stipules.

Flowers: 1.5 c.m. long, very numerous, white, with a small tinge of yellow, stamens are 10. United near the base but soon dividing into two parcels of 5 each; anthers are globose and 2 lobed.

TRADITIONAL USES

P. marsupium has been traditionally used in the treatment of leukoderma, elephantiasis, diarrhea, cough, discoloration of hair and rectalgia. It is nontoxic and useful in jaundice, fever, wounds, diabetes, stomachache and ulcer. (Mohd Saidur Rahman et al., 2018)

ETHNOBOTANICAL USES

Medicinal use of various parts of *P. marsupium* Various parts of the *P. marsupium* tree have been used as traditional ayurvedic medicine in India from time immemorial. The medicinal utilities have been described, especially for leaf, fruit and bark. The bark is used for the treatment of stomachache, cholera, dysentery, urinary complaints, tongue diseases and toothache. The gum exudes 'kino', derived from this tree, is used as an astringent. The gum is bitter with a bad taste. However, it is antipyretic, anthelmintic and tonic to liver, useful in all diseases of body and styptic vulnerant and good for griping and biliousness, ophthalmiya, boils and urinary discharges. The flowers are bitter, improve the appetite and cause flatulence. **(Yogesh Badkhane et al., 2010)**

P. marsupium has a long history of use in India as a treatment for diabetes. Various parts of Indian kino tree are used to treat antidiabetic such as seeds, roots, heartwood, bark, leaves etc... The bark and heartwood of *pterocarpus marsupium* is very effective in hypoglycemic activity and it was very popular in traditional medicine. Some studies for antidiabetic activity have conducted and reported the mechanism of action such as β -cell generation in the pancreas, insulin release, insulin like activities (increase in glucose uptake, increase in glycogen synthesis, increase in activity of oxidase enzyme) inhibition of amylase and glucosidase, increased expression of glucose transporter etc... Many studies were focused on pterostilbene and (-) epicatechin which were responsible for the antidiabetic effect of *Pterocarpus marsupium* heart wood and bark. **(Bavya.C and Bagyalakshmi. J., 2021)**

PHYTOCONSTITUENTS

P. marsupium as a very rich source of flavonoids and polyphenolic compounds. All the active phytoconstituents of *P. marsupium* were thermostable. It contains pterostilbene (45%), alkaloids (0.4%), tannins (5%) and protein. The primary phytoconstituents were liquiritigenin, isoliquiritigenin, pterostilbene, pterosupin, epicatechin, catechin, kinotannic acid, kinoin, kino red, β -eudesmol, carsupin, marsupial, marsupinol, pentosan, p-hydroxy benzaldehyde. **(Deepti Katiyar et al., 2016)**

Reported activities

Antidiabetic, Antioxidant, Antihyperlipidemic, Antibacterial, Hepatoprotective activity, Anti-inflammatory, Antidiarrheal, Antiulcer, Cardiotonic activity, Nootropic activity, Antiglycation, Anticataract, Aphrodisiac activity, Anthelmintic activity, Analgesic activity



FIG.1 *Pterocarpus marsupium* Roxb

DRUG PROFILE

METFORMIN

Metformin is considered an antihyperglycemic drug because it lowers blood glucose concentrations in type II diabetes without causing hypoglycemia. Metformin is commonly described as an *insulin sensitizer* leading to a decrease in insulin resistance and a clinically significant reduction of plasma fasting insulin levels.

IUPAC Name

1-carbamimidamido-N, N-dimethylmethanimidamide

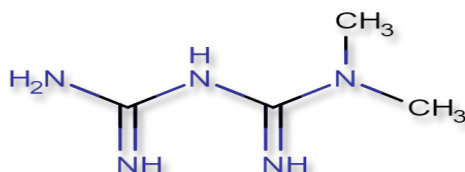
Chemical Formula

C₄H₁₁N₅

Molecular Weight

Average: 129.1636

Structure



Mechanism of action

Metformin decreases blood glucose levels by decreasing hepatic glucose production (gluconeogenesis), decreasing the intestinal absorption of glucose, and increasing insulin sensitivity by increasing peripheral glucose uptake and utilization. metformin inhibits mitochondrial complex I activity, and it has since been generally postulated that its potent antidiabetic effects occur through this mechanism.

Experimental Properties

PROPERTY	VALUE
melting point (°C)	223-226 °C
water solubility	2g of metformin hydrochloride is soluble in 10mL of water
logP	-2.6
pKa	12.4

Pharmacokinetic properties

Bioavailability	50 – 60 %
Protein binding	Minimal
Elimination half-life	4 – 8.7 hours
Excretion	Urine (90%)

GLIMEPIRIDE

Glimepiride is used for the management of type 2 diabetes mellitus (T2DM) to improve glycemic control. Glimepiride lowers blood sugar by causing the pancreas to produce insulin (a natural substance that is needed to break down sugar in the body) and helping the body use insulin efficiently.

IUPAC Name

3-ethyl-4-methyl-2-oxo-N-(2-{4-[[[(1r,4r)-4-methylcyclohexyl] carbamoyl] amino) sulfonyl] phenyl} ethyl)-2,5-dihydro-1H-pyrrole-1-carboxamide

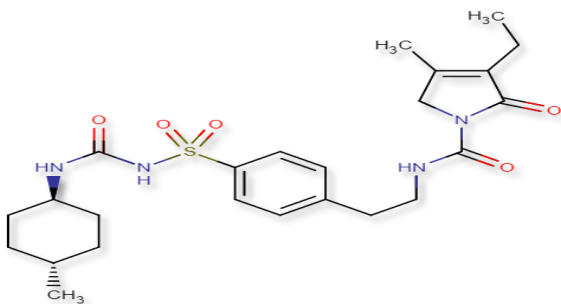
Chemical Formula

C₂₄H₃₄N₄O₅S

Molecular Weight

Average: 490.62

Structure



Mechanism of action

The primary mechanism of action of glimepiride in lowering blood glucose appears to be dependent on stimulating the release of insulin from functioning pancreatic beta cells. Glimepiride works by stimulating the secretion of insulin granules from pancreatic islet beta cells by blocking ATP-sensitive potassium channels (K_{ATP} channels) and causing depolarization of the beta cells.

Experimental properties

PROPERTY	VALUE
melting point ($^{\circ}\text{C}$)	207
water solubility	Partly miscible

Pharmacokinetic data

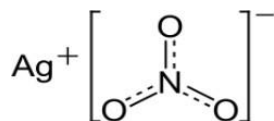
Bioavailability	100%
Protein binding	>99.5%
Elimination half-life	5–8 hours
Excretion	Urine (~60%), feces (~40%)

EXCIPIENT PROFILE

SILVER NITRATE

IUPAC name	: Silver nitrate
Molecular Formula	: Ag NO ₃
Molecular Weight	: 169.872
Color	: White
Odour	: Odour less solid
Density	: 4.35 g/cm ³
Melting point	: 209.7 °C
Boiling point	: 440 °C pH: 5.4-6.4 (100g/l, H ₂ O, 20°C)
Storage temperature	: 2- 8°C

Structure of silver nitrate



Solubility	: Soluble in Water, Acetone, Ammonia, Ether, Glycerol
Uses	: Anti-Infective Agents, Disinfection, destruction of cutaneous warts, Precursor to other silver compounds, Halide abstraction, Organic synthesis

Safety

As an oxidant, silver nitrate should be properly stored away from organic compounds. Despite its common usage in extremely low concentrations to prevent gonorrhoea and control nose bleeds, silver nitrate is still very much toxic and corrosive. Brief exposure will not produce any immediate side effects other than the purple, brown or black stains on the skin, long term exposure may cause eye damage. Silver nitrate is known to be a skin and eye irritant (https://wiki/Silver_nitrate).

EXPERIMENTAL METHODOLOGY

PART – A

SAMPLE COLLECTION

Pterocarpus marsupium bark were collected from Thalasseri, Kerala.

AUTHENTICATION

The plant specimen was identified and authenticated by Botanical survey of India, Southern regional Centre, Coimbatore.

DRYING AND PULVERIZING

The bark and wood were collected and shade dried. It was grounded into fine coarse powder with electronic blender and passed and kept in a well closed container in a dry place.

PREPARATION OF AQUEOUS EXTRACT OF *Pterocarpus marsupium* ROXB

50g of the bark powder of *Pterocarpus marsupium* was stirred with 500 mL of deionized water and kept at 65 °C for 30mins. Then the extracts were filtered by using Whatman No. 1 filter paper after cooling to room temperature. The extract was stored at 4 °C for future use. (Chen yu *et al.*, 2018)

PHYTOCHEMICAL SCREENING

PREPARATION OF TEST SOLUTION

The filtered aqueous extract of bark of *Pterocarpus marsupium* Roxb was used as a test solution for preliminary screening of phytochemical constituent.

PRELIMINARY QUALITATIVE PHYTOCHEMICAL ANALYSIS

Phytochemical screening

Chemical tests were carried out using the extract of *Pterocarpus marsupium* for the presence of phytochemical constituents.

Tests for tannins and phenolics

- **Ferric chloride test:** To the solution of the extract, the addition of 3-4 drops of 0.1% v/v Ferric chloride to the filtered sample changed the colour to brownish green or blue coloration, it indicates presences of phenols or the tannins.
- **Lead acetate test:** To the solution of the extract, 0.5 ml of 1% lead acetate solution was added the formation of precipitate indicates presence of tannins and phenolic compounds.

Tests for saponins

- **Foam test:** About 1ml of the extract was diluted with 20ml of distilled water and shaken vigorously for 15 minutes. Development of stable foam suggests the presence of saponins.

Test for flavonoids

- **Alkaline reagent test:** The plant extract is treated with 2-3 drops of sodium hydroxide solution. Acute yellow color formation, that indicates presence of the flavonoids, by the addition of some drops of sulphuric acid that changed to colorless.
- **Shinoda test:** The extract was added to pinch of magnesium turnings and 1-2 drops of concentrated hydrochloric acid were added. formation of pin color indicates the presence of flavonoids.
- **Lead acetate test:** The plant extract was taken and few drops of 10% lead acetate solution was added. Appearance of yellow color precipitates indicates the presence of flavonoids.

Tests for alkaloids

- In 1% v/v HCL the plant extract is mixed, warmed and filtered. Now this filtered is used for following test.
- **Dragendroff's test:** To the filtrate, dragendroff's reagent (potassium bismuth iodide solution) was added and an orange brown precipitate indicates the presence of alkaloids.
- **Mayers test:** With Mayer's reagent (Mercuric chloride + Potassium iodide in water) the filtrate is treated. The presence of alkaloids specifies by the formation of yellow-coloured precipitates.

Test for Starch

- **Iodine test:** To the aqueous extract add weak aqueous Iodine solution. A blue – black colour results if starch is present.

Test for Proteins

- **Warming Test:** Heat the test solution in a boiling water bath. (C. K. Kokate *et.al*)
- **Biuret test:** To the 0.5mg of extract equal volume of 40% NAOH solution and 2 drops of 1% copper sulphate solution was added. The presence of violet colour indicates the presence of protein.
- **Ninhydrin test:** About 0.5mg of extract was taken and 2 drops of freshly prepared 0.2% ninhydrin reagent were added and heated. The appearance of pink or purple colour indicates the presence of proteins.

Test for Steroids

- **Salkowski Test:** With chloroform and filtered the plant extract was mixed. 5-6 drops of conc. Sulphuric acid are treated with filtrate and shaken gently and allowed to stand carefully. The presence of triterpenes (phytosterol) indicates by the appearance of golden yellow colour. (Sheraz Khalid *et. al.*, 2018)

PREFORMULATION STUDY:

SOLUBILITY TEST

About 1 mg of *Pterocarpus marsupium* Roxb. bark extract powder was taken in a test tube and solubility in ethanol, water, chloroform and diethyl ether, dimethyl sulphoxide were checked.

UV- VISIBLE SPECTRAL ANALYSIS OF *Pterocarpus marsupium* Roxb BARK EXTRACT

1ml of *Pterocarpus marsupium* Roxb. bark extract was taken in a 10 ml standard flask and diluted with distilled water. then Uv visible spectra were taken in the range of 200- 400 nm using phosphate buffer at pH 7.4 as blank (I. Johnson. H. Joy Prabu, 2015)

PREPARATION OF CALIBRATION CURVE OF *Pterocarpus marsupium* ROXB BARK EXTRACT

Twenty-five milligrams of crude extract were dissolved in phosphate buffer with a pH 7.4 and further diluted to 50mL of solvent, in volumetric flask to get a concentration of 500 µg/mL. This was treated as stock solution. Various aliquots of stock solution were diluted further to get different concentrations. The resultant solutions were scanned for λ max in the range of 200-400nm using UV- spectrometer. (Xi-Feng Zhang *et al.*, 2016)

FTIR SPECTROSCOPY OF *Pterocarpus marsupium* ROXB BARK

50 mg each of dried *Pterocarpus marsupium* Roxb bark and wood were mixed with 100 mg of spectral grade KBr and pressed into disc under hydraulic pressure. Then FTIR spectra were recorded in the 4000- 400cm⁻¹ range.

FTIR SPECTROSCOPY OF SILVER NITRATE

100mg of silver nitrate was mixed with 100 mg of spectral grade KBr and pressed into disc under hydraulic pressure. Then FTIR spectra were recorded in the 4000- 400cm⁻¹ range (Holler, Skoog, Crouch).

GREEN SYNTHESIS OF SILVER NANOPARTICLES

Preparation of Stock Solution

1 mg of aqueous extract was weighed and diluted to 10 ml with distilled water.

Preparation of 1mM silver nitrate aqueous solution

0.017g of silver nitrate was dissolved in 100 ml of distilled water to prepare 1mM solution of silver nitrate and stored in amber colored bottle until further use

Synthesis of silver nanoparticles

An aliquot (1ml, 2ml,3ml, 4ml, 5ml) of aqueous plant extract sample was separately added to 10ml of 1mM aqueous AgNO₃. To drive nanoparticle formation the reaction mixtures were kept in magnetic stirrer with constant stirring at 120 rpm. Color change of the reaction mixtures were monitored to determine silver nanoparticle formation which is indicated by a colloidal brown color. (Shakeel Ahmed *et al.*, 2016)

Separation of AgNPs:

Centrifuged technique was used to separate the nanoparticles from the solution (AgNO₃ + plant extract). The reaction mixture (10ml AgNO₃ + 5ml leaf extract sample) was split into two equal parts and transferred to pre-weighed sterile 15ml centrifuge tubes (United Scientific, South Africa). The preparations were then centrifuged at 4000rpm for 20 mins. (Eppendorf centrifuge 5810 R, Germany). The centrifuged supernatant liquid was collected and then centrifuged twice at 10,000 rpm for 30 min. The suspended pellet was purified using ethanol. The purified pellets were then dried and the powder was taken which is used for further characterization. (I. Johnson. H. Joy Prabu, 2015)

CHARACTERIZATION OF SYNTHESIZED *Pterocarpus marsupium* ROXB SILVER NANOPARTICLE

Characterization of *Pterocarpus marsupium* Roxb. silver nanoparticles is important in order to evaluate the functional aspects of the synthesized particles. Characterization is performed using a variety of analytical techniques, including UV-vis spectroscopy, Fourier transform infrared spectroscopy (FTIR), scanning electron microscopy (SEM), particle size measurement, stability from zeta potential and drug entrapment efficacy for elemental analysis.

Visual Examination

The primary confirmation of the synthesized *Pterocarpus marsupium* silver nanoparticles is done by visual basis. The color change of reaction mixture (silver nitrate solution and leaf extract) with respect to time is observed.

UV-visible spectroscopy

UV – Visible spectroscopy analysis characterizes the formulation and completion of *Pterocarpus marsupium* silver nanoparticles. UV- Visible spectroscopy is a very useful and reliable technique for the primary characterization of synthesized nanoparticles which is also used to monitor the synthesis and stability of AgNPs. The reduction of pure silver ions was observed by measuring the UV–Visible spectrum of the reaction medium from the wavelength 400- 800 nm by using distilled water as blank. Periodic sampling at time intervals of 30mins, 60 mins, 90mins, 120 mins was carried out. (Njagi et al., 2011)

Fourier Transform Infrared (FTIR) Spectroscopy

FTIR is a suitable, valuable, non-invasive, cost effective, and simple technique to identify the role of biological molecules in the reduction of silver nitrate to silver. Dried samples of silver nanoparticles of about 100mg were mixed with 100mg of spectral grade KBr and pressed into discs under hydraulic pressure. The FTIR spectrum was recorded in the range of 4,000–400 cm⁻¹.

Determination of Entrapment Efficiency

The entrapment efficiency of nanoparticles was determined by adding 10 ml of phosphate buffer of pH 7.4 and sonicated in a bath sonicator and filtered. 1 ml of filtrate is made up to 10 ml with phosphate buffer and was assayed using UV visible spectrophotometer at 429nm using pH 7.4 phosphate buffer as blank. The amount of drug entrapped was determined by the formula. (Tenderwealth clement Jackson et al.,2019)

$$\text{Drug entrapment (\%)} = \frac{\text{weight of drug in nanoparticles}}{\text{weight of nanoparticles}} \times 100$$

Scanning Electron Microscopy

SEM is a surface imaging method, fully capable of resolving different particle sizes, size distributions, nanomaterial shapes, and the surface morphology of the synthesized particles at the micro and nanoscales. SEM analysis of *Pterocarpus marsupium* Roxb. Silver nanoparticles were performed to evaluate the surface morphology of nanoparticles. silver nanoparticles were prepared and dried well to remove the moisture content and images were taken. (Xi-feng zhang, et al., 2016)

Determination of Particle Size

The average mean diameter and size distribution of silver nanoparticles was determined by Dynamic Light Scattering method using Malvern zeta sizer at 25°C. The dried silver nanoparticles were dispersed in water to obtain proper light scattering intensity of silver nanoparticles. (Khot Uttamkumar vithal, 2013)

Determination of Zeta potential

Zeta potential is a measure of surface charge. The surface charge (electrophoretic mobility) of nanoparticles can be determined by using Zeta sizer (Malvern Instrument) having zeta cells, polycarbonate cell with gold plated electrodes and using water as medium for sample Preparation. It is essential for the characterization of stability of the silver nanoparticles. (Khot Uttamkumar vithal, 2013)

***In-vitro* methods**

α - Amylase inhibitory effect

pancreatic alpha-amylase is a one of the important enzymes, that act as a catalysis in the reaction which involves the hydrolysis of the alpha-1,4 glycosidic linkages of the starch, amylopectin, amylose, glycogen, and numerous maltodextrins and is responsible for starch digestion. The other important enzyme is alpha-glucosidase or maltase which catalyzes the final step of the digestive process of carbohydrates mainly starch by acting upon 1,4-alpha bonds and producing glucose as the final product. The large molecules like starch cannot cross the blood brain barrier as glucose has to reach the brain thus; to overcome this problem alpha-amylase cleaves the large starch molecules into smaller fragments of sugars in order to cross the blood brain barrier. If there will be excess conversion of starch to sugars, it will increase the sugar level in blood, then the role of insulin will come into action by ordering cells to metabolize the excess sugar moieties and store as energy sources i. e. glycogen. This cycle is endlessly happening in a healthy person. But in some cases, due to excess activity of amylase enzyme and insulin deficiency or resistance to insulin, level of blood glucose arises which might result in hyperglycemia. To control hyperglycemia studies on inhibition of amylase enzyme activity is being studied. **(Prashant Agarwall and Ritika Gupta, 2016)**

REAGENT PREPARATION

1. Reagent A (Sodium phosphate buffer)

Reagent A was prepared by dissolving 20 mM sodium phosphate in 6.7 mM sodium chloride using 100 ml of distilled water. The pH was adjusted to 6.9 at 20°C with 1M sodium hydroxide.

2. Reagent B (1% w/v soluble Starch solution)

Reagent B was prepared by dissolving 1% w/v of potato starch in 25 ml of reagent A. The solubilization is facilitated by heating the starch solution in a glass beaker directly on a heating stir plate, with constant stirring for 15 minutes. The solution was cooled to room temperature.

3. Reagent C (Sodium potassium tartrate solution)

Reagent C was prepared by dissolving 12 g sodium potassium tartrate tetrahydrate in 8ml of 2M sodium hydroxide solution.

4. Reagent D

Reagent D was prepared by dissolving 96mM 3,5-dinitro salicylic acid in 20ml of distilled water.

5. Reagent E (Color reagent solution)

Reagent E was prepared by adding reagent C to reagent D slowly with stirring. The solution was diluted to 40 ml with distilled water. The reagent was stored in an amber colored bottle at room temperature.

6. Reagent F

Reagent F was prepared by dissolving 1unit/ml of α -amylase in cold distilled water. The enzyme solution was prepared immediately before use.

PROCEDURE:

About 1.0 ml of reagent B (starch solution) was mixed with 1.0 ml of increasing concentration of drug (2.5 - 160 μ g/ml). To this 1ml of reagent F (enzyme solution) was added and left to react for 3 minutes at 25°C. After this 1.0 ml of calorimetric reagent E was added. The contents were heated for 10 to 15 minutes on a boiling water bath. The generation of maltose was quantified by the reduction of 3,5-nitro salicylic acid to 3-amino 5-nitro salicylic acid. This reaction, corresponding to color change from orange to red was measured at 540 nm against the reagent blank. Acarbose was used as the standard drug. The percentage of inhibition was determined by using the following formula:

$$\text{Inhibition activity\%} = \frac{\text{Abs(control)} - \text{Abs(extract)}}{\text{Abs(control)}} \times 100$$

Acarbose is an antidiabetic drug used to treat type 2 diabetes mellitus. The positive control used for this assay is **acarbose** which works by slowing the action of certain chemicals that break down food to release glucose into your blood. Slowing food digestion helps keep blood glucose from rising very high to after meals. (Preethi Johnson, et al., 2018)

INVITRO DRUG RELEASE STUDY

The antidiabetic drug *Pterocarpus marsupium* loaded silver nanoparticles (300 mg) were suspended in 10 mL of phosphate-buffered saline (PBS) in a dialysis bag. The dialysis bag was sealed and then slowly shaken in 90 mL of PBS at 37°C in a 250-mL beaker and kept in a magnetic stirrer at an rpm 170. Aliquots of the solution outside the

dialysis membrane (2 mL) were replaced with 2 mL of PBS at various times intervals and tested at 427 nm by UV Spectrophotometer. The change of the concentrations of drug with respect to different time intervals were obtained from curves of the absorbance A versus concentration C of *Pterocarpus marsupium* silver nanoparticles in PBS based on Lambert-Beer law. (Guo-Ping Yan *et al.*, 2010).

Drug release mechanism

In order to understand the mechanism of drug release, in vitro drug release data were treated to kinetic models such as zero order (Time vs Cumulative percentage drug release), first order (Time vs log cumulative percentage) and Higuchi model (Square root of time vs Cumulative percentage release) and Korsmeyer-Peppas model (Log time vs log cumulative percentage)

Zero order:

Zero-order release kinetics describe systems where the drug release rate is constant over a period of time.

$$Q_t = Q_0 + K_0 t$$

where Q_t is the amount of drug dissolved in time t , Q_0 is the initial amount of drug in the solution (most times, $Q_0 = 0$) and K_0 is the zero-order release constant expressed in units of concentration, and t is the time at which the drug release is calculated or measured

First order:

This kinetics describes concentration dependent drug release from the formulation.

$$\log C = \log C_0 - Kt / 2.303$$

where, C_0 is the initial concentration of drug, k is the first order rate constant, and t is the time. The data obtained are plotted as log cumulative percentage of drug remaining vs. time. (Suvakanta Dash, *et al.*, 2010)

Higuchi Model:

This model helps to study the release mechanism of water-soluble and less water-soluble drugs incorporated in semi-solid and solid matrixes.

The mathematical expression for drug release is,

$$Q = \sqrt{D (2C_0 - C_s) C_s \cdot t}$$

Whereas,

Q= Cumulative % of drug released in time "t" per unit area, C₀ =Initial drug concentration, C_s= Drug solubility in the matrix media, D= Diffusion coefficient

Assuming that diffusion coefficient and other parameters remain constant during release, the above equation reduces to

$$Q = K_H \cdot t^{1/2}$$

where, K_H is the Higuchi dissolution constant

Thus, for diffusion-controlled release mechanism, a plot of cumulative % of drug released vs. square root of time should be linear. The linearity of the plots can be checked by carrying out linear regression analysis and determination of regression coefficient of the plot. (Radha Kant Gouda, et al., 2017)

Korsmeyer-Peppas's model

To verify the fact that whether the diffusion follows Ficks law or not, the drug release data can also be plotted against Log time according to Peppas equation.

The drug release can be expressed as,

$$Q = K t^n$$

Taking log on both sides of equation,

$$\text{Log } Q = \text{Log } K + n \text{ Log } t$$

Where Q is the cumulative % drug release t is

the time

n is the slope of linear plot of Log Q Vs Log t

DIFFUSION MECHANISM & DIFFUSION EXPONENT (n)

DIFFUSION EXPONENT (n)	DIFFUSION MECHANISM
<0.5 or 0.5	Fickian diffusion
0.5 < n < 1.0	Non Fickian diffusion
1.0	Case 2 transport
>1.0	Super case 2 transport

PART – B

**PHARMACOKINETIC INTERACTION STUDY OF GREEN SYNTHESIZED
NANOPARTICLES AND ANTIDIABETIC DRUGS**

I.1.ESTIMATION OF METFORMIN USING UV SPECTROPHOTOMETRY

a. Preparation of stock solution

10mg of metformin in 100ml of volumetric flask dissolved in 50ml of distilled water and make up to 100ml of distilled water to obtain stock solution of 100 µg/ml.

b. Preparation of calibration curve

Dilutions from 2µg/ml – 10 µg/ml are obeyed by beer-lamberts law and a standard curve was prepared plotting absorbance measured at 233nm against concentration.

**2. DETERMINATION OF PROTEIN BINDING OF METFORMIN USING
EQUILIBRIUM DIALYSIS METHOD**

a. Preparation of 5×10^{-5} M Bovine serum albumin

0.3450g of bovine serum albumin is dissolved in 100ml of pH 7.4 phosphate buffer

b. Preparation of 3.8×10^{-8} M solution of metformin

Prepare a stock solution of 100µg/ml of metformin. From the above solution 0.5ml and diluted with 10ml with pH buffer. The above solution 10ml which contains 3.8×10^{-8} M metformin.

c. Equilibrium dialysis method

Equilibrium dialysis is one of the methods used for the determination of protein binding of any compound. This method which consists in dialyzing the unbound fraction of a compound contained in a protein (bovine serum albumin) solution through a semi-permeable membrane. In this study, this method was used for the determination of protein binding of green synthesized nanoparticle and its 1:1 mixture with metformin. In this method firstly, dialysis membrane was activated and then dialysis was performed.

d. Activation procedure:

The dialysis membrane was cut into 12 cm pieces look like a bag (also called dialysis bag) and immersed in boiling 1 M NaHCO₃ solution for about 1 h to make sure that the inside of the bag is washed as well as outside and the process was repeated once.

Then these bags were immersed in boiling demineralized water for about 1 h with intermittent change of the water making sure that all the anions and cations are washed out. Then these were well washed with demineralized water.

Then these were immersed in phosphate buffer having pH 7.4 at about 0°C for 1 h. The process was repeated once. Finally, these were rinsed with demineralized water and stored in a refrigerator with the same buffer.

e. Dialysis procedure

The activated membrane is tied at one end of a glass tube which is open at both the ends. The sac is then filled with 10 ml of bovine serum albumin ($5 \times 10^{-5} \text{ M}$) and immersed in a beaker containing 25ml of metformin ($3.8 \times 10^{-8} \text{ M}$) prepared using a phosphate buffer pH 7.4 immediately at zero time, 2ml of solution is pipetted out from the beaker and is replaced with 2 ml of buffer. Readings were taken at 10, 30, 60, 120, 240,480 mts till equilibrium is reached and absorbance is measured at 233 nm. From the absorbance by using the standard graph the concentration was determined.

f. INTERACTION STUDY OF METFORMIN WITH *Pterocarpus marsupium* SILVER NANOPARTICLES

The interaction study on metformin is carried out by adopting equilibrium dialysis method. In this type of interaction study metformin is considered as the standard and *Pterocarpus marsupium* silver nanoparticles is added i.e., 1:1 mixture of metformin and silver nanoparticle and absorbance was measured at 233 nm at different time intervals.

g. DETERMINATION OF PROTEIN BINDING PERCENTAGE

Initially, a known amount of drug was taken in the buffer compartment. The protein was added into the plasma compartment (dialysis bag). Then, concentration of drug present in the buffer (outside of this compartment) after equilibrium was measured. This measurement gave the total amount of drug that remains in the buffer compartment. Thus, we can get sum of free drug and plasma bound drug at equilibrium.

The percentage of protein binding (F) of the drug is calculated using the following equation,

$$F = \frac{\text{conc of bound drug}}{\text{conc of drug after equilibrium with the membrane}} \times 100$$

h. Determination of number of binding sites and the affinity constants

In the present study, number of binding sites and affinity constants of green synthesized nanoparticle and its 1:1 mixture with metformin were calculated by scatchard method.

In this method, a curve was produced by plotting $r/[D]$ versus r , where r is the ratio between the molar concentration of the bound drug and the molar concentration of protein i.e.,

$$\frac{[B] - [A]}{[Protein]}$$

and D is the concentration of the unbound drug i.e., $[A]$. The curve thus obtained called scatchard plot. The scatchard plot when extrapolated on Y axis, gave an intercept nK , the intersection on X-axis representing n and the slope of line AB being k . Here, k is the affinity constant and n are the number of binding sites of protein binding.

II.1. ESTIMATION OF GLIMIPRIDE USING UV SPECTROPHOTOMETRY

a. Preparation of stock solution

90mg of glimepiride is dissolved in 100ml of methanol in a volumetric flask to give a stock solution having 0.9 mg/mL concentration or 900 µg/ml concentration.

b. Preparation of calibration curve

Dilutions from 2µg/ml – 32 µg/ml are obeyed by beer-lamberts law and a standard curve was prepared plotting absorbance measured at 229nm against concentration.

2. DETERMINATION OF PROTEIN BINDING OF GLIMIPRIDE USING EQUILIBRIUM DIALYSIS METHOD

a. Preparation of 5×10^{-5} M Bovine serum albumin

0.3450g of bovine serum albumin is dissolved in 100ml of pH 7.4 phosphate buffer.

b. Preparation of 1.8×10^{-9} M solution of glimepiride

Prepare a stock solution of 900 μ g/ml of glimepiride. From the above solution 0.01ml and diluted with 10ml with methanol. The above solution 10ml which contains 1.8×10^{-9} M glimepiride.

c. Equilibrium dialysis method

This method which consists in dialyzing the unbound fraction of a compound contained in a protein (bovine serum albumin) solution through a semi-permeable membrane. In this study, this method was used for the determination of protein binding of green synthesized nanoparticle and its 1:1 mixture with glimepiride. In this method firstly, dialysis membrane was activated and then dialysis was performed.

d. Activation procedure

The dialysis membrane was cut into 12 cm pieces look like a bag (also called dialysis bag) and immersed in boiling 1 M NaHCO₃ solution for about 1 h to make sure that the inside of the bag is washed as well as outside and the process was repeated once.

Then these bags were immersed in boiling demineralized water for about 1 h with intermittent change of the water making sure that all the anions and cations are washed out. Then these were well washed with demineralized water.

Then these were immersed in phosphate buffer having pH 7.4 at about 0°C for 1 h. The process was repeated once. Finally, these were rinsed with demineralized water and stored in a refrigerator with the same buffer.

e. Dialysis procedure

The activated membrane is tied at one end of a glass tube which is open at both the ends. The sac is then filled with 10 ml of bovine serum albumin (5×10^{-5} M) and immersed in a beaker containing 25ml of glimepiride (1.8×10^{-9} M) prepared using a phosphate buffer pH 7.4 immediately at zero time, 2ml of solution is pipetted out from the beaker and is replaced with 2 ml of buffer. Readings were taken at 10, 30, 60, 120, 240,480 mts till equilibrium is reached and absorbance is measured at 229 nm. From the absorbance by using the standard graph the concentration was determined.

f. INTERACTION OF GLIMEPIRIDE WITH *Pterocarpus marsupium* SILVER NANOPARTICLES

The interaction study on glimepiride is carried out by adopting equilibrium dialysis method. In this type of interaction study glimepiride is considered as the standard and *Pterocarpus marsupium* silver nanoparticles is added i.e., 1:1 mixture of glimepiride and silver nanoparticles and absorbance was measured at 229 nm at different time intervals.

g. DETERMINATION OF PROTEIN BINDING PERCENTAGE

Initially, a known amount of drug was taken in the buffer compartment. The protein was added into the plasma compartment (dialysis bag). Then, concentration of drug present in the buffer (outside of this compartment) after equilibrium was measured. This measurement gave the total amount of drug that remains in the buffer compartment. Thus, we can get sum of free drug and plasma bound drug at equilibrium.

The percentage of protein binding (F) of the drug is calculated using the following equation,

$$F = \frac{\text{conc of bound drug}}{\text{conc of drug after equilibrium with the membrane}} \times 100$$

h. Determination of number of binding sites and the affinity constants

In the present study, number of binding sites and affinity constants of green synthesized nanoparticle and its 1:1 mixture with glimepiride were calculated by scatchard method.

In this method, a curve was produced by plotting $r/[D]$ versus r , where r is the ratio between the molar concentration of the bound drug and the molar concentration of protein i.e.,

$$\frac{[B] - [A]}{[Protein]}$$

and D is the concentration of the unbound drug i.e., $[A]$. The curve thus obtained called scatchard plot. The scatchard plot when extrapolated on Y axis, gave an intercept nK , the intersection on X-axis representing n and the slope of line AB being k . Here, K is the affinity constant and n are the number of binding sites of protein binding.

(Experimental biopharmaceutics and pharmacokinetic by C. Vijaya Raghavan page.no: 27-28)

RESULTS & DISCUSSION

SAMPLE COLLECTION

The bark of *Pterocarpus marsupium* collected from Thalassery, Kannur district in Kerala and it is cleaned with distilled water to remove any substance on the surface of the bark.

AUTHENTICATION

The bark of *Pterocarpus marsupium* had been collected from Coimbatore, Tamilnadu. The plant was identified and authenticated by Dr. M. U. Sharief, Scientist 'E', Botanical Survey of India, Tamilnadu Agricultural University (TNAU), Coimbatore, India and voucher specimen has been given the code BSI/SRC/5/23/2021/Tech.

DRYING AND PULVERIZING

The collected bark was shade dried & it was grounded into fine powder with the help of electronic blender. Then the powder obtained was stored in well closed container and kept in dry place.

PREPARATION OF AQUEOUS EXTRACT OF *Pterocarpus marsupium* ROXB

50g of *Pterocarpus marsupium* bark powder was stirred with 500 mL of deionized water and kept at 65 °C for 30mins. Then the extracts were filtered by using Whatman No. 1 filter paper after cooling to room temperature. The extract was kept in air tight container & stored at 4 °C for future use

PREFORMULATION STUDIES

1.1 Physical Characteristics

Pterocarpus marsupium was checked for its color, odor and texture. It is light yellow colored powder in appearance and has a pleasant odor. The results are shown in Table. 5

Table. 5 Phytochemical analysis of *Pterocarpus marsupium* Roxb aqueous bark extract

Chemical Constituent	Tests	PM Ag NPs
Tannins and Phenolics	Ferric chloride Test	+
	Lead acetate Test	+
Flavonoids	Alkaline reagent Test	+
	Shinoda Test	+
	Lead acetate test	+
Alkaloids	Mayer's Test	+
	Dragendroff's Test	+
Proteins	Warming Test	-
	Biuret Test	-
	Ninhydrin Test	-
Starch	Iodine Test	+
Saponins	Foam Test	+
Steroids	Salkowski's Test	+

(+) Presence of Phytoconstituents and (-) Absence of Phytoconstituents

Preliminary phytochemical screening of plant provided information regarding chemical nature of plant such as presence and absence of various phytoconstituents. The phytoconstituents screening was done for extracts of *Pterocarpus marsupium*. (C.K. Kokate et.al)

Phytochemical screening confirmed the presence of Phyto-constituents like alkaloids, flavonoids, tannins, phenols, starch, steroids, saponins. pterostilbene and (-) epicatechin which were responsible for the antidiabetic effect of *Pterocarpus marsupium* bark which is responsible for the antidiabetic activity. (Bavya. C and Bagyalakshmi. J, 2021)

Solubility studies

Solubility test for *Pterocarpus marsupium* bark was carried out in different solvents such as ethanol, water, chloroform, Diethyl ether, Dimethyl sulphoxide and results are given in Table.6

Table. 6 solubility studies of *Pterocarpus marsupium* bark in different solvents

S. No	Solvent	soluble	Sparingly soluble	Insoluble
1	Ethanol	✓	-	-
2	Water	✓	-	-
3	Chloroform	-	✓	-
4	Diethyl ether	-	✓	-
5	Dimethyl sulphoxide	-	✓	-

From the solubility studies, it was found that the *Pterocarpus marsupium* bark extract is soluble in water, ethanol and sparingly soluble in chloroform, diethyl ether & dimethyl sulphoxide. Hence, *Pterocarpus marsupium* bark extract is more soluble in polar solvents and sparingly soluble in non-polar solvents.

UV VISIBLE SPECTRAL ANALYSIS OF *Pterocarpus marsupium* ROXB BARK EXTRACT

The *Pterocarpus marsupium* stock solution of concentration 500µg/mL were prepared and the UV- visible absorption spectra for the sample were taken in the range of 200 - 800nm for λ_{max} . using double beam UV Spectrophotometer.

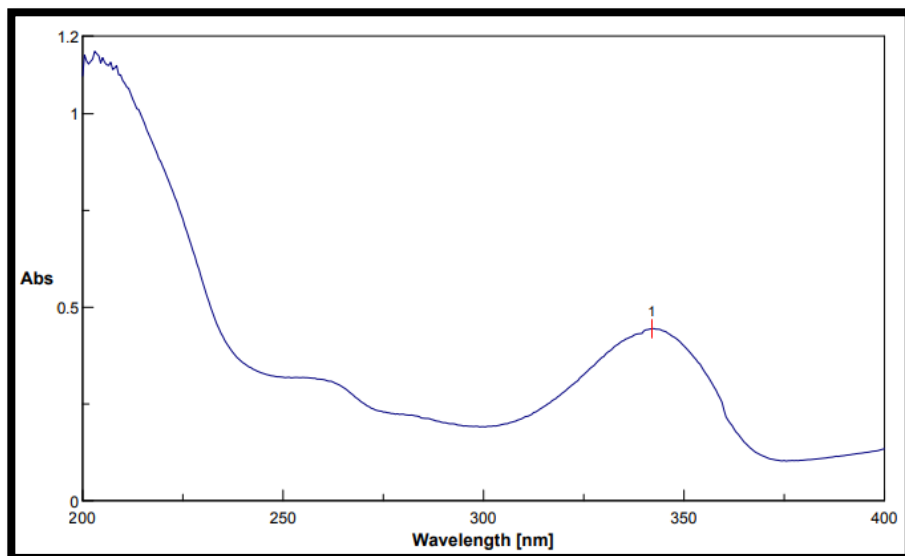


Fig.2 Uv- Visible absorption spectra of *Pterocarpus marsupium* Roxb bark extract

The maximum absorption of *Pterocarpus marsupium* Roxb bark extract was found to be at 342 nm and hence it is selected as the λ_{\max} for further studies.

CALIBRATION CURVE OF *Pterocarpus marsupium* ROXB BARK EXTRACT

To construct a calibration curve, 50 – 250 $\mu\text{g/ml}$ of *Pterocarpus marsupium* bark extract was taken & checked the linearity at 342 nm. The calibration data is shown in the Table.7

Table. 7 Calibration data of *Pterocarpus marsupium* bark extract was measured at 342 nm using Uv – visible absorption spectroscopy

S.NO	Concentration($\mu\text{g/ml}$)	Absorbance at 342 nm
1	50	0.1066
2	100	0.3063
3	150	0.5157
4	200	0.7129
5	250	0.8907

Construction of calibration curve of *Pterocarpus marsupium* bark

In the calibration curve, linearity was obtained between 50-250 $\mu\text{g/ml}$ concentration of *Pterocarpus marsupium* bark and the regression value was found to be $R^2 = 0.9992$.

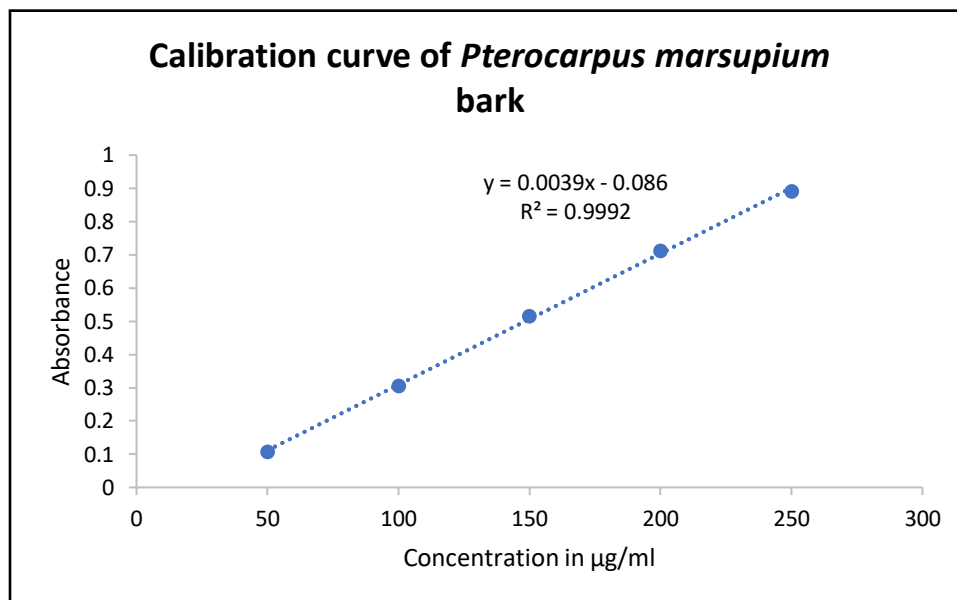


Fig.3 Calibration curve of *Pterocarpus marsupium* bark extract

Hence, the sample of *Pterocarpus marsupium* bark obeys Beer Lambert's Law at the concentration between 50-250 $\mu\text{g/ml}$.

FTIR SPECTROSCOPY OF *Pterocarpus marsupium* Roxb bark

Fourier Transform Infrared (FT-IR) spectra of the samples were obtained using a FTIR Jasco 4100 Spectrometer by KBr disc method. Number of peaks are present in the FT-IR spectra of the *Pterocarpus marsupium* Roxb. bark extract which shows the complexity of the extract.

Table. 8 FTIR interpretation of *Pterocarpus marsupium* Roxb. Bark

Materials	Test wave number cm^{-1}	Functional group assessment
<i>Pterocarpus marsupium</i> bark	3664.87	O-H stretching
	3596.40	O-H stretching
	3554.93	O-H stretching
	3511.53	O-H stretching
	3061.13	C-H bending
	1745.64	C=O stretching
	1362.75	N-O stretching
	1335.75	C-O stretching
	1318.39	C-O stretching
	1243.16	C-O stretching
	1159.26	C-O stretching
	1112.00	C-O stretching

FTIR interpretation results are given in the above table. 8 and the spectrum of *Pterocarpus marsupium* Roxb. Bark was shown in the Fig. 4

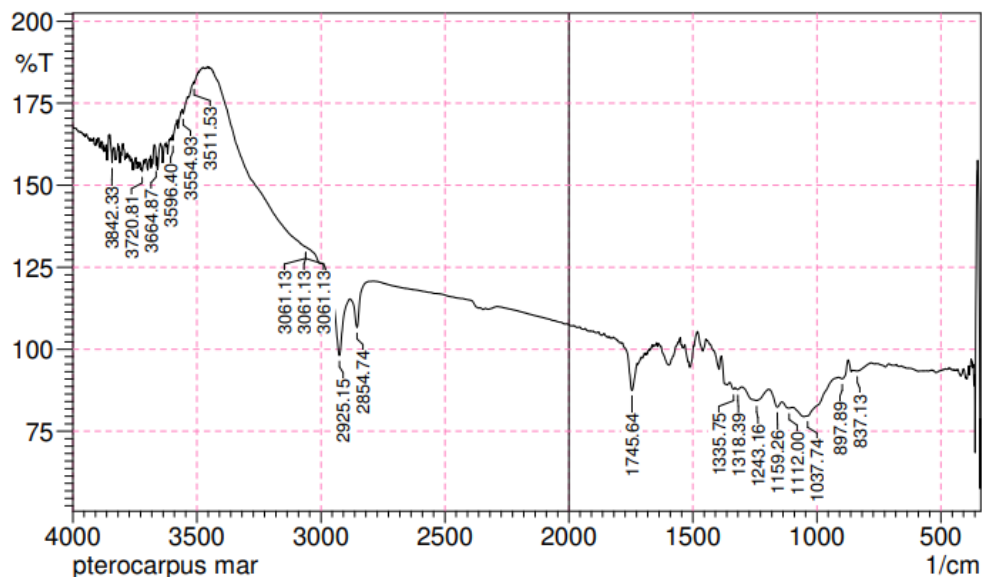


Fig.4 FTIR spectra of *Pterocarpus marsupium* Roxb. bark

FTIR SPECTROSCOPY OF SILVER NITRATE

In the FTIR spectrum of silver nitrate shows strong absorption peak at 1312.60, 1338.64, 1349.25, 1361.79 and 1393.62 indicates the presence of N-O (nitro compounds).

Table. 9 FTIR interpretation of silver nitrate

Material	Test wave number (cm-1)	Functional group assessment
Silver nitrate	1312.60	N-O stretching
	1338.64	N-O stretching
	1349.25	N-O stretching
	1361.79	N-O stretching
	1393.62	N-O stretching

FTIR interpretation results are given in the above Table.9 and the spectrum of silver nitrate was shown in the Fig.5

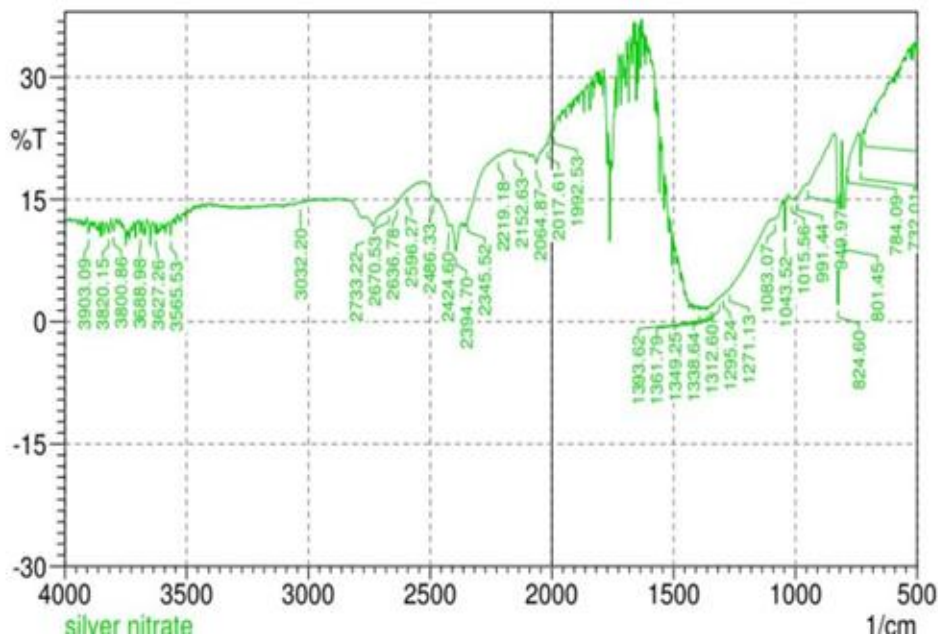


Fig.5 FTIR spectrum of silver nitrate

GREEN SYNTHESIS OF SILVER NANOPARTICLES

An aliquot (5ml) of aqueous plant extract sample was taken and added 10ml of 1mM aqueous AgNO_3 drop wise and kept in magnetic stirrer with constant stirring at 120 rpm. Color change of the reaction mixtures were monitored to determine silver nanoparticles formation which is indicated by a colloidal brown color.

SEPARATION OF SILVER NANOPARTICLES

The colloidal solution was centrifuged at 4000rpm for 20 mins. after centrifugation, the pellets were collected and washed thoroughly with deionized water to separate silver nanoparticles and they were kept for drying in desiccator to avoid moisture or dust from air. After drying, formulated *Pterocarpus marsupium* silver nanoparticles were stored in air tight container and used for further evaluation studies.

CHARACTERIZATION OF SYNTHESIZED *Pterocarpus marsupium* ROXB SILVER NANOPARTICLES

VISUAL EXAMINATION

In the experiment, addition of plant extract of *Pterocarpus marsupium* into the beakers containing aqueous solution of silver nitrate led to the change in the color of the solution from yellowish to reddish brown color. This formation indicates that silver ions in reaction medium have been converted to elemental silver having the size of nanometric range. F1, F2, F3, F4, F5 formulations of *Pterocarpus marsupium* silver nanoparticles were prepared by green synthesis method. On addition of different concentration (1 to 5 mL) of bark extracts to aqueous silver nitrate solution keeping its concentration 10 mL (1 mM) constant, the color of the solution changed from light yellow to colloidal brown indicating formation of silver nanoparticles. Hence the formulation F5 was chosen for further evaluation studies because of the formation of colloidal brown color.

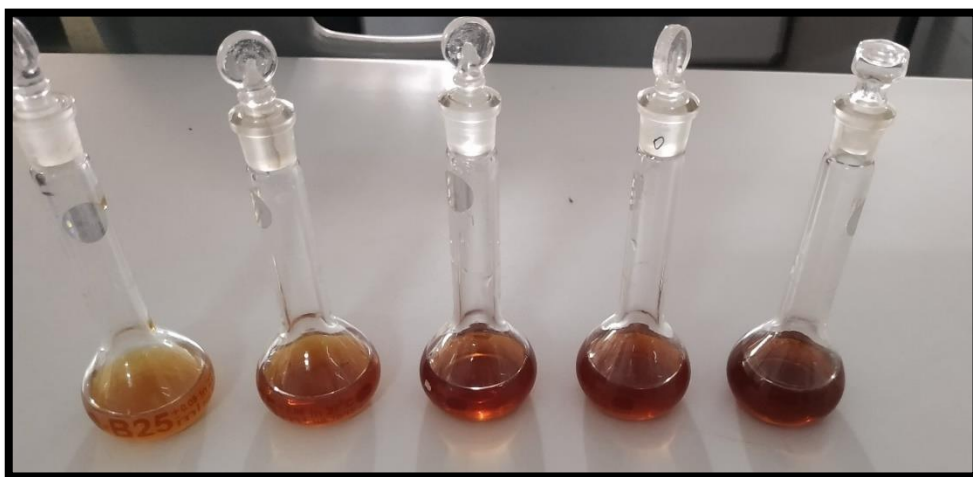


Fig. 6 Formation of *Pterocarpus marsupium* silver nanoparticles by green synthesis method

UV Visible spectral analysis of *Pterocarpus marsupium* silver nanoparticles

Uv-Visible spectral analysis characterizes the formation and completion of silver nanoparticles by using UV-Visible spectrophotometer. The reduction of silver ions in solution was

monitored by periodical sampling of aliquots at the time interval of 30min, 210min and 24hr were taken by using distilled water as blank from the wavelength of 200-800nm.

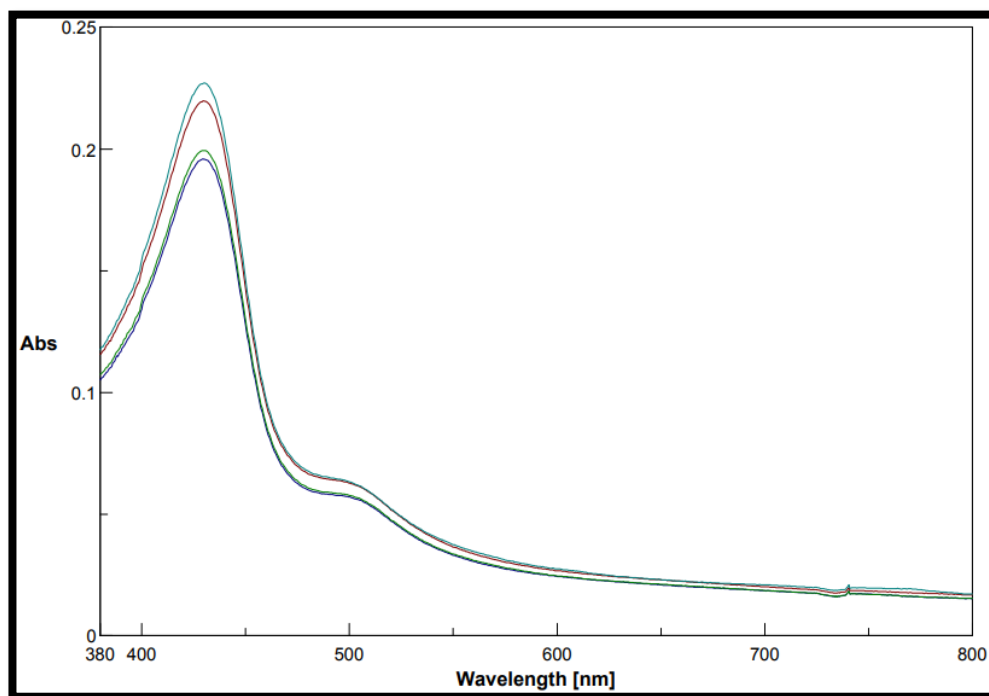


Fig. 7 UV- visible absorption spectra of *Pterocarpus marsupium* Roxb. silver nanoparticles at different time interval

The reduction of silver ions to silver nanoparticle was indicated by color change from yellow to brown color and it was reflected in spectral data obtained by using a UV-Visible spectrophotometer. The color is characteristic of the surface plasmon resonance (SPR) of silver nanoparticles. It shows an absorption peak around 429 nm which is specific for *Pterocarpus marsupium* bark silver nanoparticles. (Njagi et al., 2011)

FTIR SPECTROSCOPY OF *Pterocarpus marsupium* SILVER NANOPARTICLES

FTIR helps to identify the different functional groups in the compounds which cause the conversion of silver ion to silver nanoparticle and also used for capping or stabilization of silver nanoparticles. FTIR spectra of the *Pterocarpus marsupium* -AgNPs was recorded to identify functional groups.

Table. 10 FTIR Interpretation of *Pterocarpus marsupium* silver nanoparticles

Materials	Test wave number cm^{-1}	Functional group assessment
<i>Pterocarpus marsupium</i> silver nanoparticles	3689.95	O-H stretching
	3592.54	O-H stretching
	3544.32	O-H stretching
	3450.77	O-H stretching
	3037.99	C-H bending
	1729.24	C=O stretching
	1738.89	C=O stretching
	1124.54	C-O stretching
	1159.26	C-O stretching
	1218.09	C-O stretching
	1230.63	C-O stretching
	1316.46	N-O stretching
	1323.21	N-O stretching
	1354.07	N-O stretching
	1361.79	N-O stretching
	1367.58	N-O stretching
	1373.36	N-O stretching

FTIR interpretation results are given in the above Table.10 and the spectrum of *Pterocarpus marsupium* silver nanoparticle was shown in the Fig. 8

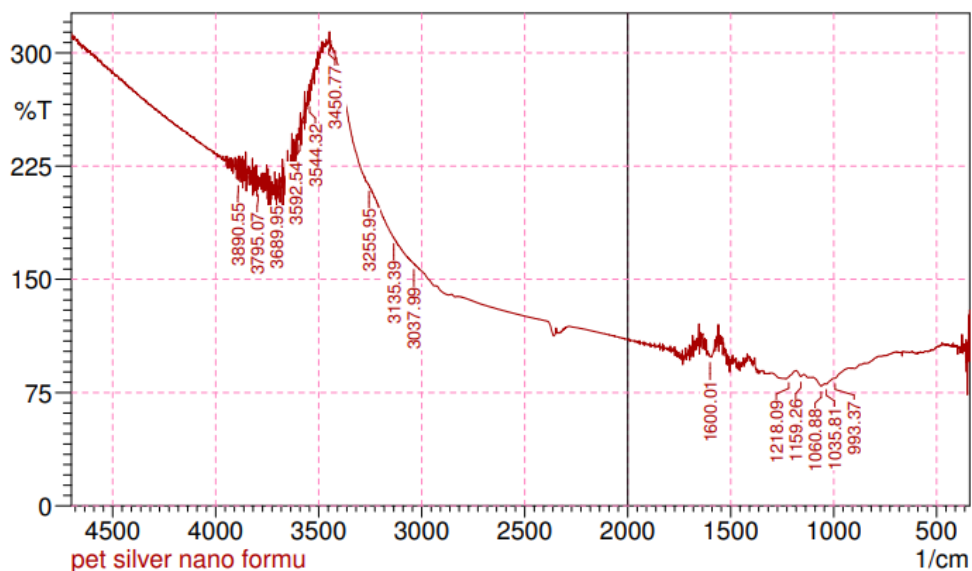


Fig. 8 FTIR spectrum of *Pterocarpus marsupium* silver nanoparticles

From the above spectral analysis, it was concluded that the drug and excipient don't have any incompatibility. since the peaks present in the drug can also be visualized in the drug and excipient spectra. Hence these excipients can be chosen for the preparation of silver nanoparticles for the further analysis. The presence of hydroxyl, carboxyl and phenolic was confirmed.

DRUG ENTRAPMENT EFFICIENCY

Drug entrapment efficacy is a measure of drug loading capacity of the system. Drug entrapment can be determined from the supernatant liquid of *Pterocarpus marsupium* bark silver nanoparticle after centrifugation by UV spectrophotometry at 429nm.

Table. 11 drug entrapment efficacy of five formulation

S. No	Formulation code	% Drug entrapment
1	F1	72%
2	F2	78%
3	F3	81%
4	F4	86%
5	F5	95%

The % entrapment of drug or drug content of *Pterocarpus marsupium* Roxb. silver nanoparticles were found to be 72% for F1, 78% for F2, 81% for F3, 86% for F4, 95% for F5. Hence the highest amount of drug was entrapped in the formulation F5 which is 95% and it was observed to be colloidal brown color which indicated the formation of *Pterocarpus marsupium* silver nanoparticles. Based on drug entrapment results, the formulation F5 was chosen for further evaluation studies as it possessed high drug entrapment capacity as compared to other formulations. (Tenderwealth clement Jackson et al.,2019)

SCANNING ELECTRON MICROSCOPY(SEM)

A SEM employed to analyze the surface morphology and size details of the silver nanoparticles. The SEM images were taken in different magnification such as 1500X, 3000X, 5000X, 15000X and shown in Fig. 9,10,11,12

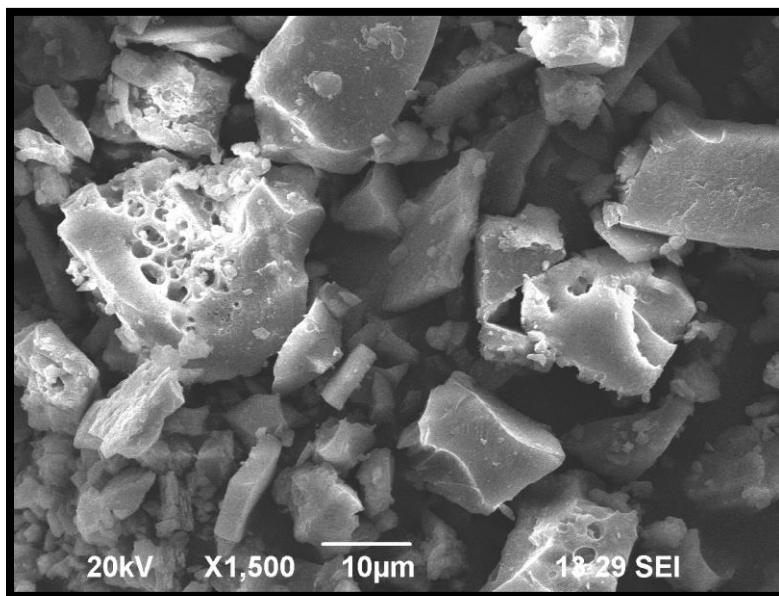


Fig.9 SEM analysis of *Pterocarpus marsupium* Roxb. Silver nanoparticle of 1500X magnification

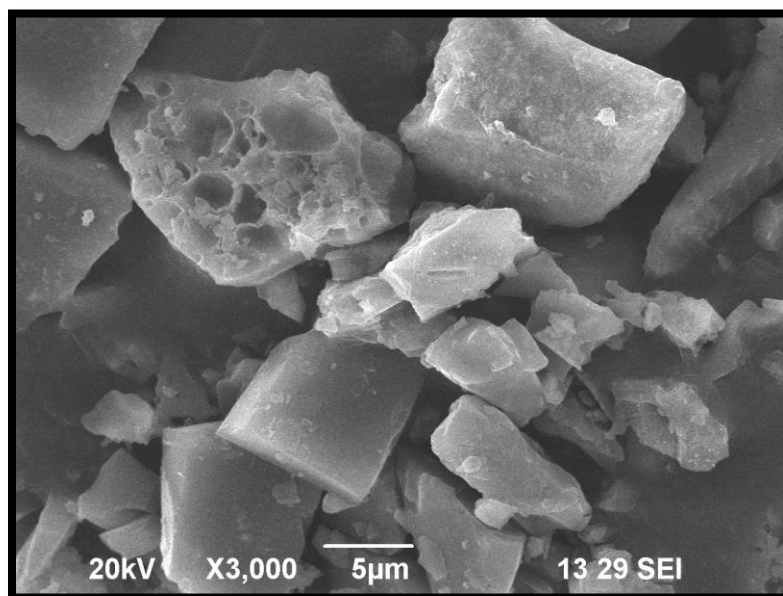


Fig. 10 SEM analysis of *Pterocarpus marsupium* Roxb. Silver nanoparticle of 3000X magnification

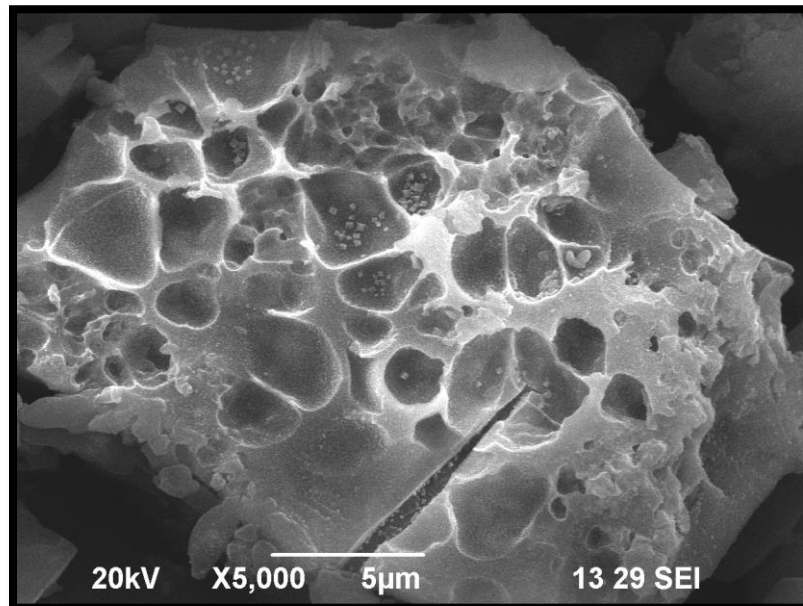


Fig. 11 SEM analysis of *Pterocarpus marsupium* Roxb. Silver nanoparticle of 5000X magnification

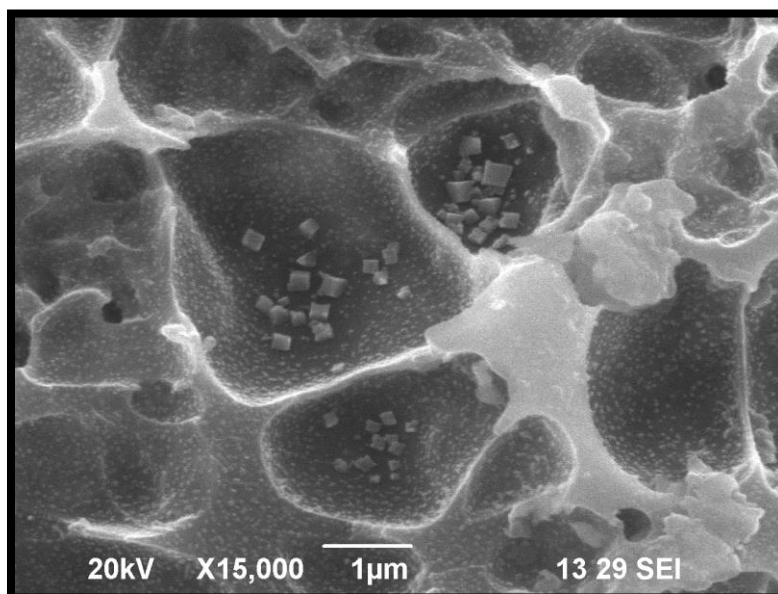


Fig. 12 SEM analysis of *Pterocarpus marsupium* Roxb. Silver nanoparticle of 15000X magnification

The SEM micrographs of *Pterocarpus marsupium* silver nanoparticles showed that the nanoparticles synthesized were polydisperse spherical shaped and highly distributed with aggregation. The SEM image showing silver nanoparticles synthesized using *Pterocarpus marsupium* aqueous extract of bark confirmed the development of silver nanostructures. (Xifeng zhang, et al., 2016)

PARTICLE SIZE MEASUREMENT

The mean particle size (z-average), polydispersity index (PI) of *Pterocarpus marsupium* silver nanoparticle were determined by dynamic light scattering technique using a zeta size analyzer (Malvern Instruments). The study revealed average particle size (z-average) is found to be 36.44nm. Particle size analysis showed the presence of nanoparticles with polydispersity indices PDI value 0.825 with intercept 0.781. it is presented in the Fig.13 (Khot Uttamkumar vithal, 2013)

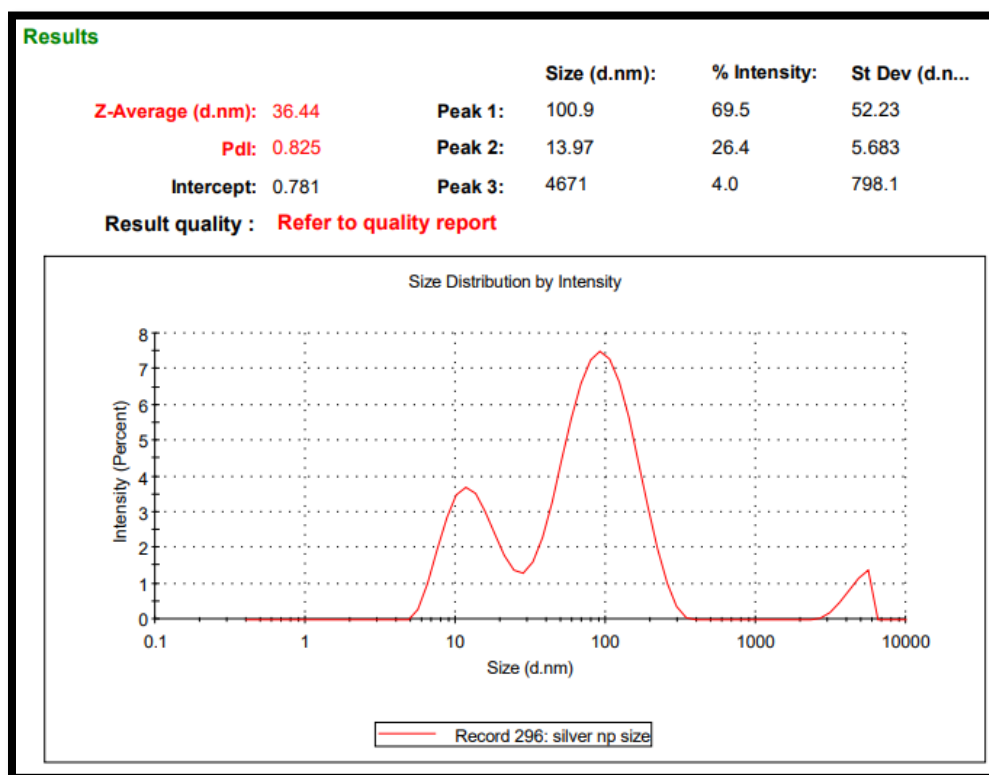


Fig. 13 Particle size measurement of *Pterocarpus marsupium* silver nanoparticles

ZETA POTENTIAL.

Zeta Potential was determined using Malvern zeta-sizer instrument. The surface charge of the particles and stability of the solution was characterized by zeta potential. For *Pterocarpus marsupium* silver nanoparticles zeta potential was found to be -22.6 mV with peak area 100 intensity. These values indicate that the formulated *Pterocarpus marsupium* silver nanoparticles are stable. Zeta potential distribution of silver nanoparticles are depicted in the Fig.14 (Khot Uttamkumar vithal, 2013)

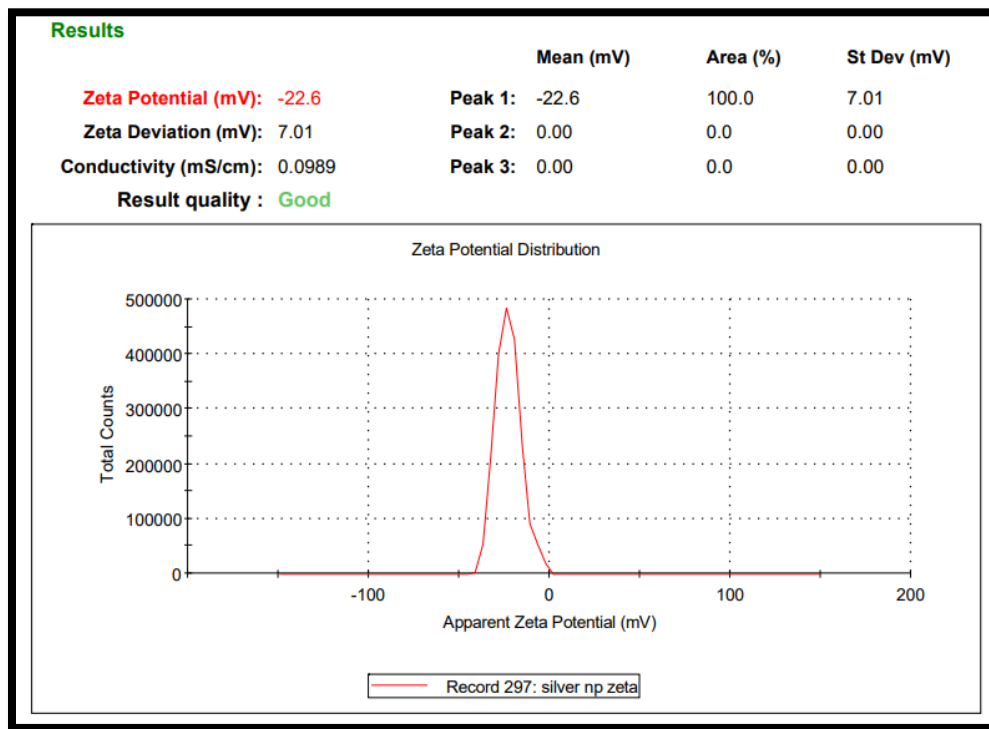


Fig. 14 Determination of zeta potential of *Pterocarpus marsupium* silver nanoparticles

IN VITRO DRUG RELEASE STUDY

The invitro release of drug from the nanoparticle was measured in phosphate buffer (pH 7.4), using dialysis bag diffusion method. Amount of drug released at different time intervals (1h,2h,3h,4h,5h and 24h) were observed.

Table.12 *In vitro* drug release study of *Pterocarpus marsupium* Roxb silver Nanoparticles

Time (in hrs)	Log time	Square root of time	Cumulative amount of drug released	Log Cumulative amount of drug released	Cumulative % Of drug released	Log cumulative % of drug released
0	0.000	0.000	0	0.000	0	0.000
1	0.000	1.000	27.1	1.433	13.55	1.132
2	0.301	1.414	41.9	1.622	20.95	1.321
3	0.477	1.732	56.21	1.750	28.10	1.449
4	0.602	2.000	72.98	1.863	36.49	1.562
5	0.699	2.236	91.11	1.960	45.55	1.658
24	1.380	4.899	181.91	2.260	90.95	1.959

The invitro drug release was fitted into different kinetic models consisting of zero order, first order, Higuchi model and Korsmeyer – Peppas model. The various profiles were evaluated by the correlation coefficient (R^2). The highest degree of correlation coefficient determines the suitable mathematical model that follows drug release kinetics.

DRUG RELEASE DATA FITTED TO VARIOUS KINETIC MODELS**Zero order**

Time vs Cumulative percentage release were plotted and shown in Fig.15 From the graph R^2 value were found to be 0.8966

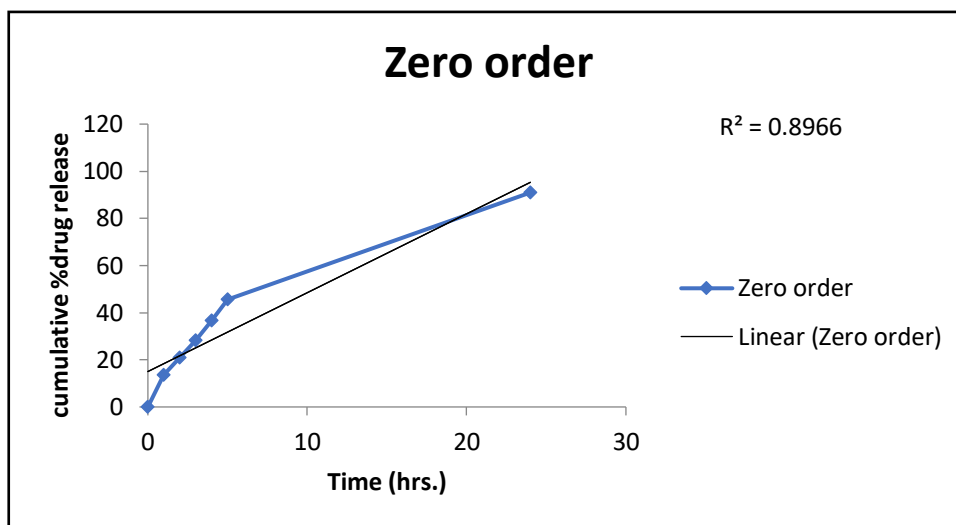


Fig. 15 Zero order plot

First order

Time vs log cumulative percentage were plotted and shown in Fig.16 From the graph R^2 value found to be 0.3223

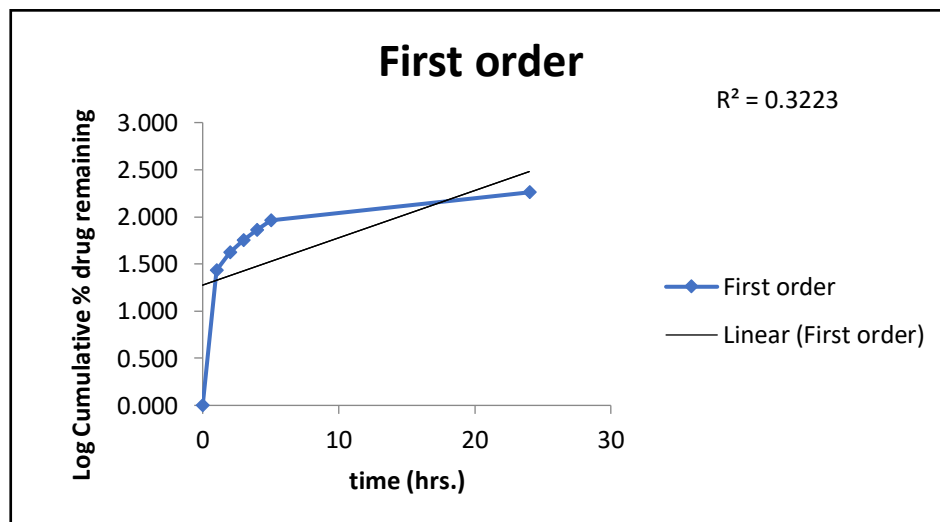


Fig.16 First order plot

Higuchi's plot

Square root of time vs cumulative percentage release and shown in the Fig.17 From the graph R^2 value was found to be 0.9877

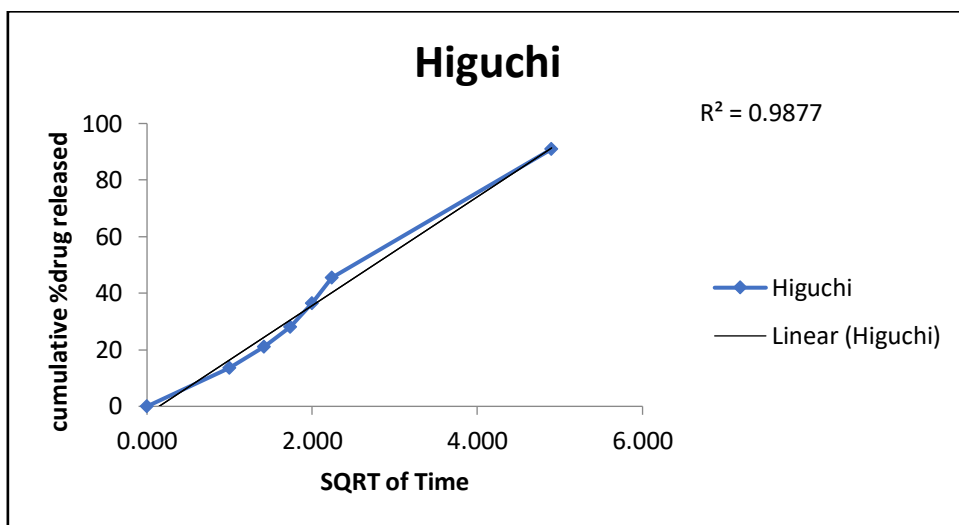


Fig. 17 Higuchi plot

Korsmeyer peppas

Log time vs log cumulative percentage and shown in the Fig. 18 From the graph was found to be 0.9692 and n value is 0.167

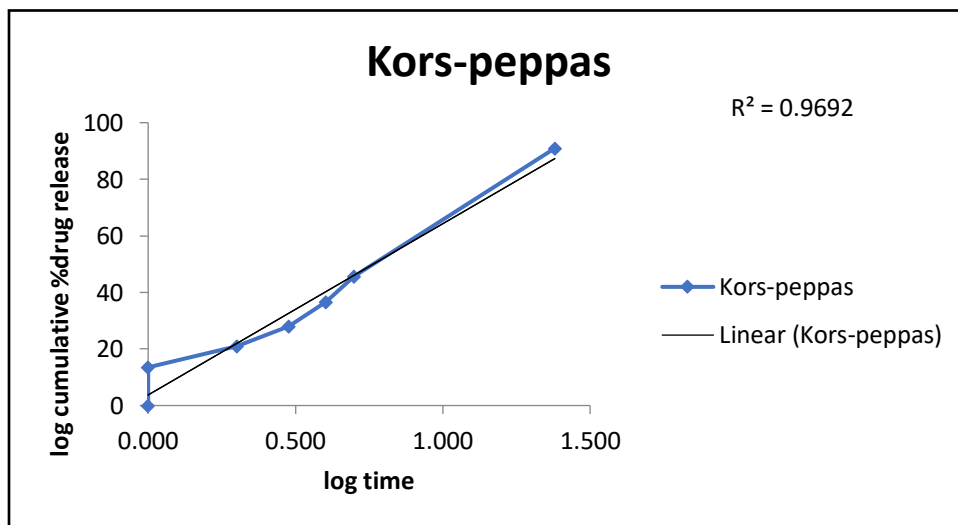


Fig. 18 Korsmeyer peppas

Table.13 R² value obtained for various kinetic models

FORMULATION	CORRELATION COEFFICIENT (R ²)				
	Zero order R ²	First order R ²	Higuchi R ²	Korsmeyer peppas	
<i>Pterocarpus marsupium</i> silver nanoparticles	0.8966	0.3223	0.9877	R ²	n
				0.9692	0.167

Based on the release kinetic analysis, the release data were best fitted with Higuchi release with R² value being 0.9877. To understand the mechanism of drug release, the data were fitted in the Korsmeyer- Peppas equation which states the type of diffusion. The corresponding plot for Korsmeyer Peppas equation also shows good linearity. the release exponent “n” was found to be 0.167, confirming that formulation followed Fickian diffusion kinetics.

From the release kinetics data, it can be concluded that the formulation *Pterocarpus marsupium* Roxb. Silver nanoparticle fit with highest correlation (R²) was resulted with Higuchi and followed by Korsmeyer peppas, zero order and first order.

INVITRO ALPHA AMYLASE INHIBITION STUDY

Alpha amylase is responsible for postprandial glucose levels therefore, *Pterocarpus marsupium* plant extracts with alpha-amylase inhibitory activity are being investigated that might decrease postprandial blood glucose levels, thus being an interesting and novel therapeutic target for diabetes mellitus treatment. A possible strategy to block dietary carbohydrate absorption is to use natural resources as carbohydrate digestive enzyme inhibitors as they have fewer side effects than synthetic drugs. Alpha-amylase inhibitory activity of *Pterocarpus marsupium* and their phytochemical compounds are explored that might be helpful within the treatment of diabetes mellitus. Acarbose is used as a standard here which is a good antidiabetic drug and works by slowing the action of certain chemicals that breakdown food to release glucose into our blood.

The result suggests that *Pterocarpus marsupium* Roxb. exhibits good alpha amylase inhibition under in vitro condition. Alpha amylase inhibitory effect of positive control.

The absorbance of control without sample is taken and it is 1.2442

Table.14 Alpha amylase inhibitory effects of positive control Acarbose

Concentration (mg/ml)	Absorbance	% Inhibition
0.2	0.8259	33.61
0.4	0.7589	39
0.6	0.6247	49
0.8	0.5378	56.77
1.0	0.4353	65

Percentage inhibition of α amylase for the positive control Acarbose was found to be 33.61% at concentration 0.2mg/ml. When the concentration is increased to 0.4 mg/ml percentage inhibition is increased by 1.1fold of when the concentration was increased to 0.6mg/ml, so the percentage inhibition is increased by 1.2fold, further the concentration was increased to 0.8mg/ml and the percentage inhibition was found to increase by 1.1-fold, when the concentration was increased to 1mg/ml which resulted in the increase of percentage inhibition was observed by 1-fold.

Table.15 α - Amylase inhibitory effects of *Pterocarpus marsupium* Roxb. silver nanoparticles

Concentration (μ g/ml)	Absorbance	% Inhibition
0.2	0.8816	29.14
0.4	0.8725	29.87
0.6	0.8162	34.39
0.8	0.7539	39.40
1.0	0.5314	57.28

Percentage inhibition of α amylase for the *pterocarpus marsupium* Roxb. silver nanoparticles were found to be 29.14% for the concentration 0.2mg/ml. When the concentration was increased to 0.4mg/ml percentage inhibition was observed to increase by 1-fold when the concentration was increased to 0.6mg/ml, so the percentage inhibition was also found to increase by 1.1-fold. Further the concentration was increased to 0.8mg/ml then the percentage inhibition was increased by 1.1-fold, when the concentration was increased to 1mg/ml which resulted in the increase of percentage inhibition by observed to 1.4-fold high.

Comparison of alpha amylase inhibition of acarbose vs *Pterocarpus marsupium* Roxb. Silver nanoparticles were shown in Fig.19. From the figure we compare the percentage inhibition of both positive control and test drug.

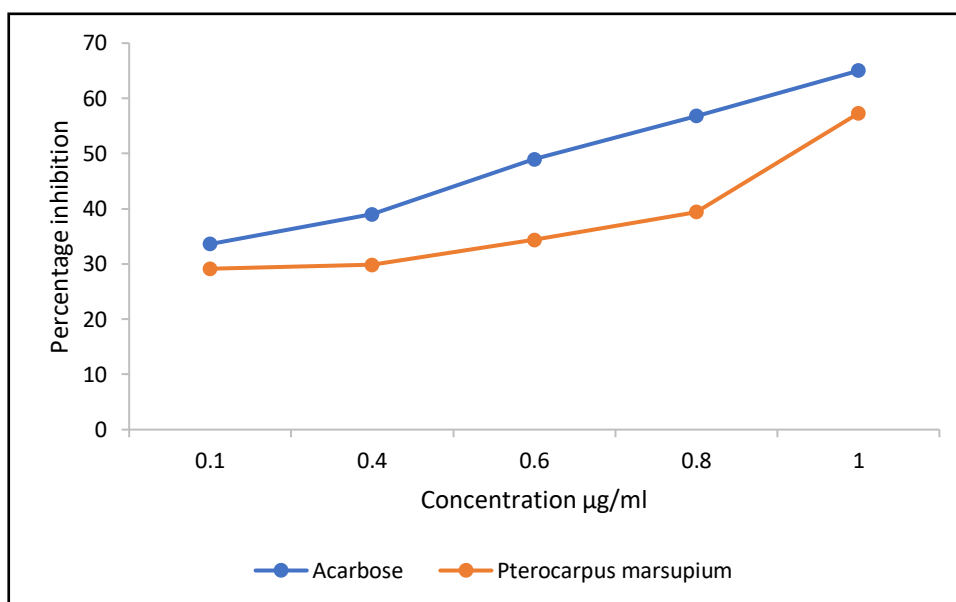


Fig. 19 comparison of α -amylase inhibition of *Pterocarpus marsupium* silver nanoparticles & acarbose on alpha amylase enzyme

The percentage α amylase inhibition of positive control Acarbose at lower(0.2mg/ml) and higher (1 mg/ml) concentration were found to be 33.61% and 65% respectively and for the test *Pterocarpus marsupium* Roxb. silver nanoparticles, the percentage α - amylase inhibition at lowest (0.2mg/ml) and highest (1mg/ml) concentration were found to be 29.14% and 57.28% respectively.

PART – B

**PHARMACOKINETIC INTERACTION STUDY OF GREEN SYNTHESIZED
NANOPARTICLES AND ANTIDIABETIC DRUGS**

ESTIMATION OF METFORMIN USING UV SPECTROPHOTOMETRY

The calibration graph of metformin was revalidated. Metformin shows good linearity with the range of 2 to 10 µg/ml. when measured at 233nm using uv spectrophotometry and it was reported in below Table.16 and Fig. 20

Table.16 Calibration curve of Metformin

S.NO	Concentration(µg/ml)	Absorbance at 233nm
1	2	0.2252
2	4	0.5166
3	6	0.7757
4	8	0.9878
5	10	1.308

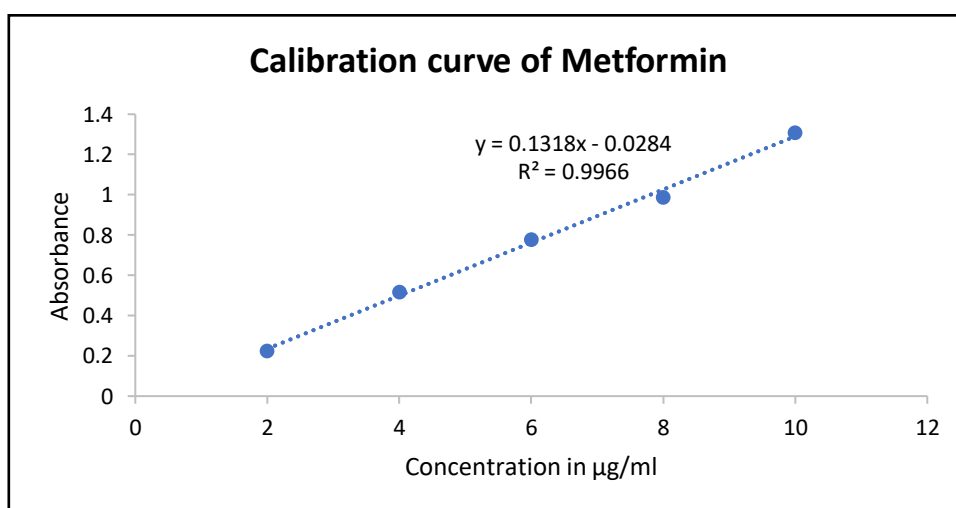


Fig.20 Calibration curve of metformin measured at 233 nm using uv spectrophotometry

DETERMINATION OF PROTEIN BINDING OF METFORMIN USING EQUILIBRIUM DIALYSIS METHOD

The concentration of unbound metformin and percentage protein binding of metformin was determined using equilibrium dialysis method. The study was carried out with concentration ($3.8 \times 10^{-8} \text{ M}$) of metformin. It is represented in Table.17

Table. 17 shows the unbound concentration and percentage protein binding of metformin individually

Time (mins)	Unbound concentration ($\mu\text{g/ml}$)	Unbound concentration (M)	% Protein binding
10	1.75	1.33×10^{-8}	48
30	1.79	1.36×10^{-8}	41
60	2.01	1.52×10^{-8}	33
120	2.04	1.55×10^{-8}	31
180	2.07	1.57×10^{-8}	30
240	2.17	1.64×10^{-8}	24
300	2.20	1.67×10^{-8}	21

In case of $3.8 \times 10^{-8} \text{ M}$ concentration of metformin individually, the percentage protein binding of metformin at different time intervals like 10, 30, 60, 120, 180, 240, 300 min was 41%, 33%, 31%, 30%, 24%, 21% respectively. The concentration of metformin individually was found to increase by 1.01, 1.12, 1.0, 1.01, 1.04, 1.01 fold respectively as compared to the concentration at 10, 30, 60, 120, 180, 240, 300 min respectively was as represented in Fig.21

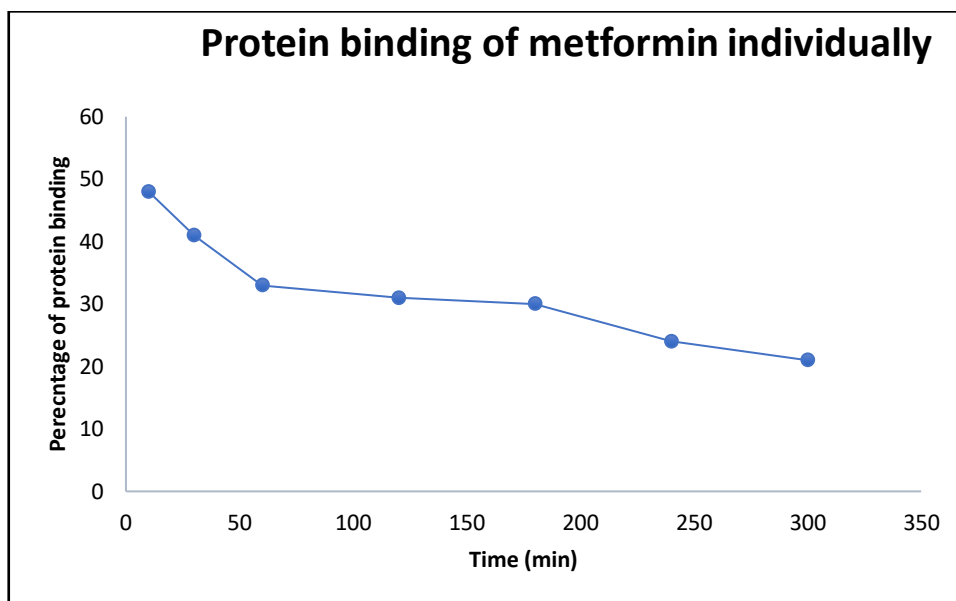


Fig.21 Protein binding of metformin individually

As the time of contact with drug and protein increases, there is a decrease in percentage of protein binding which may be due to the number of binding sites and affinity constant.

INTERACTION STUDY OF METFORMIN WITH *Pterocarpus marsupium* SILVER NANOPARTICLES

The concentration of unbound drug and percentage protein binding of metformin in the presence of *Pterocarpus marsupium* silver nanoparticles is determined using the equilibrium dialysis method. The study was carried out with a concentration ($3.8 \times 10^{-8} \text{M}$) of metformin and 20ml of *Pterocarpus marsupium* silver nanoparticles. It is represented in Table.18

Table.18 shows the unbound concentration and percentage protein binding of metformin in presence of *Pterocarpus marsupium* silver nanoparticles

Time (mins)	Unbound concentration (µg/ml)	Unbound concentration (M)	% Protein binding
10	2.60	0.19x10 ⁻⁹	45
30	2.69	0.20x10 ⁻⁹	44
60	2.77	0.21x10 ⁻⁹	41
120	2.91	0.22x10 ⁻⁹	38
180	3.22	0.23x10 ⁻⁹	31
240	3.27	0.24x10 ⁻⁹	30
300	3.38	0.25x10 ⁻⁹	28

In case of (3.8×10^{-8} M) concentration of metformin with 20ml *Pterocarpus marsupium* silver nanoparticle, the percentage protein binding of metformin in presence of silver nanoparticle at different time intervals like 10, 30, 60, 120, 180, 240, 300 min was 45%, 44%, 41%, 38%, 31%, 30%, 28% respectively are as represented in figure. The concentration of metformin with silver nanoparticles was found to increase by 1.03, 1.02, 1.05, 1.10, 1.01, 1.03-fold respectively as compared to the concentration at 10, 30, 60, 120, 180, 240, 300 min respectively was as represented in Fig.22

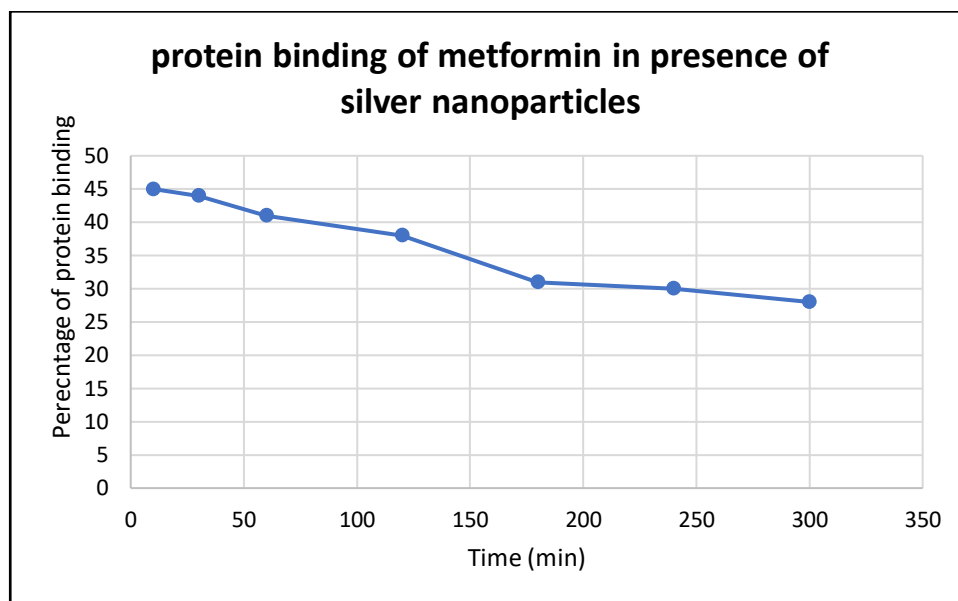


Fig. 22 Protein binding of metformin in presence of *Pterocarpus marsupium* silver nanoparticles (1:1) mixture

DETERMINATION OF PROTEIN BINDING PARAMETERS

SCATCHARD PLOT

In case of scatchard plot, the x-axis is specific binding (usually labeled 'bound') and the y-axis is the ratio of specific binding to concentration of free radioligand (usually labeled 'unbound or free'). Numbers of binding sites were obtained by dividing the intercept (nk) by slope (k) of the straight lines. The values for affinity constants associated with respective class of binding sites were obtained directly from the slope of the straight lines (Scatchard, 1949).

NUMBER OF BINDING SITES AND AFFINITY CONSTANT OF METFORMIN

From scatchard plots, x – intercept was found to be 0.0025 and y – intercept was found to be 6.243. The number of binding sites for metformin individual in BSA was found to be 8.81 and affinity constant were found to be 0.70 respectively are as represented in Fig.23

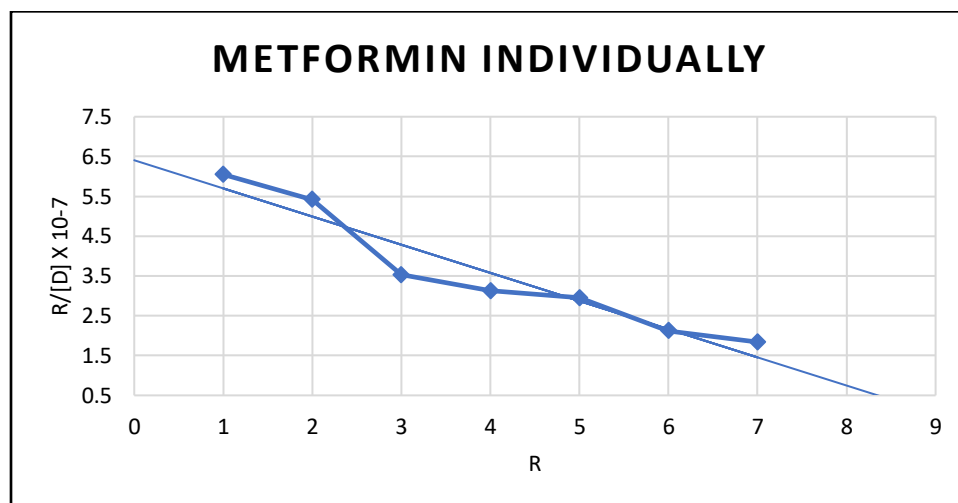


Fig. 23 Scatchard plot for protein binding of metformin individually

NUMBER OF BINDING SITES AND AFFINITY CONSTANT OF METFORMIN IN PRESENCE OF *Pterocarpus marsupium* SILVER NANOPARTICLES

From scatchard plots, x – intercept was found to be 0.00036 and y – intercept was found to be 2.490. The number of binding sites for metformin in presence of *Pterocarpus marsupium* silver nanoparticles in BSA was found to be 11.19 and affinity constant were found to be 0.22 respectively. When metformin is combined with silver nanoparticles the number of binding sites found to be increased when compared to metformin individually.

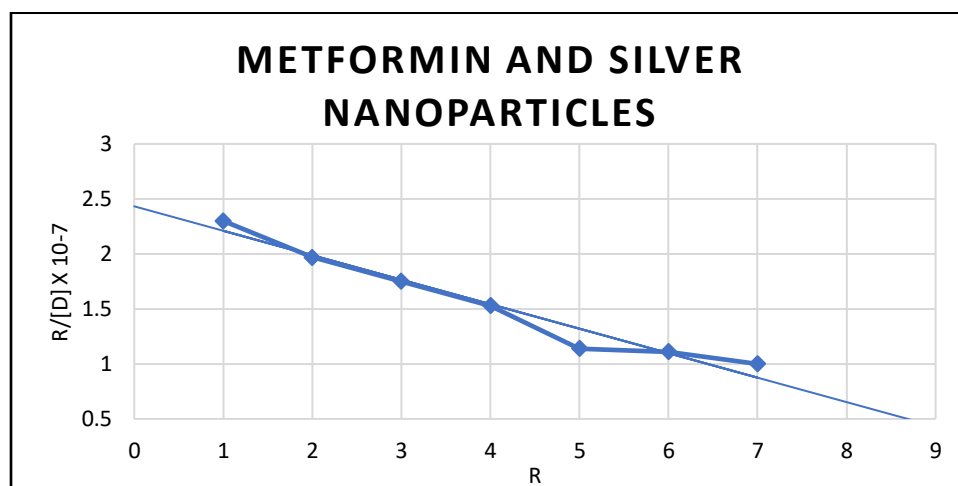


Fig. 24 Scatchard plot for protein binding of metformin in presence of *Pterocarpus marsupium* silver nanoparticles (1 :1 mixture)

ESTIMATION OF GLIMEPIRIDE USING UV SPECTROPHOTOMETRY

The calibration graph of glimepiride was revalidated. Glimepiride shows good linearity with the range of 9 to 36 $\mu\text{g/ml}$. when measured at 229nm using uv spectrophotometry and it was reported in below Table. 19 and Fig. 25

Table.19 Calibration curve of Glimepiride

S.NO	Concentration($\mu\text{g/ml}$)	Absorbance at 229nm
1	9	0.3915
2	18	0.8974
3	27	1.3940
4	36	1.8356

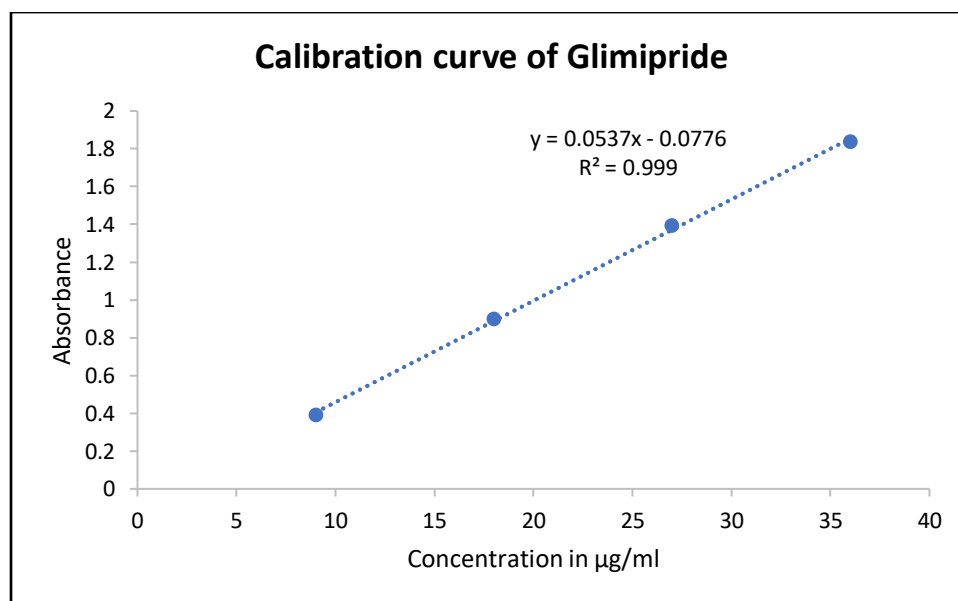


Fig.25 Calibration curve of glimepiride measured at 229 nm using uv spectrophotometry

DETERMINATION OF PROTEIN BINDING OF GLIMEPIRIDE USING EQUILIBRIUM DIALYSIS METHOD

The concentration of unbound glimepiride and percentage protein binding of glimepiride is determined using equilibrium dialysis method. The study was carried out with concentration ($1.8 \times 10^{-9} \text{M}$) of glimepiride. It is represented in Table.20

Table.20 shows the unbound concentration and percentage protein binding of glimepiride individually

Time (mins)	Unbound concentration ($\mu\text{g/ml}$)	Unbound concentration (M)	% Protein binding
10	0.09	1.96×10^{-10}	88
30	0.10	2.18×10^{-10}	85
60	0.12	2.48×10^{-10}	83
120	0.13	2.68×10^{-10}	81
180	0.17	3.44×10^{-10}	75
240	0.20	4.08×10^{-10}	70
300	0.24	4.42×10^{-10}	67

In case of $1.8 \times 10^{-9} \text{M}$ concentration of glimepiride, the percentage protein binding of glimepiride at different time intervals like 10, 30, 60, 120, 180, 240, 300 min was 88%, 85%, 83%, 81%, 75%, 70%, 67%. The concentration of glimepiride individually was found to increase by 1.11, 1.2, 1.08, 1.12-fold respectively as compared to the concentration at 10, 30, 60, 120, 180, 240, 300 min respectively as represented in Fig.26

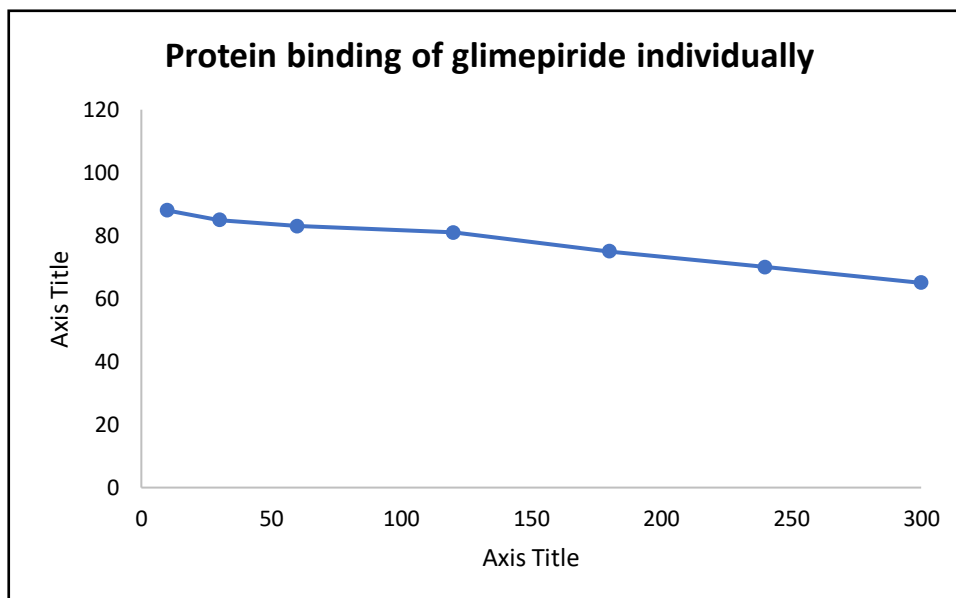


Fig.26 Protein binding of glimepiride individually

As the time of contact with drug and protein increases, there is a decrease in percentage of protein binding which may be due to the number of binding sites and affinity constant.

INTERACTION STUDY OF GLIMEPIRIDE WITH *Pterocarpus marsupium* SILVER NANOPARTICLES

The concentration of unbound drug and percentage protein binding of glimepiride in presence of *Pterocarpus marsupium* silver nanoparticles is determined using equilibrium dialysis method. The study was carried out with concentration ($1.8 \times 10^{-9} \text{M}$) of glimepiride and 20ml of *Pterocarpus marsupium* silver nanoparticles. It is represented in Table.21

Table.21 shows the unbound concentration and percentage protein binding of glimepiride in presence of *Pterocarpus marsupium* silver nanoparticles

Time (mins)	Unbound concentration (µg/ml)	Unbound concentration (M)	% Protein binding
10	2.15	4.3×10^{-9}	68
30	2.50	5.0×10^{-9}	61
60	2.64	5.28×10^{-9}	58
120	2.68	5.36×10^{-9}	57
180	2.89	5.78×10^{-9}	52
240	2.92	5.84×10^{-9}	51
300	2.97	5.94×10^{-9}	50

In case of (1.8×10^{-9} M) concentration of glimepiride with 20ml *Pterocarpus marsupium* silver nanoparticles, the percentage protein binding of glimepiride in presence of silver nanoparticles at different time intervals like 10, 30, 60, 120, 180, 240, 300 min was 68%, 61%, 58%, 57%, 52%, 51%, 50% respectively. The concentration of glimepiride with silver nanoparticles was found to increase by 1.16, 1.05, 1.01, 1.0, 1.01, 1.01-fold respectively as compared to the concentration at 10, 30, 60, 120, 180, 240, 300 mins respectively as represented in Fig.27

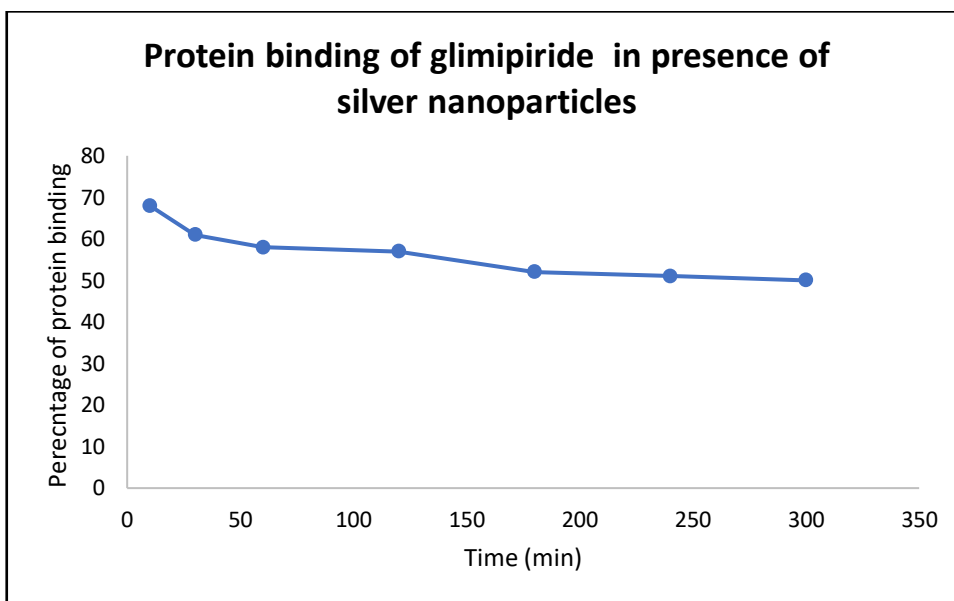


Fig.27 Protein binding of glimepiride in presence of *Pterocarpus marsupium* silver nanoparticles (1:1) mixture

DETERMINATION OF PROTEIN BINDING PARAMETERS

NUMBER OF BINDING SITES AND AFFINITY CONSTANT OF GLIMEPIRIDE

From scatchard plots, x – intercept was found to be 0.00031 and y – intercept was found to be 7.310. The number of binding sites for glimepiride individual in BSA was found to be 8.50 and affinity constant were found to be 0.85 respectively are as represented in Fig.28

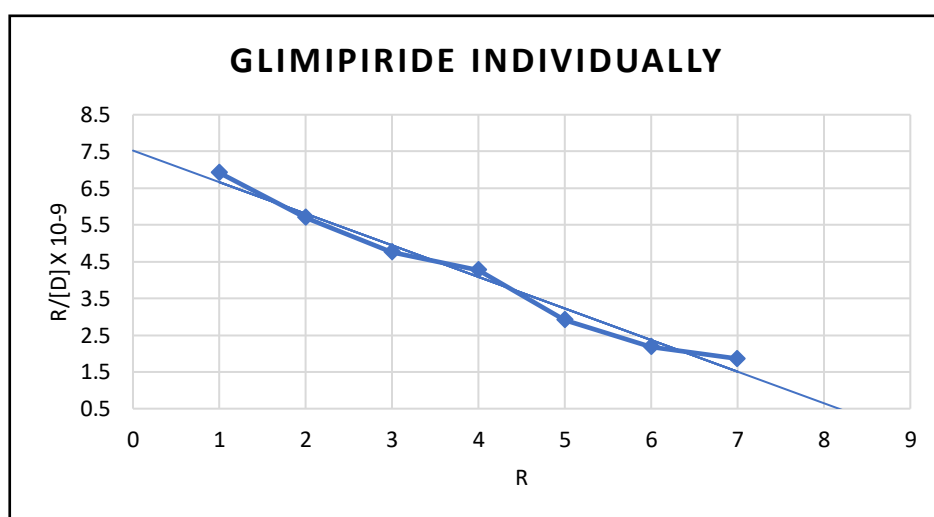


Fig.28 Scatchard plot for protein binding of glimepiride individually

NUMBER OF BINDING SITES AND AFFINITY CONSTANT OF GLIMEPIRIDE IN PRESENCE OF *Pterocarpus marsupium* SILVER NANOPARTICLES

From scatchard plots, x – intercept was found to be 0.00022 and y – intercept was found to be 2.346. The number of binding sites for glimepiride in presence of *Pterocarpus marsupium* silver nanoparticles in BSA was found to be 19.32 and affinity constant were found to be 0.12 respectively. When glimepiride is combined with silver nanoparticles the number of binding sites found to be increased when compared to glimepiride individually.

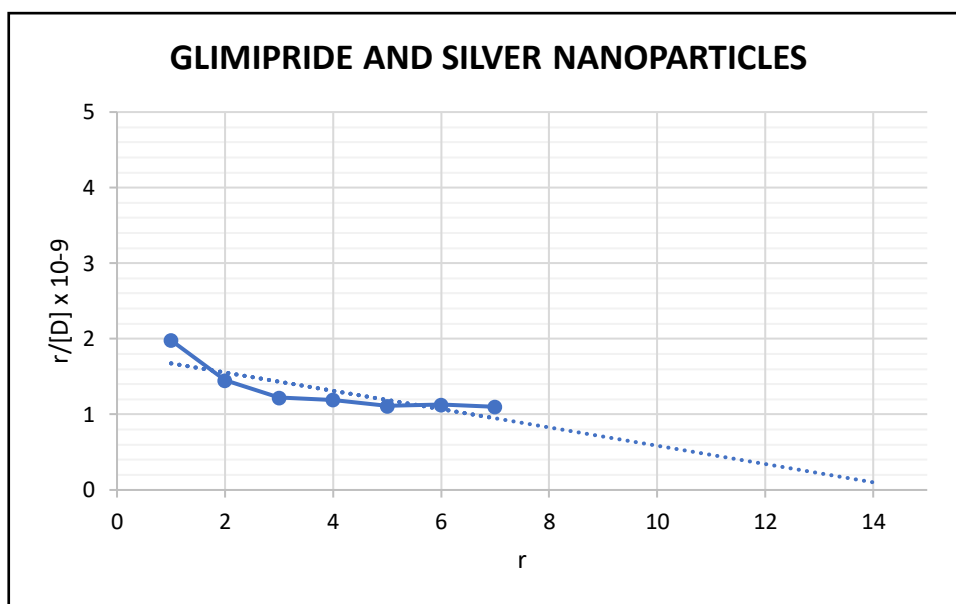


Fig. 29 Scatchard plot for protein binding of glimepiride in presence of *Pterocarpus marsupium* silver nanoparticles (1 :1 mixture)

SUMMARY & CONCLUSION

Nanotechnology is a rapidly growing field due to its unique functionality and a wide range of applications. Nanomedicine explores the possibilities of applying the knowledge and tools of nanotechnology for the prevention, treatment, diagnosis and control of disease.

Diabetes mellitus is a group of metabolic disorders that is characterized by elevated blood glucose levels driven by insulin deficiency or resistance. As diabetes has become a serious chronic illness, the number of diabetic patients is increasing at an alarming rate which makes it an important topic of research.

Silver nanoparticles with nano size and well-defined structure was synthesized by the green chemistry approach using *Pterocarpus marsupium* Roxb. bark extract. This green chemistry approach towards the synthesis of silver nanoparticle is highly essential effort being addressed in nanomedicine because of its varied advantages. The biosynthesis of nanoparticles has been proposed as a cost-effective and environmentally friendly alternative to chemical and physical methods.

The objective of the study is to investigate antidiabetic effect of green synthesized silver nanoparticle from aqueous extract of *Pterocarpus marsupium* and to study pharmacokinetic interaction with antidiabetic drug.

Preformulation studies were carried out to find the solubility of *Pterocarpus marsupium* Roxb bark is soluble in polar solvents and sparingly soluble in non-polar solvents.

Uv- visible absorption spectra for *Pterocarpus marsupium* Roxb. bark the λ_{max} was observed to be 342 nm. The calibration curve of *Pterocarpus marsupium* Roxb. bark extract was found to be linear with R^2 value was found to be 0.999 for the concentration between 50-250 μ g/ml.

Green synthesized silver nanoparticles were done using the *Pterocarpus marsupium* bark extract along with the silver nitrate solution. Silver nanoparticles formation was confirmed by the formation of dark brown from solution of silver nitrate, where the reduction of silver ion occurs which leads to the formation of silver nanoparticles. The UV-visible spectra peak at 429 nm confirmed the reduction of silver ions leading to synthesis of silver nanoparticle.

FTIR measurement of *Pterocarpus marsupium* Roxb. was carried out to identify the possible biomolecules responsible for capping and efficient stabilization of Ag nanoparticles synthesized and found to be hydroxyl, carboxyl and phenolic group which acts as a reducing, stabilizing and capping agent.

Drug entrapment efficacy test was carried out and the percentage of drug entrapment efficacy was found to be 95%.

SEM analysis was carried out to study Structural and morphological features of synthesized *Pterocarpus marsupium* silver nanoparticles and outcome shows that, there is a formation of polydisperse spherical shaped.

Particle size distribution is analyzed by using zeta sizer and average particle size was found to be 36.44nm with polydispersity index of 0.825 and intercept 0.781.

Zeta potential measurement was found to be -22.6 mV with the peak areas of 100% intensity and these values indicate formulated nanoparticles are stable.

In vitro drug release data have been observed in different time intervals and release kinetics data were evaluated by zero order, Higuchi, Korsmeyer-Peppas models. Based on the release kinetic analysis, the release data were best fitted with Higuchi release with R^2 value being 0.9877. The corresponding plot for Korsmeyer Peppas equation also shows good linearity. the release exponent “n” was found to be 0.167, confirmed that formulation followed Fickian diffusion kinetics.

In vitro α amylase exhibited potential inhibitory activity for the aqueous extract of *Pterocarpus marsupium* silver nanoparticles and it was compared with standard acarbose. Percentage inhibition of positive control acarbose at lower and higher concentration was found to be 33.61% and 65% and *Pterocarpus marsupium* Roxb. silver nanoparticle was found to be 29.14% and 57.28%.

About 463 million people worldwide have diabetes, it is predicted that by 2045 may afflict up to 700 million people. In India, currently 77 million individuals have diabetes and it was expected to double in 2045. A study revealed a varying range of complementary and alternative medicine (CAM) use rates among diabetic patients in India (67.7%). CAM can affect

the management of diabetes by herb – drug interaction with use of herbal medicine. To find out any such interaction this research work has been carried out with antidiabetic drug metformin and glimepiride.

The protein binding studies can be done to study pharmacokinetic interaction between silver nanoparticle and antidiabetic drug using equilibrium dialysis method.

Estimation of metformin shows good linearity with the range of 2 to 10 µg/ml. when measured at 233nm using uv spectrophotometry.

The protein binding of metformin was studied using equilibrium dialysis method. Data of the metformin have been used to find the protein binding percentage.

In case of (3.8×10^{-8} M), the percentage protein binding of metformin at different time intervals like 10, 30, 60, 120, 180, 240, 300 min are 41%, 33%, 31%, 30%, 24%, 21%. The percentage of protein binding decreases with the increase in time of contact with the drug. Due to the number of binding sites and affinity constant. The concentration of metformin individually was found to increase by 1.01, 1.12, 1.0, 1.01, 1.04, 1.01-fold as compared to the concentration at 10, 30, 60, 120, 180, 240, 300 min respectively.

In case (3.8×10^{-8} M) concentration of metformin with presence of *Pterocarpus marsupium* silver nanoparticles, the percentage protein binding of metformin in presence of silver nanoparticles at different time intervals like 10, 30, 60, 120, 180, 240, 300 min is 45%, 44%, 41%, 38%, 31%, 30%, 28%. The percentage of protein binding decreases with the increase in time of contact with the drug. Due to the number of binding sites and affinity constant. The concentration of metformin with silver nanoparticles was found to increase by 1.03, 1.02, 1.05, 1.10, 1.01, 1.03-fold as compared to the concentration at 10, 30, 60, 120, 180, 240, 300 min respectively.

From scatchard plot of metformin individual, x – intercept was found to be 0.0025 and y – intercept was found to be 6.243. The number of binding sites in BSA was found to be 8.81 and affinity constant were found to be 0.70 respectively.

From scatchard plot of metformin in the presence of *Pterocarpus marsupium*, x – intercept was found to be 0.00036 and y – intercept was found to be 2.490. The number of

binding sites for metformin in presence of *Pterocarpus marsupium* silver nanoparticles in BSA was found to be 11.19 and affinity constant were found to be 0.22 respectively. When metformin is combined with silver nanoparticle the number of binding sites found to be increased when compared to metformin individually.

Estimation of glimepiride shows good linearity with the range of 9 to 36 µg/ml. when measured at 229nm using uv spectrophotometry.

The protein binding of glimepiride was studied using equilibrium dialysis method. Data of the glimepiride have been used to find the protein binding percentage.

In case of ($1.8 \times 10^{-9} \text{ M}$), the percentage protein binding of glimepiride at different time intervals like 10, 30, 60, 120, 180, 240, 300 min are 88%, 85%, 83%, 81%, 75%, 70%, 67%. The percentage of protein binding decreases with the increase in time of contact with the drug. Due to the number of binding sites and affinity constant. The concentration of glimepiride individual was found to increase by 1.11, 1.2, 1.08, 1.2-fold as compared to the concentration at 10, 30, 60, 120, 180, 240, 300 min

In case ($1.8 \times 10^{-9} \text{ M}$) concentration of glimepiride with presence of *Pterocarpus marsupium* silver nanoparticles, the percentage protein binding of glimepiride in presence of silver nanoparticle at different time intervals like 10, 30, 60, 120, 180, 240, 300 min is 68%, 61%, 58%, 57%, 52%, 51%, 50%. The percentage of protein binding decreases with the increase in time of contact with the drug. Due to the number of binding sites and affinity constant. The concentration of glimepiride with silver nanoparticles was found to increase by 1.16, 1.05, 1.01, 1.0, 1.01, 1.01-fold as compared to the concentration at 10, 30, 60, 120, 180, 240, 300 min respectively.

From scatchard plot of glimepiride individually, x – intercept was found to be 0.00031 and y – intercept was found to be 7.310. The number of binding sites in BSA was found to be 8.50 and affinity constant were found to be 0.85 respectively.

From scatchard plot of glimepiride in presence of *Pterocarpus marsupium* silver nanoparticle, x – intercept was found to be 0.00022 and y – intercept was found to be 2.346. The number of binding sites in BSA was found to be 19.32 and affinity constant were found to be 0.12 respectively. When glimepiride is combined with silver nanoparticle the number of binding sites found to be increased when compared to glimepiride individually.

The current study was pursued using green synthesis of silver nanoparticles was prepared using the *Pterocarpus marsupium* Roxb. Bark since this method helps bark extract (*Pterocarpus marsupium*) to serve as a reductant and a stabilizing agent for the synthesis of AgNPs. These nanoparticles were characterized and evaluated by various test such as visual examination, uv visible spectral analysis, FTIR spectroscopy, drug entrapment efficacy, determination of particle size and zeta potential, SEM analysis, invitro antidiabetic study, invitro drug release kinetics study. Literature survey regarding diabetes mellitus have revealed that the patient administered with complementary or alternative medicine like herbal medicine along with synthetic drugs has led to the herb – drug interaction. Hence this research work has been carried out to find any pharmacokinetic interaction between green synthesized *Pterocarpus marsupium* silver nanoparticles with metformin and glimepiride using equilibrium dialysis method. The study was carried out by assessing percentage protein binding using metformin and glimepiride individually and in combination with green synthesized silver nanoparticles of *Pterocarpus marsupium*. The percentage protein binding of metformin and glimepiride individually and in combination with silver nanoparticles were found to decrease with the increase in time of contact. The concentration of metformin and glimepiride was found to get altered at different time interval. From the scatchard plot number of binding sites and affinity constant was found. The interaction study of green synthesized silver nanoparticles with metformin was observed to be increase in free drug concentration of metformin in blood plasma. The interaction study of green synthesized silver nanoparticles with glimepiride was observed to be increase in free drug concentration of glimepiride in blood plasma.

Hence it can be inferred that, the concomitant administration of *Pterocarpus marsupium* silver nanoparticles with metformin and glimepiride should be avoided as the pharmacokinetic properties of the metformin and glimepiride was getting altered in presence of *Pterocarpus marsupium* silver nanoparticles.

BIBLIOGRAPHY

1. Agarwal, H., Kumar, S.V. and Rajeshkumar, S., 2021. Antidiabetic effect of silver nanoparticles synthesized using lemongrass (*Cymbopogon Citratus*) through conventional heating and microwave irradiation approach. *Journal of Microbiology, Biotechnology and Food Sciences*, 2021, pp.371-376.
2. Agarwal, P. and Gupta, R., 2016. Alpha-amylase inhibition can treat diabetes mellitus. *Res. Rev. J. Med. Health Sci*, 5(4), pp.1-8.
3. Ahmed, S., Ahmad, M., Swami, B.L. and Ikram, S., 2016. A review on plants extracts mediated synthesis of silver nanoparticles for antimicrobial applications: a green expertise. *Journal of advanced research*, 7(1), pp.17-28.
4. Alam, S.M., Akter, M.J., Reza, M.N., Israt, F., Ahmed, F. and Shilpi, J.A., 2004. Drug-drug interactions between ciprofloxacin and captopril at binding sites of bovine serum albumin. *Pak J Biol Sci*, 7, pp.79-81.
5. Alkaladi, A., Abdelazim, A.M. and Afifi, M., 2014. Antidiabetic activity of zinc oxide and silver nanoparticles on streptozotocin-induced diabetic rats. *International journal of molecular sciences*, 15(2), pp.2015-2023.
6. Almatroudi, A., 2020. Silver nanoparticles: Synthesis, characterization and biomedical applications. *Open Life Sciences*, 15(1), pp.819-839.
7. Alzahrani, A.S., Price, M.J., Greenfield, S.M. and Paudyal, V., 2021. Global prevalence and types of complementary and alternative medicines use amongst adults with diabetes: systematic review and meta-analysis. *European journal of clinical pharmacology*, 77(9), pp.1259-1274.
8. Archit, R., Gayathri, M. and Punnagai, M., 2013. An in-vitro investigation into the mechanism of antidiabetic activity of selected medicinal plants. *Int J Drug Dev Res*, 5(3), pp.221-26.
9. Badkhane, Y., Yadav, A.S., Sharma, A.K., Raghuwanshi, D.K., Uikey, S.K., Mir, F.A., Lone, S.A. and Murab, T., 2010. *Pterocarpus marsupium* Roxb-Biological activities and medicinal properties. *International Journal of Advances in Pharmaceutical Sciences*, 1(4).
10. Bagyalakshmi, J. and Haritha, H., 2017. Green synthesis and characterization of silver nanoparticles using *Pterocarpus marsupium* and assessment of its in vitro Antidiabetic activity. *American Journal of Advanced Drug Delivery ISSN*.

11. Balan, K., Qing, W., Wang, Y., Liu, X., Palvannan, T., Wang, Y., Ma, F. and Zhang, Y., 2016. Antidiabetic activity of silver nanoparticles from green synthesis using *Lonicera japonica* leaf extract. *Rsc Advances*, 6(46), pp.40162-40168.
12. Bavya, C., Bagyalakshmi, J., 2021. Silver nanoparticle of *pterocarpus marsupium* demonstrating antidiabetic activity in rats. *Determinations Nanomed Nanotechnol.* 2(2). DNN. 000532.
13. Brahmanekar, D.M. and Jaiswal, S.B., 2005. *Biopharmaceutics and pharmacokinetics: A treatise*. Vallabh prakashan.
14. Chintamani, R.B., Salunkhe, K.S. and Chavan, M.J., Emerging use of green synthesis silver nanoparticle: an updated.
15. Dash, S., Murthy, P.N., Nath, L. and Chowdhury, P., 2010. Kinetic modeling on drug release from controlled drug delivery systems. *Acta Pol Pharm*, 67(3), pp.217-223.
16. Ealia, S.A.M. and Saravanakumar, M.P., 2017, November. A review on the classification, characterisation, synthesis of nanoparticles and their application. In *IOP Conference Series: Materials Science and Engineering* (Vol. 263, No. 3, p. 032019). IOP Publishing.
17. Eriksson, M.A., Gabrielsson, J. and Nilsson, L.B., 2005. Studies of drug binding to plasma proteins using a variant of equilibrium dialysis. *Journal of pharmaceutical and biomedical analysis*, 38(3), pp.381-389.
18. Evans, G., 2004. *A handbook of bioanalysis and drug metabolism*. CRC press.
19. Gerber, W., Steyn, J.D., Kotzé, A.F. and Hamman, J.H., 2018. Beneficial pharmacokinetic drug interactions: a tool to improve the bioavailability of poorly permeable drugs. *Pharmaceutics*, 10(3), p.106.
20. Dag, B., 2021. Green synthesis, characterization, and antioxidant activity of silver nanoparticles using *Stachys annua* L. subsp. *annua* var. *annua*. *Particulate Science and Technology*, pp.1-9.
21. Gouda, R., Baishya, H. and Qing, Z., 2017. Application of mathematical models in drug release kinetics of carbidopa and levodopa ER tablets. *J. Dev. Drugs*, 6(02), pp.1-8.
22. Govindappa, M., Hemashekhar, B., Arthikala, M.K., Rai, V.R. and Ramachandra, Y.L., 2018. Characterization, antibacterial, antioxidant, antidiabetic, anti-inflammatory and antityrosinase activity of green synthesized silver nanoparticles using *Calophyllum tomentosum* leaves extract. *Results in Physics*, 9, pp.400-408.

23. Gupta, R.C., Chang, D., Nammi, S., Bensoussan, A., Bilinski, K. and Roufogalis, B.D., 2017. Interactions between antidiabetic drugs and herbs: an overview of mechanisms of action and clinical implications. *Diabetology & metabolic syndrome*, 9(1), pp.1-12.
24. Skoog, D.A., Holler, F.J. and Crouch, S.R., 2017. *Principles of instrumental analysis*. Cengage learning. page number: 459- and 461.
25. Huang, S.M., Lertora, J.J. and Atkinson Jr, A.J. eds., 2012. *Principles of clinical pharmacology*. Academic Press.
26. Hugar, A.L. and Londonkar, R.L., 2020. Green synthesis, characterization and pharmacological activities of silver nanoparticles prepared from pterocarpus marsupium. *European Journal of Biomedical*, 7(10), pp.528-534.
27. Jackson, T.C., Agboke, A.A., Udofa, E.J., Ucheokoro, A.S., Udo, B.E. and Ifekpolugo, N.L., 2019. Characterization and Release Kinetics of Metronidazole Loaded Silver Nanoparticles Prepared from Carica papaya Leaf Extract. *Advances in Nanoparticles*, 8(3), pp.47-54.
28. Jini, D. and Sharmila, S., 2020. Green synthesis of silver nanoparticles from Allium cepa and it's in vitro antidiabetic activity. *Materials Today: Proceedings*, 22, pp.432-438.
29. Johnson, I. and Prabu, H.J., 2015. Green synthesis and characterization of silver nanoparticles by leaf extracts of Cycas circinalis, Ficus amplissima, Commelina benghalensis and Lippia nodiflora. *International Nano Letters*, 5(1), pp.43-51.
30. Johnson, P., Krishnan, V., Loganathan, C., Govindhan, K., Raji, V., Sakayanathan, P., Vijayan, S., Sathishkumar, P. and Palvannan, T., 2018. Rapid biosynthesis of Bauhinia variegata flower extract-mediated silver nanoparticles: an effective antioxidant scavenger and α -amylase inhibitor. *Artificial Cells, Nanomedicine, and Biotechnology*, 46(7), pp.1488-1494.
31. Karthik, V.P., Suresh, P. and David, D.C., 2016. In vitro nitric oxide scavenging activity and alpha amylase inhibitory activity of pterocarpus marsupium extract. *International Journal of Phytopharmacology*, 7(2), pp.85-88.
32. Katiyar, D., Singh, V. and Ali, M., 2016. Phytochemical and pharmacological profile of Pterocarpus marsupium: A review. *The Pharma Innovation*, 5(4, Part A), p.31.
33. Khadayat, K., Marasini, B.P., Gautam, H., Ghaju, S. and Parajuli, N., 2020. Evaluation of the alpha-amylase inhibitory activity of Nepalese medicinal plants used in the treatment of diabetes mellitus. *Clinical Phytoscience*, 6(1), pp.1-8.

34. Khalid, S., Shahzad, A., Basharat, N., Abubakar, M. and Anwar, P., 2018. Phytochemical screening and analysis of selected medicinal plants in Gujrat. *Journal of Phytochemistry and Biochemistry*, 2(1), pp.1-3.
35. Kifle, Z.D., 2021. Prevalence and correlates of complementary and alternative medicine use among diabetic patients in a resource-limited setting. *Metabolism Open*, 10, p.100095.
36. Kokate C. K, A.P. Purohit, S.B. Gokhale, Pharmacognosy, volume 1 & 2, edition: 45, page number: A.1 to A.6
37. Lal, B.S., 2016. Diabetes: causes, symptoms and treatments. *Public health environment and social issues in India*, 1.
38. Luhar, S., Kondal, D., Jones, R., Anjana, R.M., Patel, S.A., Kinra, S., Clarke, L., Ali, M.K., Prabhakaran, D., Kadir, M.M. and Tandon, N., 2021. Lifetime risk of diabetes in metropolitan cities in India. *Diabetologia*, 64(3), pp.521-529.
39. Maruthupandian, A. and Mohan, V.R., 2011. Antidiabetic, antihyperlipidaemic and antioxidant activity of Pterocarpus marsupium Roxb. in alloxan induced diabetic rats. *Int J Pharm Tech Res*, 3(3), pp.1681-1687.
40. McCabe-Sellers, B., Frankel, E.H. and Wolfe, J.J., 2003. *Handbook of food-drug interactions*. CRC press.
41. Mekala, S. and Mchenga, S.S.S., 2020. Antidiabetic effect of Pterocarpus marsupium seed extract in gabapentin induced diabetic rats.
42. Mohiuddin, M., Azam, A.Z., Amran, M.S. and Hossain, M.A., 2009. on the Protein Binding of Caffeine in the Aqueous Media. *Journal of Biological Sciences*, 9(5), pp.476-481.
43. Nath, A.K., Jenny, A., Uddin, M.Z., Dutta, M., Chowdhury, S., Saha, D. and Morshed, M.M., 2011. In vitro interaction of metformin hydrochloride with levofloxacin and its influence on protein binding. *Bang Pharm J*, 14, pp.121-125.
44. Njagi, E.C., Huang, H., Stafford, L., Genuino, H., Galindo, H.M., Collins, J.B., Hoag, G.E. and Suib, S.L., 2011. Biosynthesis of iron and silver nanoparticles at room temperature using aqueous sorghum bran extracts. *Langmuir*, 27(1), pp.264-271.
45. Patra, J.K., Das, G., Fraceto, L.F., Campos, E.V.R., Rodriguez-Torres, M.D.P., Acosta-Torres, L.S., Diaz-Torres, L.A., Grillo, R., Swamy, M.K., Sharma, S. and Habtemariam, S., 2018. Nano based drug delivery systems: recent developments and future prospects. *Journal of nanobiotechnology*, 16(1), pp.1-33.

46. Rahman, M.S., Mujahid, M.D., Siddiqui, M.A., Rahman, M.A., Arif, M., Eram, S., Khan, A. and Azeemuddin, M.D., 2018. Ethnobotanical uses, phytochemistry and pharmacological activities of *Pterocarpus marsupium*: a review. *Pharmacognosy Journal*, 10(6s).
47. Reddy Yp, Sowmya C, Raja Ms, Kumar Kr, Suresh B, Chaithanya T. Spectrophotometric Method for The Estimation of Glimepiride in Bulk and Pharmaceutical Formulations
48. Rekha, B.C., Tangeti, S., Madhavi, L. and Pathapati, R.M., 2016. Toxicity, Acute and Longterm Anti-Diabetic Profile of Methanolic Extract of Leaves of *Pterocarpus Marsupium* on Alloxan Induced Diabetic Albino Rats. *The Pharma Innovation*, 5(7, Part B), p.90.
49. Saratale, R.G., Shin, H.S., Kumar, G., Benelli, G., Kim, D.S. and Saratale, G.D., 2018. Exploiting antidiabetic activity of silver nanoparticles synthesized using *Punica granatum* leaves and anticancer potential against human liver cancer cells (HepG2). *Artificial cells, nanomedicine, and biotechnology*, 46(1), pp.211-222.
50. Seedher, N. and Kanojia, M., 2008. Reversible binding of antidiabetic drugs, repaglinide and gliclazide, with human serum albumin. *Chemical biology & drug design*, 72(4), pp.290-296.
51. Shah, J.M., Bukhari, S.A.H., ZENG, J.B., QuAN, X.Y., Ali, E., Muhammad, N. and ZHANG, G.P., 2017. Nitrogen (N) metabolism related enzyme activities, cell ultrastructure and nutrient contents as affected by N level and barley genotype. *Journal of Integrative Agriculture*, 16(1), pp.190-198.
52. Shah, M., Nawaz, S., Jan, H., Uddin, N., Ali, A., Anjum, S., Giglioli-Guivarc'h, N., Hano, C. and Abbasi, B.H., 2020. Synthesis of bio-mediated silver nanoparticles from *Silybum marianum* and their biological and clinical activities. *Materials Science and Engineering: C*, 112, p.110889.
53. Shargel, L., Wu-Pong, S. and Yu, A.B.C., 2012. Applied biopharmaceutics and pharmacokinetics, McGraw-Hill. *New York, NY*.
54. Shouip, H.A., Signs and symptoms.
55. Tran, N., Pham, B. and Le, L., 2020. Bioactive compounds in anti-diabetic plants: From herbal medicine to modern drug discovery. *Biology*, 9(9), p.252.

56. Vallinayagam, S., Rajendran, K. and Sekar, V., 2021. Green synthesis and characterization of silver nanoparticles using Naringi crenulate leaf extract: Key challenges for anticancer activities. *Journal of Molecular Structure*, 1243, p.130829.
57. Vijaya Raghavan, C. and Justin, J., 2006. Experimental Biopharmaceutics and Pharmacokinetics. *New century book house*.
58. Vitthal, K.U., Pillai, M. and Kininge, P., 2013. Study of solid lipid nanoparticles as a carrier for bacoside. *Int. J. Pharma Biosci*, 3, pp.414-426.
59. Yu, C., Tang, J., Liu, X., Ren, X., Zhen, M. and Wang, L., 2019. Green biosynthesis of silver nanoparticles using Eriobotrya japonica (Thunb.) leaf extract for reductive catalysis. *Materials*, 12(1), p.189.
60. Zhang, X.F., Liu, Z.G., Shen, W. and Gurunathan, S., 2016. Silver nanoparticles: synthesis, characterization, properties, applications, and therapeutic approaches. *International journal of molecular sciences*, 17(9), p.1534.



भारतसरकार
GOVERNMENT OF INDIA
पर्यावरण, वन और जलवायु परिवर्तन मंत्रालय
MINISTRY OF ENVIRONMENT, FOREST & CLIMATE CHANGE
भारतीय वनस्पति सर्वेक्षण



BOTANICAL SURVEY OF INDIA

दक्षिणीक्षेत्रीयकेन्द्र / Southern Regional Centre
टी.एन.ए.यू.कैम्पस/ T.N.A.U. Campus
लाउलीरोड/ Lawley Road
कोयंबटूर/ Coimbatore - 641 003

टेलीफोन / Phone: 0422-2432788, 2432123, 2432487
टेलीफैक्स/ Telefax: 0422- 2432835
ई-मेल/E-mail id: sc@bsi.gov.in
bsisc@rediffmail.com


सं. भा.व.स./द.क्षे.के./No.: BSI/SRC/5/23/2021/Tech

109

दिनांक/Date: 13.09.2021

पौधा प्रमाणीकरण प्रमाणपत्र / PLANT AUTHENTICATION CERTIFICATE

The plant specimen which has been given by you for authentication is identified as *Pterocarpus marsupium* Roxb. – FABACEAE. The identified specimen is returned herewith for preservation in your College/ Department/ Institution Herbarium.


डॉ.एम. यू. शरीफ/Dr. M.U. Sharief
वैज्ञानिक 'ई' एवं कार्यालयाध्यक्ष/
Scientist 'E' & Head of Office
13/9/2021

सेवा में / To

Ms. C. Bavya
II Year M. Pharm Student
Department of Pharmaceutics, College of Pharmacy
Sri Ramakrishna Institute of Paramedical Sciences
Coimbatore Dist. – 641 044, Tamil Nadu